DSPACE

https://dspace.org/

Hydrogeochemical characterisation of groundwater in fractured aquifers at Konkola mine in Chililabombwe, Zambia

Sakala, Vincent

2025
University of the Witwatersrand, Johannesburg
https://hdl.handle.net/10539/50292
Sakala, Vincent. (2025). Hydrogeochemical characterisation of groundwater in fractured aquifers at Konkola mine in Chililabombwe, Zambia [Master's dissertation, University of the Witwatersrand, Johannesburg]. WIReDSpace. https://hdl.handle.net/10539/50292

Downloaded from a DSpace repository. https://dspace.org/

Hydrogeochemical characterisation of groundwater in fractured aquifers at Konkola Mine in Chililabombwe, Zambia



WITS
UNIVERSITY

HYDROGEOLOGY RESEARCH REPORT (GEOL7052)

A research report submitted to the Faculty of Science for the partial *Fulfilment* of the degree *MSc in Hydrogeology* at the University of the Witwatersrand

Submitted by

Vincent Sakala

2633542

Supervisor: Prof. Tamiru Abiye

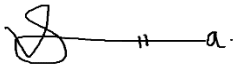
November 2025

DECLARATION

I, Vincent Sakala (Student Number: 2633542), declare that 'Hydrogeochemical characterisation of groundwater in fractured aquifers at Konkola Mine in Chililabombwe, Zambia' is my personal original work and has not been presented for academic credit or assessment at any other institution. I have properly credited all sources used in this study. All sources cited or utilised in this work have been fully acknowledged with appropriate citations.

Additionally, I acknowledge the subsequent:

- I understand that using another person's work without due citation or authorisation constitutes academic misconduct.

Signature of candidate:  Date: 3rd November 2025

ABSTRACT

An extensive hydrogeological investigation was carried out at the Konkola Copper Mine (KCM), a major mining operation located in Chililabombwe, Zambia, to explore the hydrogeochemical properties of groundwater in fractured aquifers. The approach integrated multiple datasets, including a review of the regional and local geological settings, site-specific meteorological data, environmental isotopes, hydrochemical analyses and previous hydrogeological studies conducted at KCM. The primary aim was to enhance the understanding of both fractured and unfractured aquifers at KCM, which will contribute to the development of a more effective dewatering strategy for the mine. The study established a hydraulic link between fractured and unfractured aquifers as supported by similarities in $\delta^{2}H$ and $\delta^{18}O$ isotopic signatures that indicate shared recharge sources and groundwater mixing.

In the investigated site, the prevailing hydrochemical facies is classified as Ca-HCO_3, indicating that the chemistry of groundwater is dominantly influenced by rock-water interactions, particularly with the carbonaceous and siliceous rock formations affected by percolating water. The hydrochemical results revealed aquifer connectivity and inflow direction, supporting dewatering planning.

The stable isotope ($\delta^{2}H$ and $\delta^{18}O$) analysis suggests that groundwater recharge primarily occurs through rainfall originating from high latitudes and regional air circulations associated with cooler climate conditions, as evidenced by the depleted isotope signatures. Additionally, the similarities in isotopic (stable) signatures indicate a possible hydraulic linkage among the aquifers at KCM. Tritium analysis reveals ranges between 0.1 and 1.0 T.U., suggesting a mix of recently recharged and sub-modern water, further supporting the presence of hydraulic connections between the aquifers. Higher tritium levels indicate rapid infiltration within permeable aquifer systems, while lower values suggest deep-circulating or confined groundwater. Variations in tritium concentrations across and within aquifers, especially in the Hangingwall Aquifer (HWA) and fractured aquifer, highlight the mixing of distinct water sources.

Based on the integrated hydrogeological investigation, the fractured aquifer at KCM has been identified as a zone of groundwater mixing. The overall groundwater flow is directed from the HWA and Lower Porous Conglomerate (LPC) towards the Footwall Aquifer (FWA) and the fractured aquifer.

This report recommends that ongoing sampling of isotopes and water chemistry from rainfall, surface water bodies, and underground sources within the study area should continue. Such efforts are important for gaining a better understanding of the area's hydrogeochemistry. Additionally, measures to exclude surface water should be improved

to minimize seepage, as this study has observed a connection between surface water and groundwater.

DEDICATION

This work is lovingly dedicated to the memory of my late father

Michael Sakala

1955–2021

May the comfort and blessing of his memory remain forever

ACKNOWLEDGEMENTS

I want to sincerely thank Konkola Copper Mines plc for providing me with the incredible opportunity to access mine data and conduct my research in the mining area. Thank you very much to the following General Managers, Mr. Kasanda Allam (GM Technical Services), Mr. Cornelius Chimbanga (GM Konkola Mine) and Mr. Mubita Davy (GM Technical Services - Projects) for their immense support and encouragement during the course of this study.

These studies could not have been possible without the invaluable contribution and advice of Mr. John Ngambi (Former Manager, Hydrogeology at KCM) and Mr. Jasper Manyika (Manager, Geology, at Konkola). Their suggestions helped me to expand the research ideas.

I am profoundly thankful to Professor Tamiru Abiye, my research supervisor, for his invaluable guidance, patience and technical expertise throughout this project. The thought provoking lectures I attended under his mentorship inspired my research and enhanced my comprehension of the topic. I am deeply grateful for the assistance I received with stable isotope analysis.

I want to express my gratitude to Mr. Mike Butler and iThemba Labs for their support with tritium analysis. This work would not have been possible without their assistance.

My gratitude extends to the Konkola Copper Mines Hydrogeology team for their unwavering support during my research journey. I am also thankful to my teammates at KCM; Sibongile Kanyungu, Banda Masinge, Evans Luma, Masinge Banda, Emmanuel Mwila, Davies Kashimu, and Alex Mwewa for their valuable input and engaging discussions that enriched this research project.

I wish to express my deep appreciation to my mother, Charity Nanyangwe, my siblings, and my entire family for their unwavering support. Their encouragement has been fundamental to my success.

Lastly, I would like to extend my love and gratitude to my wonderful wife, Priscilla S. Siachobe, and our sons, Vincent Jnr and Michael, for their understanding and support during the long hours I dedicated to this study. To my late father, Michael Sakala, thank you for instilling in me the values of hard work and education, which have guided me to this point.

TABLE OF CONTENTS

DECLARATION ..... **i**
ABSTRACT ..... **ii**
DEDICATION ..... **iv**
ACKNOWLEDGEMENTS ..... **v**
LIST OF FIGURES ..... **ix**
LIST OF TABLES ..... **xi**
1. INTRODUCTION **1**
1.1 General 1
1.3 Research Objectives 3
1.4 Research Limitations 3
2. LITERATURE REVIEW **4**
2.1 Introduction 4
2.2 The Role of Hydrochemical and Environmental Tracer Techniques in Characterising Groundwater in Mines 4
2.3 Hydrochemical Techniques in Groundwater Studies 5
2.4 Environmental Tracer Techniques in Groundwater Studies 7
2.4.1 Environmental Stable Isotopes (ESI) 7
2.4.2 Radioactive Isotopes 8
2.5 Application of Hydrochemical and Environmental Tracers Techniques to Characterise Groundwater in Mining Environments 9
2.6 Application of Hydrogeochemical and Environmental Tracers Techniques to Characterise Groundwater at KCM 11
3. DESCRIPTION OF THE STUDY AREA **12**
3.1 Location of study area 12
3.2 Climate 14
3.2.1 Precipitation 15
3.2.2 Evaporation 16
3.2.2 Surface Topography and Drainage 17
3.2.3 Land Use and Land Cover 19
3.3 Geology of the Zambian Copperbelt 20

3.3.1 Regional Geology 20
3.3.2 Konkola Area Local Geology 23
3.3.2 Stratigraphy of Konkola Mining Areas 24
3.3.2 Structural setting 30
3.5 Hydrogeology 31
3.5.1 Aquifers 33
3.4.2 Aquicludes 34
4. METHODOLOGY 36
4.1 Desktop investigations 36
4.2 Fieldwork 37
4.2.1 Geological survey 37
4.2.2 Core logging 37
4.2.3 Hydrogeological Investigations 38
4.2.4 Water Sampling 38
4.3 Laboratory analyses 39
4.3.1 Analytical Description and Preservation 39
4.3 Data Presentation 40
4.3.1 Water Chemistry 40
4.3.2 Stable isotope 41
4.3.3 Tritium 41
5. RESULTS AND DISCUSSION 43
5.1. Physiochemical and Hydrochemistry 44
5.1.1 Temperature (°C) 44
5.1.2 pH (Hydrogen ion activity) 44
5.1.3 Total dissolved solids (TDS) 44
5.1.4 Electrical conductivity (EC) 45
5.1.5 Hydrochemical facies 45
5.2 Stable Isotopes 51
5.2.1 Deuterium excess or D-excess 55
5.3 Tritium Dating 57

5.3 Tracing the Possible Pathways of the Water and Mixing of Groundwater Flow in Aquifers in the Konkola Flats area at KCM. 60
5.3 Mixing of Groundwater in Aquifers at KCM (Konkola Flats Area) 67
5.4 Dewatering Principle for the Fractured Aquifer 70
5.4.1 Proposed Dewatering Methods 70
6. CONCLUSION AND RECOMMENDATIONS 73
6.1 Conclusion 73
6.2 Recommendations 74
7. REFERENCES 76

LIST OF FIGURES

Figure 2-1: Schematic diagram illustrating the evolution of groundwater along a flow path from the recharge zone to the confined segment, highlighting key hydrochemical processes that influence groundwater chemistry (Hiscock and Bense, 2014). 6

Figure 3-1: Location map of the KCM 13

Figure 3-2: Konkola deposit top-down view, highlighting Konkola Flats mining sector alongside other sectors and their related resource timetable (Konkola Copper Mines, 2024). 14

Figure 3-3: KCM annual rainfall from 1957 to 2023 (Source: Konkola Copper Mines Rainfall Records, 2024). 15

Figure 3-4: Rainfall change from the mean for KCM from 1957 to 2023, calculated from Konkola Copper Mines Rainfall Records, (2024). 16

Figure 3-5: Surface topography and drainage at KCM (WSP, 2018). 18

Figure 3-6: Digital Elevation Model (DEM) showing the topography of KCM 19

Figure 3-7: Generalized geological maps illustrating the tectonic framework, a cross-sectional profile along line A–A', and the LFB structural features. (Source: Selley *et al.,* 2005). 20

Figure 3-8: Lithostratigraphy of the Katangan Supergroup in the Zambian Copperbelt, showing approximate average strata thicknesses. (Source: Selley et al. (2005). 22

Figure 3-9: Konkola Mine geological map. (modified from WSP, 2018) 24

Figure 3-10: Field appearance of the Muliashi Porphyry with rounded microcline porphyroblasts. 25

Figure 3-11: Field appearance of the (A) LPC and the (A and B) lower portion of the FWQ which is highly jointed. 26

Figure 3-12: General stratigraphic column of the Konkola Mine (Konkola Copper Mines, 2010). 28

Figure 3-13: Photographs of rock units from the field and diamond drill cores. 29

Figure 3-14: Structural map of Konkola Mine depicting the Kirilabombwe anticline surface outline (Torremans *et al.*, 2013). 30

Figure 3-15: 760m level plan of the Konkola Flats area showing plotted diamond drill holes and West to East section line BB'. 34

Figure 3-16: A West (B) to East (B') cross-section parallel to KON 09 (BPN 898) sampling point showing mapped geological structures. 35

Figure 5-1: Piper diagram presenting surface and groundwater of water sampled from KCM. 46

Figure 5-2: Stiff diagram (Stiff, 1951) graphically representing hydrochemical facies of water at KCM. 48

Figure 5-3: TDS vs Na/ (Na/(Na+Ca) diagrams of all water samples from the KCM area.The diagrams depict water chemistry for surface water (Gibbs, 1970) diagram (A) and in groundwater (B). The evolution of groundwater quality caused by (C) the dissolution of evaporite minerals (Sahib et al., 2016).The grey patterned cloud on B and C represents the groundwater samples taken from the USGS Brackish Groundwater Database(Qi and Harris, 2017). 49

Figure 5-4: Expanded Durov diagram for KCM representing hydrochemical processes. 50

Figure 5-5: Stable isotope correlation diagram of water samples at KCM with associated LMWL 53

Figure 5-6: Scatter plots of δ18O and deuterium excess for water samples from KCM .. 56

Figure 5-7: Scatter plot of Tritium and $\delta^{18}O$ within the KCM area. 59

Figure 5-8: Scatter plot depicting the correlation between Tritium levels and mine depths. 60

Figure 5-9: Observed Fractured Zone of the footwall sandstone in DVN 898 that allows water flow and is associated with sample KON 08. The oxidized, fractured footwall sandstone comprises variable stains of iron oxide. 61

Figure 5-10: Underground picture showing massive quartz vein within the footwall sandstone; pen for scale 63

Figure 5-11: Water collection points from surface and underground at KCM. (A) KON 08, (B) KON 10, (C) KON 01 and (D) KON 05..... 64

Figure 5-12: Schematic figure of KCM in 3D (Surpac DTM), showing No. 3 Shaft and the sampling points 65

Figure 5-13: Mixing graph of $\delta^{18}O$ versus chloride of the water samples from the sampling sites at KCM 68

Figure 5-14: Change relationships of environmental stable isotopes with TDS in groundwater flowing direction in the KCM aquifers..... 69

Figure 5-15: Conceptual hydrogeological sectional of KCM showing the three main aquifers and proposed boreholes. Modified after KCM (2010)..... 71

LIST OF TABLES

Table 3-1: Summary data on monthly evaporation and rainfall (WSP, 2018). 17

Table 3-2: Konkola Mine Hydrostratigraphic column (Advisian WorleyParsons Group, 2017) 32

Table 4-1: Drilled diamond drill boreholes in the Konkola Flats area at KCM. 37

Table 4-2: Surface and underground sampling points and physical appearance of the samples..... 38

Table 5-1: Surface and groundwater hydrochemical analyses of samples at KCM. 43

Table 5-2: Simple classification of groundwater based on TDS content, modified after Freeze and Cherry (1979). 44

Table 5-3: Water types based on Stiff diagram interpretation of samples at KCM..... 48

Table 5-4: Results of ESIs in surface water and groundwater for KCM. 54

Table 5-5: Stable isotope of surface water and groundwater from KCM with associated deuterium excess. 56

Table 5-6: Tritium concentrations and associated mean residence times for samples from KCM. 58

Table 5-7: Detailed description of rock units and lithological attributes for BPN 898 61

ABBREVIATIONS

D-excess: Deuterium excess

EC: Electrical Conductivity

ESI: Environmental Stable Isotope

FWA: Footwall Aquifer

GMWL: Global Meteoric Water Line

HWA: Hangingwall Aquifer

ITCZ: Intertropical Convergence Zone

KCM: Konkola Copper Mine

LMWL: Local Meteoric Water Line

LPC: Lower Porous Conglomerate

MWL: Meteoric Water Line

TDS: Total Dissolved Solids

1. INTRODUCTION

1.1 General

In the mining sector, understanding the sources of water recharge, the interactions between surface water and groundwater, and the relationships between rocks and water is essential for developing effective water resource management strategies. As mining activities increase in depth, intensity and scale, groundwater-related issues tend to become more severe and hazardous (Zhang *et al.*, 2019). Therefore, tracing groundwater sources in mining environments is essential. Additionally, groundwater is essential for agriculture, industry and human consumption, existing within various geological formations. These formations are influenced by geological features such as faults, fractures and folds. The lithology, stratigraphy and structural characteristics of these formations and deposits determine the type and distribution of aquifers and aquitards within a given geological system (Clark and Fritz, 1997).

Moreover, mining, particularly underground mining, can alter underground flow patterns and hydrogeological parameters by increasing rock permeability and creating networks of fractures (Bridgwood *et al.*, 1983). Fractured aquifers in underground mines represent unique hydrogeological systems, presenting both opportunities and challenges for environmentally sustainable mining practices. Conducting hydrogeochemical assessments of groundwater in these contexts is essential for understanding water quality, predicting future contaminant migration and developing effective groundwater management strategies (Smedley and Kinniburgh, 2002). Water seepage through fractures in underground mining operations poses significant challenges, impacting stability, safety and overall operational efficiency. Managing water inflow through processes such as pumping, treatment and disposal presents a particularly complex problem in these environments (Vutukuri and Singh, 1995). Therefore, for sustainable groundwater control and effective dewatering in underground mines, it is important to comprehend the hydrogeochemical properties of groundwater. This knowledge helps determine optimal groundwater flow pathways, water sources and groundwater mixing (Mazor, 2003; Abiye *et al.*, 2013; Cook, 2020).

On a global scale, numerous incidents of mine water inflow and uncontrolled water inflows have been documented (Sammarco and Eng, 1986; Polak *et al.*, 2016; Guan *et al.*, 2019). Nevertheless, there have been a limited number of studies carried out in Africa, including works by Funke (1990), Mulenga (1991) and Ashton *et al.*(2001). Several studies suggest that water inflow, seepage and flooding in mines can be attributed to various factors. These

include the proximity of tailings dams, geological formations such as faults and dykes, fractures induced by mining activities, the presence of significant surface water bodies near the mining site and inadequate management of mine water (Singh, 1986; Mulenga, 1993; Mengistu *et al.*, 2015).

In Zambia, limited research has focused on the hydrogeochemical characterisation of aquifers within mining operations(Mulenga, 1991; Dildar *et al.*, 2023; Mbilima, 2023). However, a substantial body of literature focuses on how mining operations affect water resources. Since mining began in 1957, managing large groundwater inflows at Konkola Copper Mine (KCM) has remained a significant operational challenge (Mulenga, 1991). Effective dewatering of aquifers is required during mine development to facilitate ore extraction in the dewatered strata. Therefore, a thorough understanding of the mine area's structural geology and hydrogeology is essential for developing a robust dewatering strategy. According to Mulenga (1991), the need for improved water control in mines is primarily assessed based on the direct and indirect expenses associated with working in wet conditions. A comprehensive investigation into the sources of groundwater recharge and its chemical evolution is essential for enhancing the dewatering strategy at KCM. This requires hydrogeochemical studies that integrate both environmental isotope analysis and hydrochemical investigations.

Previous hydrogeological studies have been conducted at KCM, focused on groundwater flow, impact, characterisation and modelling (Singh, 1986; Mulenga, 1991; Mulenga and De Freitas, 1991; Straskraba *et al.*, 1991; Mulenga *et al.*, 1992; Naish, 1993). However, stable isotopes of water (δ^2H and δ^{18}O) have never been employed to assess the hydrogeochemical properties of water at KCM. Therefore, this study aims to incorporate stable isotopes to improve the comprehension of recharge sources, flow paths of groundwater and the interaction between different water sources within the aquifers at KCM. Mulenga (1991) asserted that groundwater enters KCM primarily through areas with high conductivity, such as fractures and fissures.

Therefore, to enhance the dewatering strategy at the KCM, it is essential to thoroughly understand the sources of recharge, flow paths and the mixing of waters. This can be achieved through hydrogeochemical research, geophysical studies, numerical modelling and an integrated approach, as suggested by (Clark and Fritz, 1997; Mazor, 2003). Hence, this study will focus on examining the hydrochemical and isotopic properties (δ^2H, δ^{18}O and tritium) of groundwater in both primary and secondary (fractured) aquifers. This investigation aims to deepen the understanding of recharge origins, water flow paths and the mixing of different water sources.

1.2 Research Objectives

This research seeks to identify and describe the hydrogeological characteristics of groundwater in both unfractured and fractured aquifers at KCM in Chililabombwe, Zambia. It employs an integrated approach that combines environmental isotopes and hydrochemical analyses. A better understanding of the fractured aquifers at KCM will aid in developing a more effective dewatering strategy for the mine.

The objectives of this research include:

- identifying the sources of major ions and the factors controlling them in fractured zones;
- examining water-rock interactions in fractured aquifers;
- analysing surface water and groundwater using different methods and constituents;
- groundwater recharge assessment inferred from stable isotopes and tritium ; and
- interpret hydrochemical and isotopic data to infer aquifer connectivity and its implication on mine dewatering.

1.3 Research Limitations

The data collected exhibited shortcomings due to challenges encountered during the research, including limited access to some underground sampling locations because of safety concerns for personnel in the area of study. Additionally, the costs associated with laboratory examination of the collected water samples restricted both the number of samples collected and the range of parameters analysed. Furthermore, Sampling was limited to a single instance due to access restrictions in the active mine area, preventing the evaluation of temporal variations. As a result, interpretations are therefore based on hydrogeochemical trends observed at the time of sampling, using representativeness to ensure reliable conclusions

2. LITERATURE REVIEW

2.1 Introduction

The hydrogeochemical characterisation of groundwater in underground mines has been studied globally. However, characterising groundwater in underground mines, particularly within fractured aquifers, presents unique challenges for groundwater management (Mulenga, 1991; Mengistu *et al.*, 2015; Guan *et al.*, 2019; Ramangoa, 2021) due to the complexity of varying hydrogeological and geological conditions in specific areas. Research worldwide has employed various techniques, including multivariate statistical methods, geochemical modelling, hydrochemical analysis, environmental stable isotopes (ESIs) and tritium, to identify pollution sources, geochemical evolution, water-rock interactions and groundwater movement patterns in aquifers (Mulenga, 1991; Straskraba *et al.*, 1991; Abiye *et al.*, 2013; Ma *et al.*, 2015; Mengistu *et al.*, 2015; Qian *et al.*, 2017; Ramangoa, 2021).

Hydrochemical, stable isotopes and tritium analyses provide valuable insights into groundwater movement, recharge processes and residence time of water (Clark and Fritz, 1997; Mazor, 2003). This is because water acquires traceable isotopic signatures along its flow pathway (Abiye *et al.*, 2013). Therefore, understanding hydrochemistry is essential for the effective and sustainable management of water resources in fractured aquifers within underground mines, ensuring long-term water management.

The following sections provide a comprehensive understanding of (i) the role of hydrochemical and environmental tracer techniques in characterising groundwater in mines; (ii) hydrogeochemical techniques in groundwater studies; (iii) stable isotope techniques in groundwater studies; (iv) the use of environmental tracer and hydrochemical methods to characterise groundwater in mining environments; and (v) The use of environmental tracer and hydrochemical and methods to characterise groundwater at KCM.

2.2 The Role of Hydrochemical and Environmental Tracer Techniques in Characterising Groundwater in Mines

Hydrochemical and ESI tracer techniques have been widely used to understand the complexity of groundwater in mining environments (Mulenga, 1991; Abiye *et al.*, 2015; Ma *et al.*, 2015a; Mengistu *et al.*, 2015; Zhang *et al.*, 2019; Ramangoa, 2021). By analysing the isotopic signatures and chemical composition of groundwater samples, researchers have gained valuable knowledge about the sources, flow paths and interactions of groundwater with surface water and surrounding rock, as well as potential contamination risks. These techniques are essential for effective mine water management, environmental impact assessment and the development of sustainable mining practices. In particular,

underground mining operations significantly impact the surrounding geological environment, leading to complex interactions between surface water and groundwater.

Abiye et al. (2015) conducted a study in the Upper Crocodile River Basin in South Africa, employing environmental isotopes to investigate the relationship between groundwater and surface water. This region is characterised by fractured crystalline rocks and dolomitic aquifers influenced by mining activities. The study revealed that mine water contaminates both shallow groundwater and streams. By employing environmental isotopes, the researchers tracked the source and movement of water, demonstrating that mine water consists of a combination of deep-circulating groundwater and rainwater. Furthermore, the study quantified the volume of mine water infiltrating the dolomitic aquifer, a significant concern due to its potential impact on water quality and archaeological sites. This research underscores the importance of comprehending the interactions between surface water and groundwater, particularly in mining regions, to facilitate effective water resource management and conservation.

2.3 Hydrochemical Techniques in Groundwater Studies

Hydrochemical techniques involve analysing various chemical characteristics of groundwater, including major ions (e.g. Ca^{2+}, Mg^{2+}, Na^{+}, K^{+}, Cl^{-}, SO_4^{2-} and HCO_3^{-}), trace elements (e.g. Fe, Mn, Zn and As) and other parameters (e.g. pH, dissolved oxygen and electrical conductivity [EC]). These measurements are essential for identifying groundwater sources, tracing flow paths, assessing surface and groundwater interactions, assessing water-rock interactions and detecting contamination (Mulenga and De Freitas, 1991; Abiye *et al.*, 2015; Leketa *et al.*, 2018; Leketa and Abiye, 2021).

Groundwater is a complex mixture of various dissolved substances. The chemical and biochemical interactions between groundwater and the geological materials of soils and rocks lead to a diverse range of dissolved inorganic and organic substances (Hiscock, 2005). Other important factors include the varying composition of rainfall and atmospheric dry deposition in recharge areas, the modification of atmospheric inputs through evapotranspiration, differential absorption by biological processes in the soil zone and mixing with seawater in coastal regions (Hiscock, 2005).

Furthermore, the specific composition of groundwater depends on factors such as rock type, residence time and temperature (Mazor, 2003). For example, groundwater flowing through limestone typically has higher concentrations of calcium and bicarbonate ions (Zhang *et al.*, 2019). The chemical composition of groundwater is dynamic, evolving due to both natural (geogenic) and human-induced (anthropogenic) processes. Human activities, particularly agriculture, mining and industrial processes, can significantly influence groundwater chemistry. Agricultural practices, for example, introduce fertilisers and pesticides, which can leach into groundwater, increasing nitrate levels and other contaminants (Singhal *et al.*, 2010). The relative concentrations of major ions and trace

elements can help differentiate between various groundwater sources, such as meteoric water, connate water (trapped in rock formations during deposition) and deep-seated water. For instance, high chloride and sodium concentrations may indicate saline water intrusion or the dissolution of evaporite minerals (Freeze and Cherry, 1979). Analysing changes in hydrogeochemical parameters along flow paths can also provide insights into groundwater movement. For instance, elevated calcium and sulphate concentrations may suggest the presence of gypsum or anhydrite minerals along the flow path.

Groundwater's chemical composition changes along its flow path. Hiscock and Bense (2014) provided a pictorial representation of the typical variations in hydrochemical facies along a groundwater flow path (see Figure 2-1).

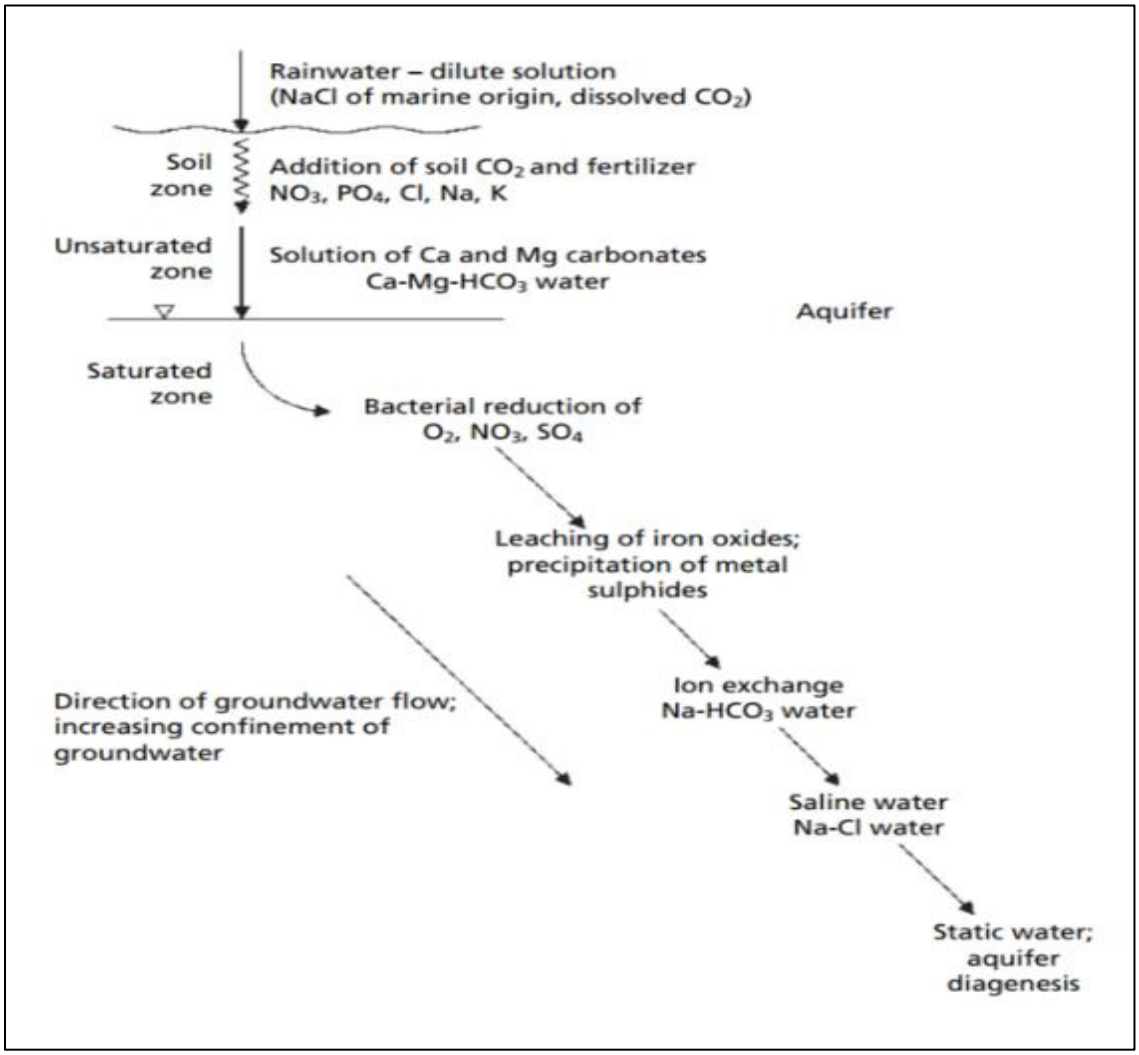


Figure 2-1: Schematic diagram illustrating the evolution of groundwater along a flow path from the recharge zone to the confined segment, highlighting key hydrochemical processes that influence groundwater chemistry (Hiscock and Bense, 2014).

A hydrochemical facies refers to a specific groundwater zone characterised by particular concentrations of cations and anions within defined limits (Hiscock, 2005). Essentially, it delineates distinct areas based on the composition of dissolved chemicals in the water. Geochemical reactions between groundwater and surrounding rocks can significantly influence water chemistry (Ma *et al.*, 2015). Groundwater from different sources can mix, resulting in blended chemical signatures. Water-rock interactions play a crucial role in shaping groundwater chemistry. As water moves through geological formations, it dissolves minerals and absorbs their chemical signatures. This process is influenced by factors such as rock type, temperature, pressure and contact time. Additionally, reactions involving ion exchange between water and minerals can change the proportion of ions present in the solution. Redox reactions, which involve the transfer of electrons between chemical species, can also modify groundwater chemistry. For example, a common redox reaction in groundwater that takes place when bacteria are present is the reduction of sulphate to sulphide (Singhal and Gupta, 2010).

2.4 Environmental Tracer Techniques in Groundwater Studies

Environmental tracers are naturally occurring (geogenic) or artificially introduced (anthropogenic) isotopes, elements or compounds present throughout the Earth's subsurface. Their varying abundances help scientists learn about and understand different environmental processes (Cook, 2020). As noted by Abiye *et al.* (2013), these tracers are widely used to investigate groundwater and surface water, providing insights into water transport and interconnectivity. Consequently, the use of environmental isotopes in mining-related studies has proven effective in global water resource management (Leketa and Abiye, 2021; Mulenga, 1991; Qian et al., 2017; Ramangoa, 2021; Verhagen et al., 2013; Xu et al., 2022; Zhang et al., 2019). The selection of tracers depends on specific hydrogeological conditions and research objectives. Among the most commonly used environmental tracers are:

2.4.1 Environmental Stable Isotopes (ESI)

ESI are non-radioactive atoms of the same chemical element that have the same number of protons and electrons but different numbers of neutrons. They can also be produced through radioactive decay (Cook, 2020). In hydrology, the stable isotopes of hydrogen ($^{2}H/^{1}H$) and oxygen ($^{18}O/^{16}O$) are particularly significant, as variations in their ratios provide valuable insights into water sources and chemical reactions (Clark, 2015). Water's isotopic makeup is typically reported in comparison to the Standard Mean Ocean Water (SMOW), an internationally recognised reference sample (Craig, 1961). These ratios are represented using delta (δ) notation in per mil (‰) as illustrated in Equation 1.

$$\boldsymbol{\delta}\ (‰) = \frac{\mathbf{Rsample - Rstd}}{\mathbf{Rstd}} * \mathbf{1000} \qquad \textbf{Equation 1}$$

Here,

R = ratio of isotope amount (usually less abundant to most abundant isotope)

The isotope ratios, represented by Rsample and Rstd, refer to the ratios of oxygen ($^{18}O/^{16}O$) or hydrogen ($^{2}H/^{1}H$) in the standard and sample. Typically, the measurement accuracy is within ± 0.2‰ and ± 2‰ for $\delta^{18}0$ and $\delta^{2}H$, respectively (Freeze and Cherry, 1979).

Furthermore, isotopic data obtained from precipitation samples generally align with a meteoric water line (MWL), which is determined using local, regional or global precipitation data. The Global Meteoric Water Line (GMWL), first identified by Craig (1961), is an equation that represents a real-world connection illustrating the typical correlation between $\delta^{18}O$ and $\delta^{2}H$ values in precipitation. Terzer *et al.* (2013) proposed a new approach known as the regionalised cluster-based water isotope prediction (RCWIP) for improving the prediction of stable isotope composition ($\delta^{2}H$, $\delta^{18}O$) in precipitation globally. This model is an improvement over older models, in particular, the equation for the GMWL of $\delta^{2}H = 7.91\delta^{18}O + 8.72‰$ (see Equation 2), as it incorporates regional climatic variations and a broader range of climatic and spatial variables.

$$\mathbf{\delta^{2}H = 7.91\ \delta^{18}0 + 8.72‰} \qquad \textbf{Equation 2}$$

Changes in $^{2}H/^{1}H$ and $^{18}O/^{16}O$ ratios in natural waters primarily occur due to isotopic fractionation during evaporation and condensation. Heavier water isotopes tend to remain in the liquid phase during evaporation or transition into the liquid phase during condensation (Cook, 2020). The equation illustrates a real-world correlation between $\delta^{18}O$ and $\delta^{2}H$ values in precipitation. It is possible to ascertain whether there was substantial evaporation prior to the water being replenished in the aquifer by using this analysis. It also allows for inferences about whether recharge was primarily influenced by direct rainfall infiltration or by a preferential flow mechanism (Mazor, 2004).

2.4.2 Radioactive Isotopes

Radioactive isotopes are isotopes of an element with an unstable nucleus that release excess energy through the spontaneous emission of alpha, beta and/or gamma rays (Cook, 2020). The radioisotopes routinely used in hydrogeology include tritium (^{3}H) and carbon-14 (^{14}C), which help estimate residence time and groundwater age, respectively, providing insights into flow paths and recharge areas (Clark and Fritz, 1997). The measurement of

radioactivity is based on the decay rate, which represents the change in the number of radioisotope atoms per second. Each radioisotope has a unique rate of decay, often characterised by its half-life. For example, ^{36}Cl has a half-life of 301,000 years, ^{14}C has a half-life of 5,730 years and ^{3}H has a half-life of 12.43 years (Clark and Fritz, 1997). This rate of decay is represented by the decay constant (λ), which is specific to each radioisotope. Consequently, the decay equation, which describes the time required for the number of atoms, *n*, to reduce to half of the initial amount ($n_o/n_t = 2$), defines the half-life ($T_{½}$) of a given radioisotope, as shown in Equation 3:

$$\boldsymbol{\lambda = \frac{\mathbf{In2}}{T_{1/2}} (time^{-1})}$$ **Equation 3** (Clark, 2015)

Therefore, combining multiple tracers with hydrochemical data provides a comprehensive understanding of complex hydrogeological processes, including groundwater flow, recharge and potential contamination risks.

2.5 Application of Hydrochemical and Environmental Tracers Techniques to Characterise Groundwater in Mining Environments

Managing groundwater entering mine operations can be a lengthy and expensive process because of the costs associated with pumping, as well as the additional wear on equipment, particularly when dealing with acidic water(Mulenga, 1991). Therefore, understanding groundwater characteristics is crucial for sustainable water management in mining environments, as its chemical composition can change along its flow path (Hiscock, 2005). Hydrochemical and environmental tracer techniques have been widely used to analyse the complexity of groundwater composition in mining settings (Mulenga, 1991; Abiye *et al.*, 2015; Ma *et al.*, 2015; Mengistu *et al.*, 2015; Zhang *et al.*, 2019; Ramangoa, 2021).

In South Africa, Leketa and Abiye (2021) employed these techniques to investigate groundwater flow mechanisms in fractured crystalline and karst aquifers in the Upper Crocodile River Basin, Johannesburg. Their study revealed direct recharge mechanisms in the fractured quartzite aquifer and emphasised the importance of collecting multiple samples for precise groundwater characterisation. Additionally, Levin and Verhagen (2013) utilised the environmental isotope technique alongside traditional methods to investigate potential leakage from the Osplaas Dam into a nearby railway tunnel. The collected water samples from the dam, boreholes and tunnel were analysed for chemical composition and stable isotope ratios. The results indicated no direct link between the dam water and the observed seepage in the tunnel. Furthermore, a radon emanation investigation was conducted to identify geological structures that might facilitate water movement

between the two locations. The study concluded that the increase in seepage within the tunnel after the dam was filled was likely due to the additional hydraulic pressure exerted on the groundwater system. Ramangoa (2021) investigated possible seepage water sources at a Gold Mine within South Africa using combined tracer and hydrochemical analysis. The findings indicated that water seepage in the mine was predominantly linked to or found near backfilled regions, areas adjacent to active mining operations, abutment zones, and geological features like faults and fractures caused by mining activities, further exacerbated by poor mine management. Mengistu *et al.* (2015) utilised ESI, hydrochemical, and tritium data integration to enhance the conceptualisation of a groundwater flow model at a nearby pumping shaft in South Africa. The study, conducted in a South African mining town, aimed to understand the origin of excessive water at the pumping shaft. Based on the findings, the study concluded that incorporating additional methods, such as ESI and hydrochemical analyses, could improve flow conceptualisation and numerical modelling.

In China, Huang *et al.*(2018) characterised the groundwater and hydrogeochemical processes of the Ningtiaota Coalfield using hydrochemical and ESI-integrated techniques to understand the mechanisms and sources of groundwater recharge. The study found that groundwater in this area originates from atmospheric precipitation, with weak evaporation during infiltration. Additionally, natural geochemical processes primarily drive the hydrochemistry, with minimal impact from coal mining activities. (Guan *et al.*, 2019) conducted a study to determine the sources of inflow water at a coal mine in China, using hydrogeochemical and isotope analyses. The study identified aquifers 1 and 2, along with the Yimin River, as potential sources of water inflow, contributing 30.8%, 60.6% and 8.6%, respectively. The authors also highlighted that employing multiple analytical methods could enhance result comparability and improve the understanding of inflow sources in a mining environment.

Therefore, an integrated approach using hydrochemical and environmental isotopic techniques would be advantageous at KCM for characterising groundwater within fractured aquifers. This approach will help determine the sources of groundwater recharge, the mixing of multiple groundwater reservoirs and the residence time of groundwater within the fractured aquifer. Understanding the hydrogeochemical progression of the groundwater will enable the mine to develop effective management and mitigation strategies for future groundwater-related concerns. For instance, if the investigation finds that groundwater is being replenished by surface water, the mine could take measures to reduce surface water seepage. Similarly, if the groundwater is found to have a significant age and prolonged residence time, the mine could implement safeguards to protect it from contamination.

2.6 Application of Hydrogeochemical and Environmental Tracers Techniques to Characterise Groundwater at KCM

Effective mine water management in fractured rock aquifers is problematic due to the complexity of flow patterns and the risk of contamination. However, hydrogeochemical and environmental isotope data serve as valuable tools for addressing these challenges and improving water management practices. Mulenga (1991) conducted a comprehensive study on groundwater flow at KCM, integrating ongoing and historical mining and dewatering and mining data with surface water hydrology, structural geological information, geochemistry and hydrogeochemistry. The study included analyses of major ions, pH, total dissolved solids (TDS), conductivity and temperature. Mine water was found to originate from both surface recharge and deeper regional aquifers, with flow primarily controlled by fractures and fissures. A numerical model was developed to predict groundwater outflow and the decrease in water levels, leading to the recommendation of a water-exclusion groundwater management solution to significantly reduce water inflow and associated costs. Understanding the origin and flow paths of groundwater in fractured rock aquifers is crucial for effective mine water management. In this study, tracers such as *Escherichia coli* and residual xanthates were used to confirm the hydraulic connection between surface water bodies, specifically the Lubengele Tailings Dam and the Kafue River and mine groundwater. Additionally, tritium dating was employed to differentiate recent water sources from older ones.

Given the success of this integrated approach in other studies, KCM would benefit from employing similar techniques, including the use of oxygen and hydrogen stable isotopes, which have not yet been applied in the mine for hydrogeochemical analyses. This would enhance the understanding of groundwater recharge sources and the mixing of various groundwater bodies. Furthermore, analysing the hydrogeochemical evolution of groundwater would enable the mine to develop effective, continuous management and mitigation strategies for potential groundwater-related issues, as demonstrated in studies by Huang *et al.* (2018), Levin and Verhagen (2013) and Guan *et al.* (2019).

Generally, the project examines both previously conducted studies and new investigations to advance the understanding of selected individual studies. The interpretation of isotopes' role in water resource assessment has been refined, where additional data collected after the initial investigation. The focus is on integrating hydrochemical, ESI and tritium data to improve insights into groundwater systems within underground mines, particularly on water recharge sources and flow paths, with practical applications for water management.

3. DESCRIPTION OF THE STUDY AREA

3.1 Location of study area

This study focuses on KCM, formerly known as Bancroft Mine. It is a Zambian-registered mine owned by Konkola Copper Mines Plc, situated in Chililabombwe town, Zambia's Copperbelt Province (Figure 3-1). Geographically, Chililabombwe is situated at an elevation of 1,360 metres above sea level (m a.s.l), while the Konkola Mine lies at an altitude of 1,331 m a.s.l. The town of Chililabombwe, where this study was conducted, is located 25 km northwest of Chingola and approximately 25 km from the Kasumbalesa border with the Democratic Republic of the Congo. It is also about 450 km north of the capital, Lusaka. The mine's geographical coordinates range from 27.357° to 28.467° longitude and -12.28° to -12.45° latitude.

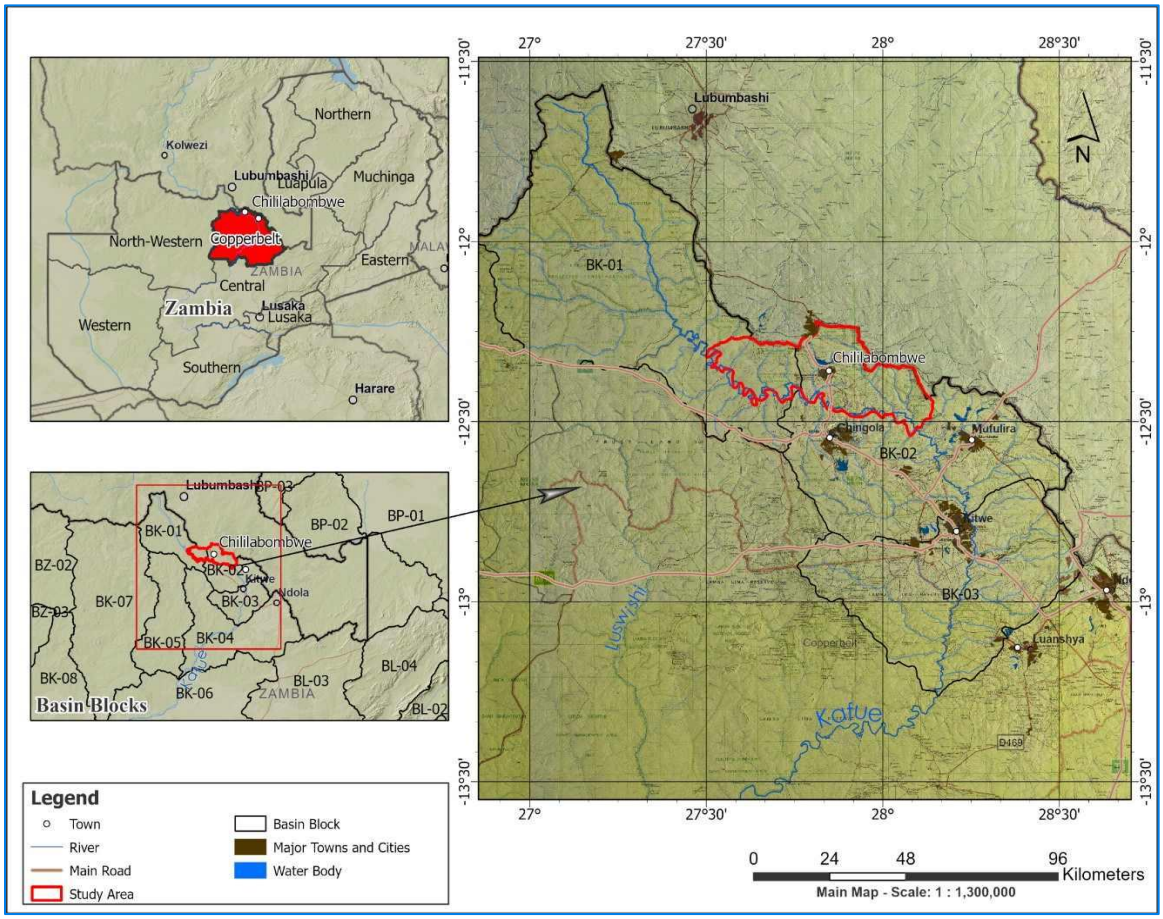


Figure 3-1: Location map of the KCM

KCM is mined through three shafts (1, 3 and 4) and is divided into six mining sectors: Bancroft Deeps, Bancroft Central, Bancroft North, Konkola Extension, Konkola Flats and Konkola East. This study focuses on the Konkola Flats mining blocks, which fall within the northern part of the Konkola deposit, as highlighted in Figure 3-2.

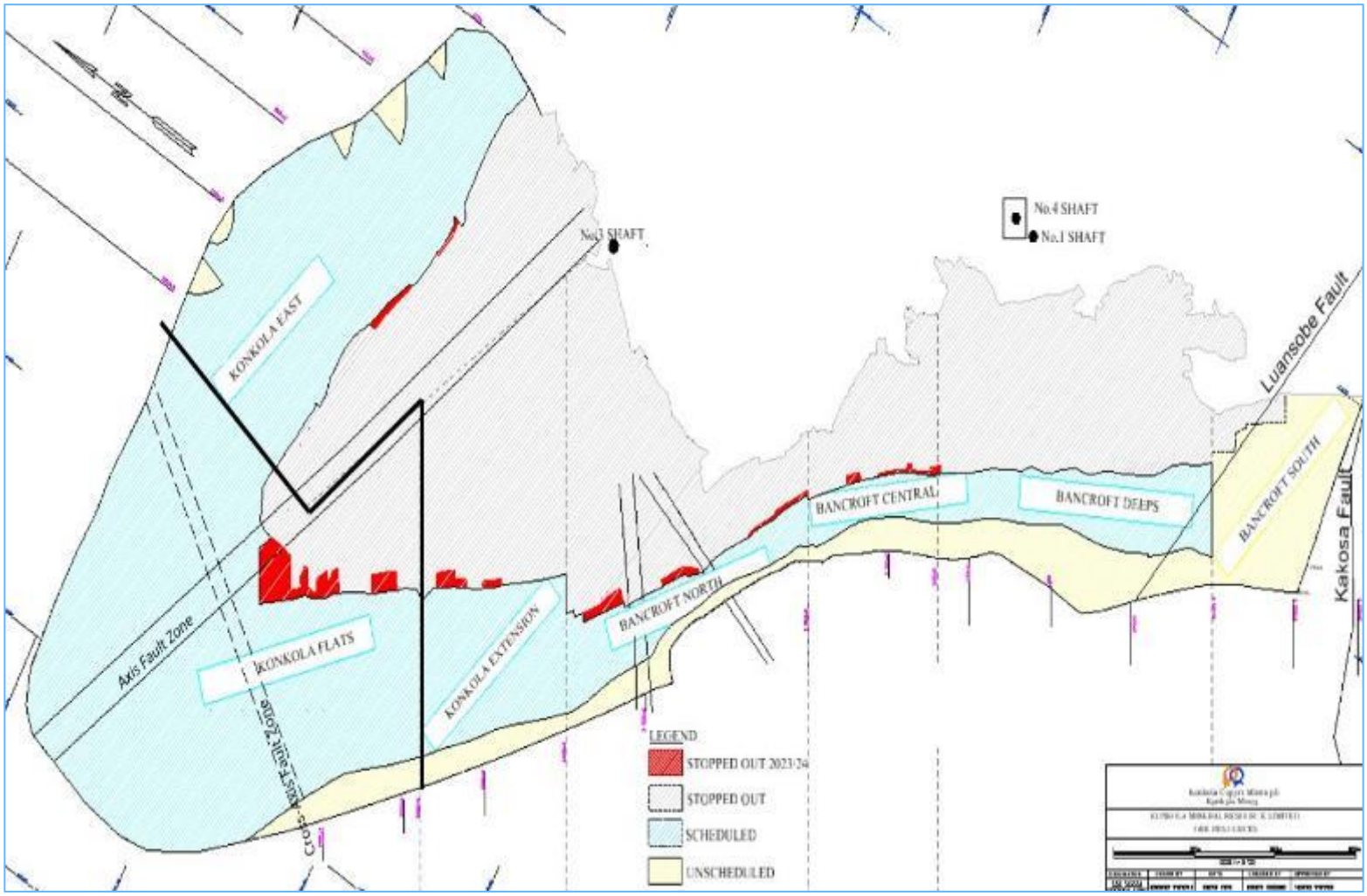


Figure 3-2: Konkola deposit top-down view, highlighting Konkola Flats mining sector alongside other sectors and their related resource timetable (Konkola Copper Mines, 2024).

3.2 Climate

Regionally, Zambia experiences two primary climatic seasons. The first is a hot and humid summer lasting from October to April, characterised by temperatures ranging from 25°C to 35°C. The second is a cooler and drier winter occurring from May to September, with temperatures typically between 10°C and 15°C. The amount of rainfall is significantly influenced by the shifting of the Intertropical Convergence Zone (ITCZ) and the El Niño–Southern Oscillation (ENSO) phenomenon (*World Bank Climate Change Knowledge*

Portal, 2025). The country's average annual rainfall ranges from 600 mm in the southern region to 1,300 mm in the north. Due to its proximity to the equator, Zambia experiences a tropical climate.

KCM is located near the northern watershed of the Zambezi River system, at an elevation of approximately 1,300 m a.s.l. Consequently, it falls within Zambia's high-rainfall belt. The area's climate is influenced by the periodic north-south migration of the equatorial low-pressure system.

3.2.1 Precipitation

KCM lies within the country's high-rainfall belt, with nearly all precipitation occurring between November and March. Annual rainfall ranges from 570 mm to 1,800 mm, with an average of 1,250 mm (Figure 3-3). December and January are typically the wettest months, while May and June are usually the driest. During the wet season, rainfall can occur on more than 20 days each month, accompanied by dense cloud cover that persists almost continuously. Temperatures during this period range from 25°C to 35°C. In contrast, the months from April to August are generally dry, clear and relatively cool, with temperatures ranging from 10°C to 20°C. September and October are characterised by rising temperatures and occasional thunderstorms.

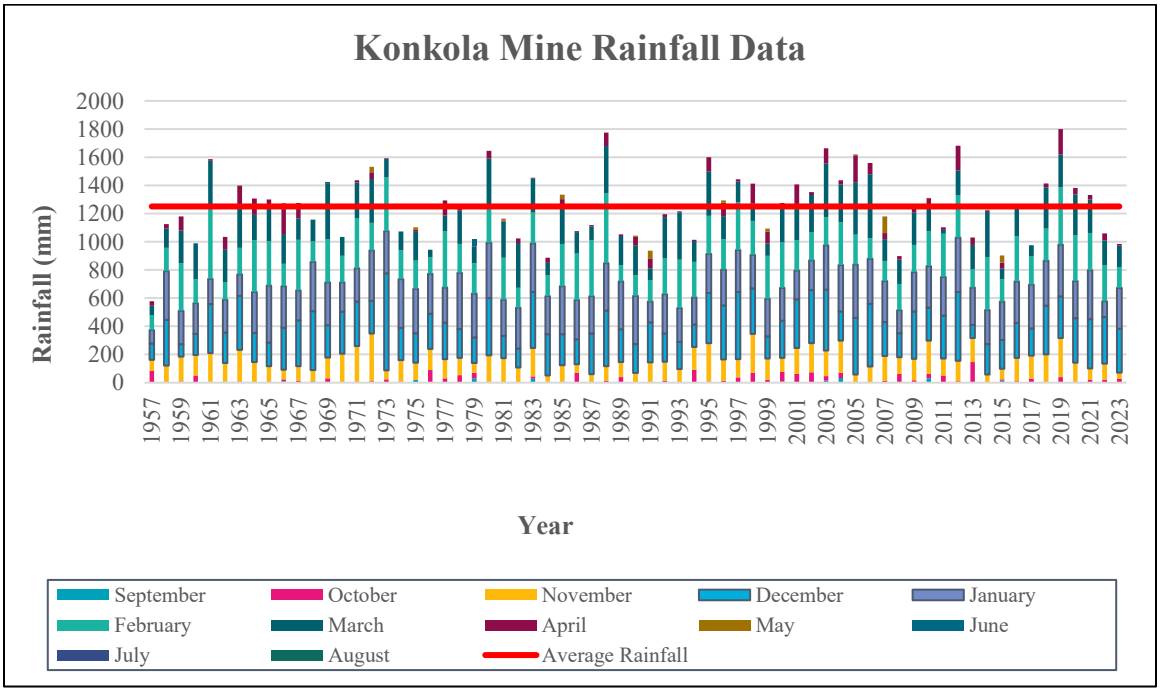


Figure 3-3: KCM annual rainfall from 1957 to 2023 (Source: Konkola Copper Mines Rainfall Records, 2024).

Figure 3-4 presents the rainfall change from the mean graph for KCM. The rainfall change from the mean frequently applied to estimate recharge quantities in semi-arid areas such as Southern Africa involves calculating the difference between monthly rainfall and the average monthly rainfall (Xu and Beekman, 2003). An upward trend in the plot indicates that rainfall is exceeding the average, likely enhancing groundwater recharge, as reflected in rising water levels in the region. Conversely, a downward trend in the plot suggests that rainfall is below average, leading to decreased groundwater recharge, which is reflected in declining water levels.

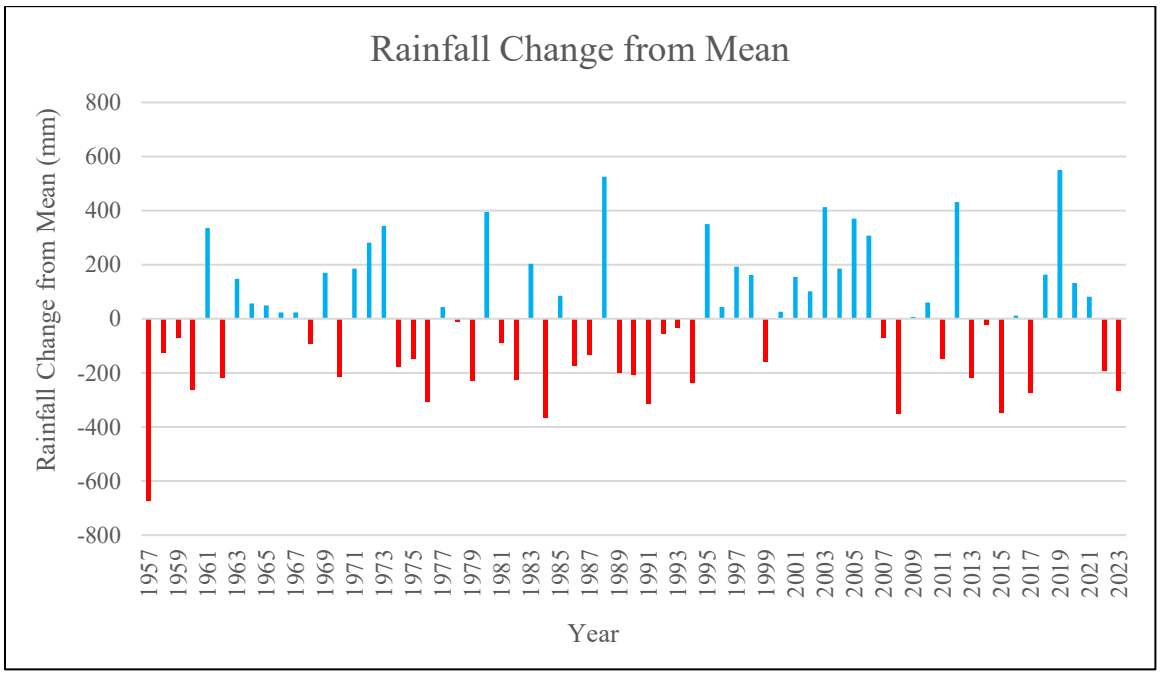


Figure 3-4: Rainfall change from the mean for KCM from 1957 to 2023, calculated from Konkola Copper Mines Rainfall Records (2024).

3.2.2 Evaporation

The annual pan evaporation rate averages around 2,200 mm per year (Chilillabombwe Municipal Council, 2022). Evaporation peaks in October at 215.2 mm/month, while the lowest evaporation occurs in June at 118.6mm/month, as shown in Table 3-1.

Table 3-1: Summary data on monthly evaporation and rainfall (WSP, 2018).

Month	Average Monthly Rainfall (mm)	Median Monthly Rainfall (mm)	Lowest Recorded Monthly Rainfall (mm/month)	Highest Recorded Monthly Rainfall (mm)	Average Class A-Pan Evaporation (mm/month)
September	3.90	0	0	33.8	195.2
October	27.90	18.3	0	143.5	215.2
November	141.70	138.6	46.7	276.9	167.2
December	277.80	263.4	91.4	487.4	130.4
January	291.90	290.5	109.5	426	122.8
February	255.40	253.2	1515	493.6	119.4
March	215.30	210.8	27.9	455.5	131.6
April	52.90	33.3	0	237	134.2
May	7.40	0	0	117.1	136
June	0.00	0.00	0.00	0.00	118.6
July	0.00	0.00	0.00	0.00	134.4
August	0.00	0.00	0.00	0.00	157.8

3.2.3 Surface Topography and Drainage

The study area's topographical setting and drainage are illustrated in Figures 3-5 and 3-6. Elevation ranges from 1,320 metres in the northern part of the Lubengele drainage basin, near Konkola Township at the Zambia-Congo border, to 1,265 metres at the confluence of the Lubengele and Kafue rivers. Overall, elevation tends to decrease moving southward from the highlands in the north. Within the mining zone, the surface drainage system is primarily influenced by the Kafue River network, including key tributaries, notably the Kakosa and Lubengele Streams.

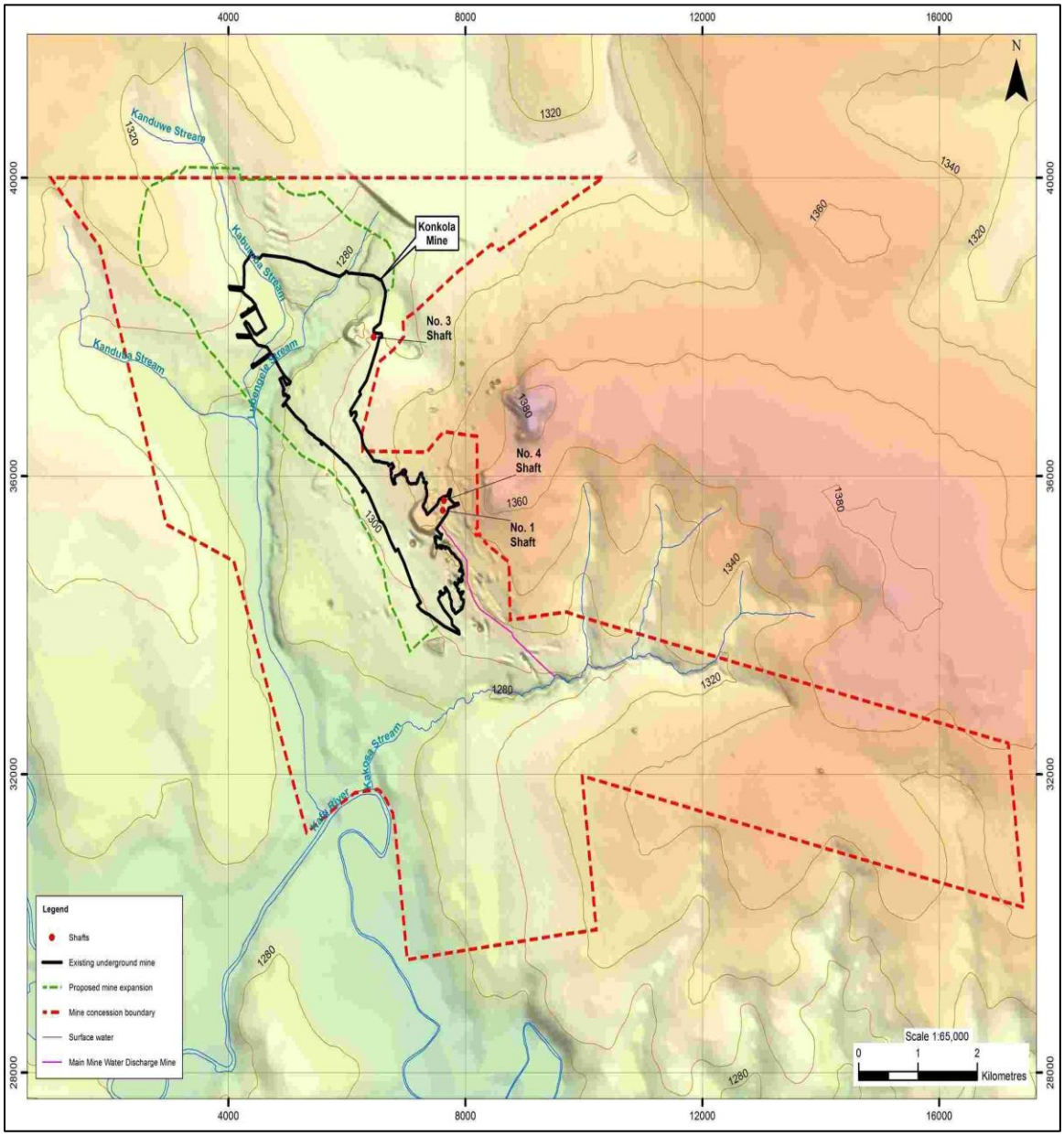


Figure 3-5: Surface topography and drainage at KCM (WSP, 2018).

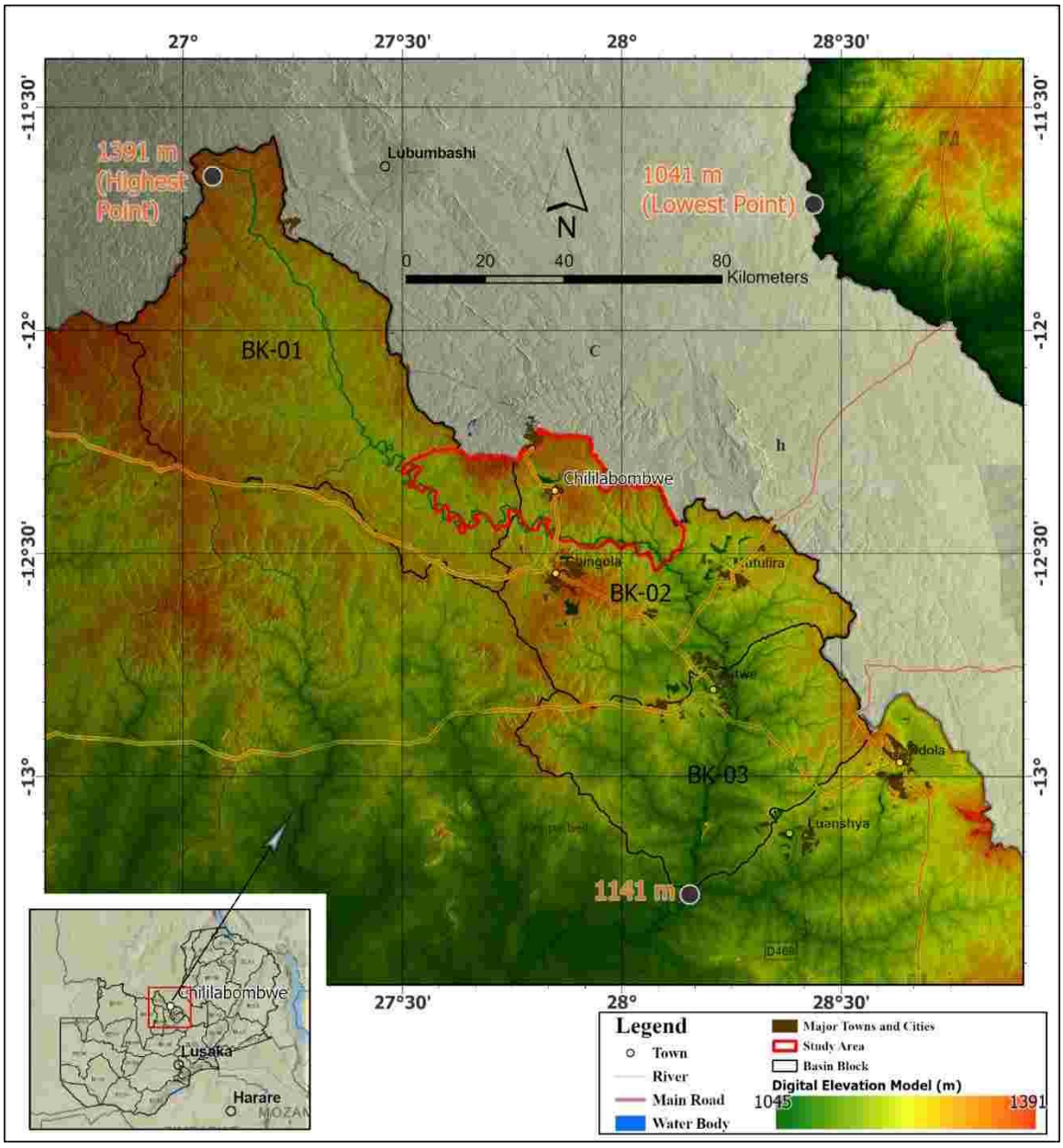


Figure 3-6: Digital Elevation Model (DEM) showing the topography of KCM

3.2.4 Land Use and Land Cover

In the study site, land is predominantly used for subsistence farming, degraded woodland and deforested areas. Within the surface rights, approximately 8% of the land comprises wetlands and tailings facilities.

3.3 Geology of the Zambian Copperbelt

3.3.1 Regional Geology

The Konkola deposit is situated in the Central African Copperbelt, known as one of the largest deposits of sediment-hosted stratiform copper and cobalt globally. This belt includes the Zambian Copperbelt (ZCB), the Congolese Copperbelt (also referred to as the Katangan Copperbelt) found north of the DR Congo-Zambia border, and deposits in Zambia's North-Western Province (Hitzman *et al.*, 2012). The Central African Copperbelt is part of the Lufilian Fold Belt (LFB), as shown in Figure 3-7. This fold structural belt belongs to the Pan-African mobile belts that delineate the Kalahari and Congo Cratons. According to Muchez et al. (2010), the LFB was formed through Neoproterozoic extensional tectonics during the breakup of the supercontinent Rodinia, followed by late Neoproterozoic to early Phanerozoic collision, deformation and metamorphism. The belt is oriented northward, measuring 700 km in length and 150 km in width (Selley *et al.*, 2005). The LFB consists of four distinct zones, each exhibiting unique deformation characteristics. From north to south, these are the External Fold and Thrust Belt, the Domes Region, the Synclinorial Belt and the Katanga High (Cailteux *et al.*, 2005; Selley *et al.*, 2005; Muchez *et al.*, 2010). The Zambian Copperbelt is situated within the Domes Region and is characterised by greenschist and amphibolite facies (Selley *et al.*, 2005).

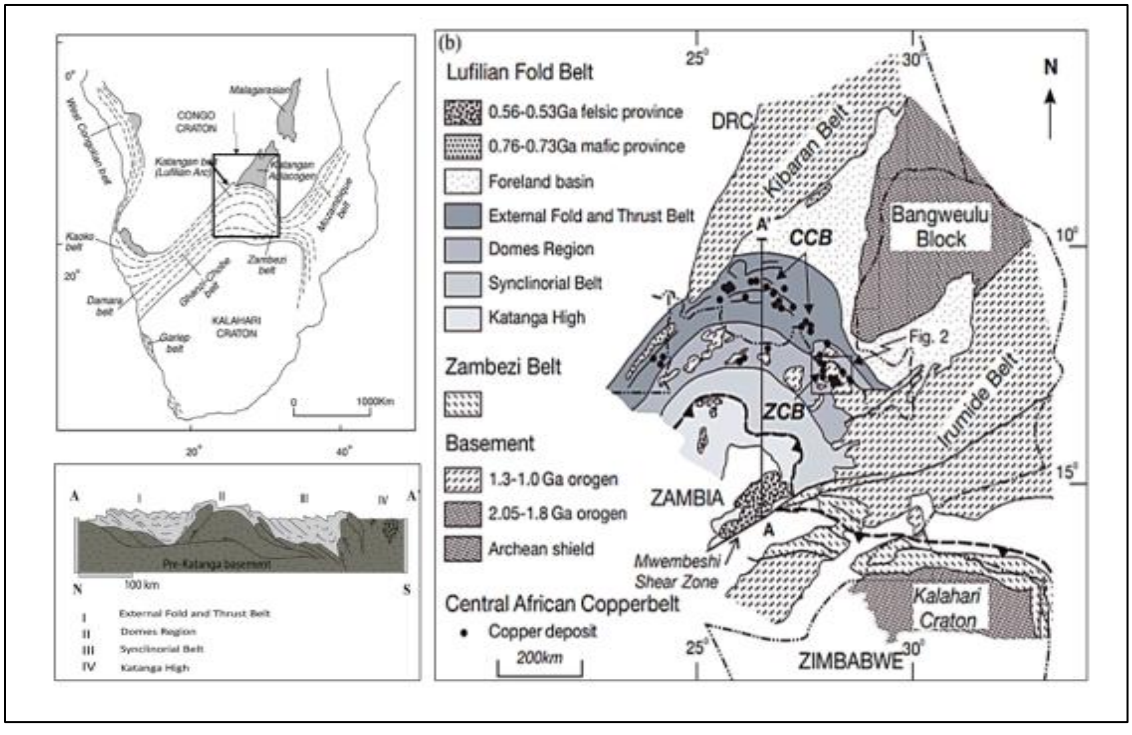


Figure 3-7: Generalised geological maps illustrating the tectonic framework, a cross-sectional profile along line A–A', and the LFB structural features. (Source: Selley *et al.,* 2005).

In the Zambian Copperbelt, three main tectonic events have been identified (Hitzman *et al.*, 2012). Fault-bounded basins were created as a result of rifting along major fault lines during the first phase. The subsequent rifting episode was associated with mafic magmatic activity and occurred during the deposition of the lower Nguba Group and the upper Mwanshya Subgroup. Compressional tectonics, basin reversal, and the appearance of greenschist facies metamorphism were characteristics of the last stage, referred to as the Lufilian Orogeny (Hitzman *et al.*, 2012).

3.3.1.1 Regional Stratigraphy

The stratigraphy of the Zambian Copperbelt is illustrated in Figure 3-8, depicting the Basement Complex overlain by the Katanga Supergroup.

Basement Complex

The Basement Complex consists of Pre-Neoproterozoic metapelites and quartzites belonging to the Muva and Lufubu Supergroups, deposited between approximately 1941 Ma and 1000 Ma (Kampunzu and Cailteux, 1999; De Waele and Mapani, 2002; Selley *et al.*, 2005). It is believed to date back to the Eburnean period (McGowan *et al.*, 2006) and comprises reworked metagranites, migmatites, metavolcanic and metasedimentary units from the Archean to Mesoproterozoic eras, along with relatively weakly reworked metagranites (Selley *et al.*, 2005).

The Katanga Supergroup

The Katanga Supergroup is a sedimentary sequence composed of continental and marine meta-sedimentary rocks, carbonates and mafic igneous rocks, which uncomformably overlie the Basement Complex (Selley *et al.*, 2018). This Supergroup has a thickness ranging from approximately 5 to 10 kilometres, with its earliest deposition dated to around 883 ± 10 million years ago, based on the Nchanga Granite age (Cailteux *et al.*, 2005). Most of the sediments in the Supergroup are derived from the Nchanga Granite and the Paleoproterozoic basement (Cailteux *et al.*, 1994; Twite *et al.*, 2019). The Katanga Supergroup is categorised into the Roan, Nguba and Kundelungu groups, which are distinguished by two regionally correlated glaciogenic diamictites: the Grand Conglomerate and the Petit Conglomerate (Muchez *et al.*, 2010).

The Roan Group, which overlies the basement, forms the lowest stratigraphic unit in the Katanga sequence and is divided into three main subdivisions: the Lower Roan, Upper Roan and Mwashya Group. It consists of siliciclastic, carbonate and plutonic rocks deposited in a continental rift (Porada and Berhorst, 2000). The Lower Roan comprises siliciclastic units formed during the initial syn-rift phase, originating from basement erosion. These consist of tectonically formed conglomerates, quartzite, arkose, and shale (Master *et al.*, 2005). The Upper Roan overlies the Lower Roan and consists of a substantial sequence of carbonates that contains evaporites, which range from stratiform to discordant,

along with mega-clastic breccias. These breccias likely originated from the dissolution of pre-existing evaporite layers following brittle fracturing during the Lufilian Orogeny (Cailteux *et al.*, 2005). Above this unit is the Mwashya Subgroup, comprising platform carbonates, sandstones, dolomitic shales, and carbon-rich shales, as well as being intruded by mafic volcanic rocks that date back around 765 million years, linked to a subsequent extensional phase in the basin (Kampunzu and Cailteux, 1999).

The graciogenic Grand Conglomerate defines the base of the overlying Nguba Group and serves as a regional marker throughout the Central African Copperbelt. The highest preserved unit is the Kundelungu Group, which shares similarities with the Nguba Group and is distinguished by a glacial tillite at its base, referred to as the Petit Grand Conglomerate. The characteristics of the sedimentary rocks in each group suggest that basin expansion occurred due to extensional processes (Cailteux *et al.*, 2005).

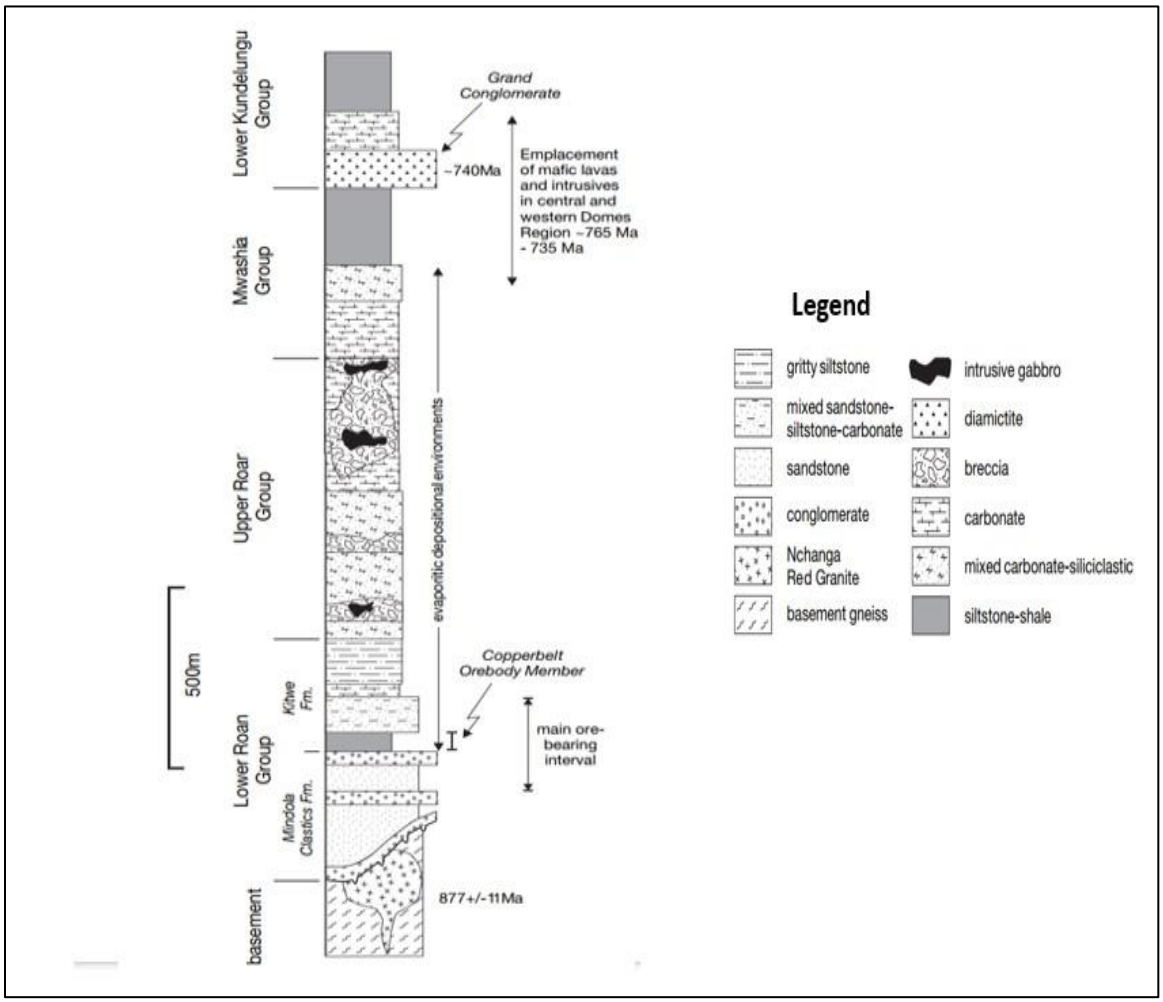


Figure 3-8: Lithostratigraphy of the Katangan Supergroup in the Zambian Copperbelt, showing approximate average strata thicknesses. (Source: Selley et al. (2005).

3.3.2 Konkola Area Local Geology

On the southeastern flank of the Lufilian Arc, the geological framework consists of an alternating pattern of domes and basins. This configuration results from the interplay between Lufilian tectonic activities and the natural contours of the pre-existing underground landscape (Muchez *et al.*, 2010; Hitzman *et al.*, 2012). The formations of the Katanga Supergroup, which are significant for containing copper-cobalt mineral deposits, are distributed across these domes (referred to as 'basement highs') and fill the basins (Bull *et al.*, 2011). Figure 3-9 depicts the geology in the area surrounding the Konkola Mine, which is part of the Katanga Supergroup. These formations are situated on the western flank of the Kafue Anticline and include a Basement Complex at the bottom, which is overlain unconformably by the Roan Group, followed by the Nguba and then the Kundelungu sedimentary successions.

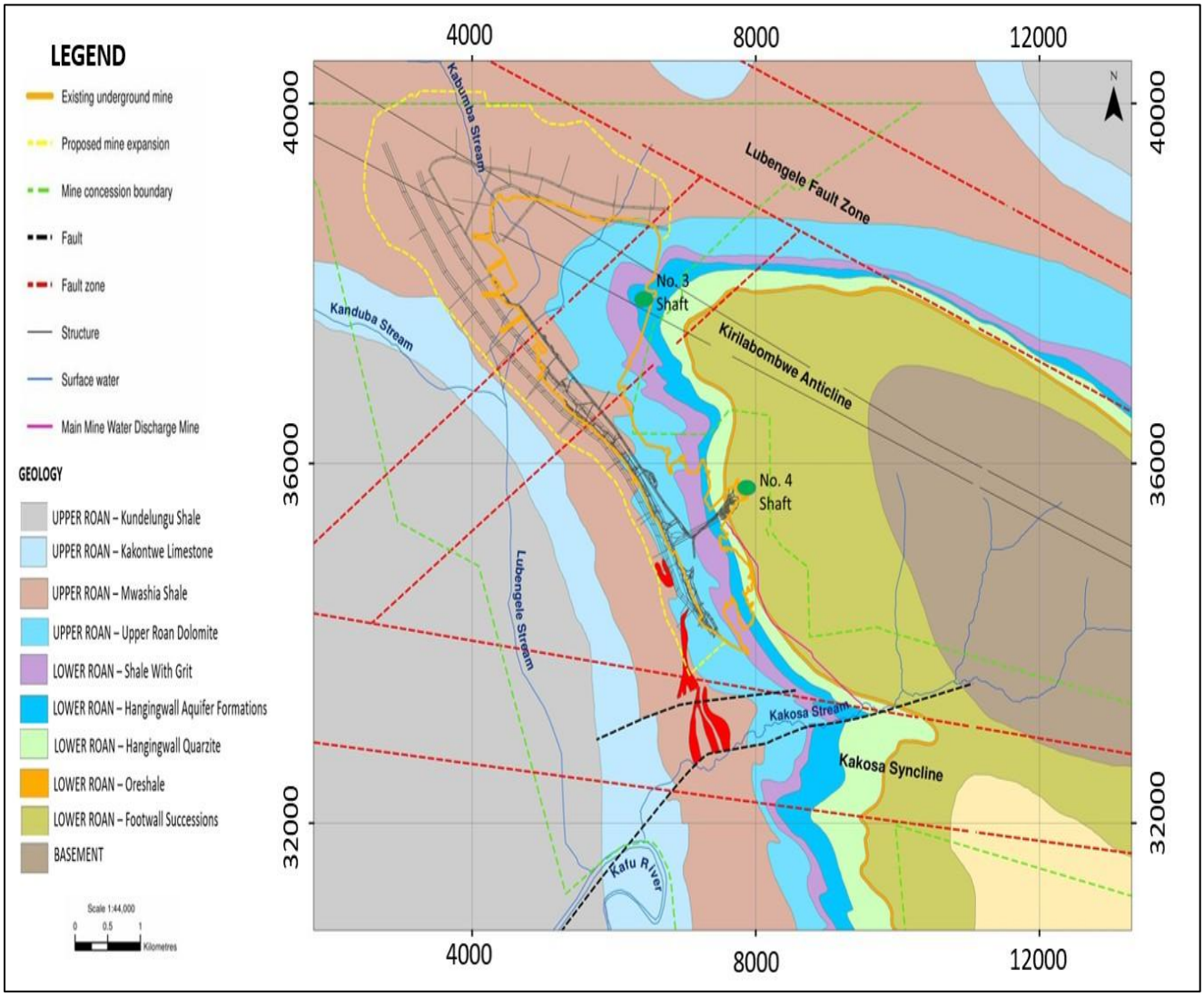


Figure 3-9: Konkola Mine geological map. (modified from WSP, 2018)

3.3.3 Stratigraphy of Konkola Mining Areas

The lithostratigraphy of the Konkola Mining area, including its supergroups, subgroups and formations, is illustrated in Figure 3-11. Additionally, Figure 3-12 features photographs of rock units collected from the field and diamond drill cores. The mine is situated on the western flank of the Kafue Anticline, where the lowest geological unit consists of Basement Complex rocks. The Roan Group unconformably overlain this unit, followed by the Nguba and Kundelungu sedimentary layers.

The Basement Complex

Basement Complex comprises of Proterozoic basement rocks of the Kirilabombwe Dome, which form the core of the Kirilabombwe Anticline. These rocks include granites, gneisses,

schists and quartzites, which have been intruded by the Muliashi Porphyry (Figure 3-10). The Muliashi Porphyry contains large, rounded microcline porphyroblasts that resemble pebbles within a gneissic matrix composed of oligoclase, quartz, biotite, and epidote.



Figure 3-10: Field appearance of the Muliashi Porphyry with rounded microcline porphyroblasts.

Katanga Supergroup

The rocks of the Katanga Supergroup unconformably overlie the basement rocks and have undergone deformation (Torremans et al., 2013). The Katanga Supergroup is made up of the Lower Roan, Upper Roan, and Mwashia Groups, with the Copperbelt ore deposits mostly located within the Lower Roan Group. At the Konkola Mining area, the Lower Roan succession unconformably overlies the basement rocks, with the Boulder Conglomerate as its lowest formation. This formation is a coarse-grained, vuggy conglomerate that is loosely cemented, with boulders composed mainly of quartz.

The Pebble Conglomerate overlies the Boulder Conglomerate and is typically a medium- to coarse-grained conglomerate with interbedded quartzite. In most areas, the upper portion of the Pebble Conglomerate is leached and porous, containing a micaceous or clay-rich matrix. This upper section is known as the Lower Porous Conglomerate (LPC), which is characterised by its coarse texture and poor sorting.

Above the Pebble Conglomerate (PBC) lies the Footwall Quartzite (FWQ), a grey, medium-grained, massive quartzite characterised by cross-bedding and is highly jointed in its lower portions (Figure 3-11 A and B). When combined with the LPC, it forms a major aquifer at Konkola Mine (Mulenga, 1991). Above the FWQ lies the argillaceous sandstone, characterised by a grey colour and a medium-grained texture, with a sequence of interbedded argillites.

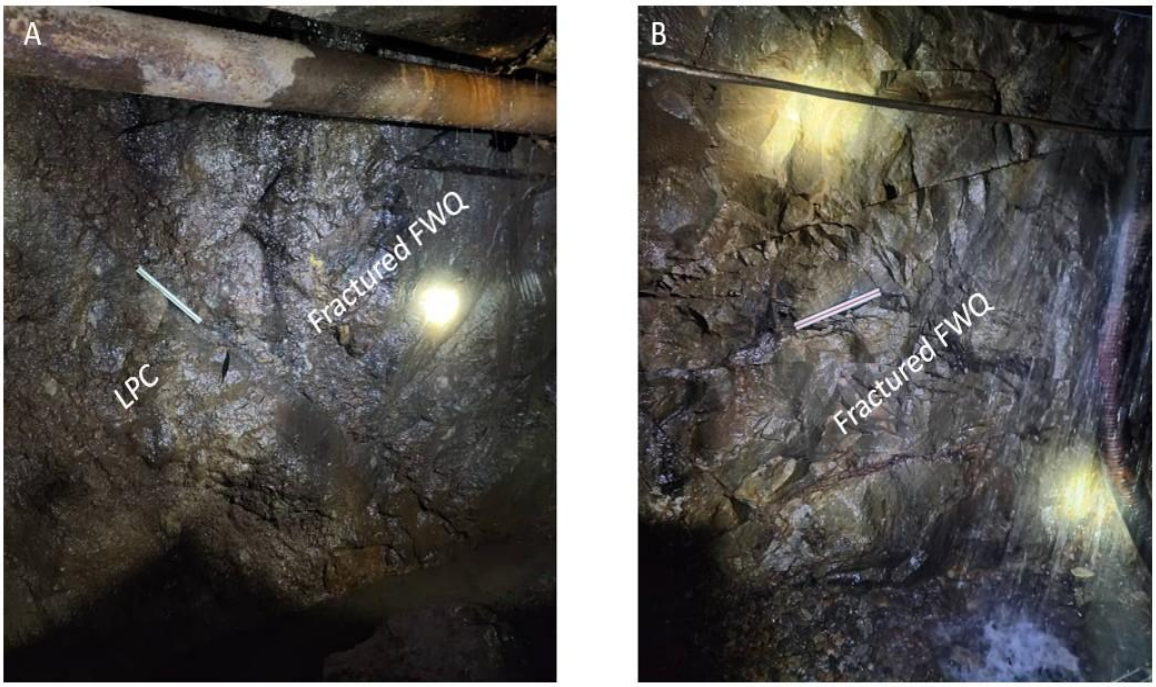


Figure 3-11: Field appearance of the (A) LPC and the (A and B) lower portion of the FWQ, which is highly jointed.

The Footwall Aquifer (FWA), which is the second significant aquifer at KCM, consists of the Porous Conglomerate (PC), Footwall Sandstone (FWSST) and Footwall Conglomerate (FWC)(Mulenga, 1991). It overlies the FWQ. Both the FWSST and the PC are characterised by pebbles composed of quartzite, feldspar and granite, embedded within a micaceous or clay matrix. However, the Footwall Conglomerate lacks continuity and has weak cementation. These two conglomerates sandwich the Footwall Sandstone, which is distinguished by its medium-grained, feldspathic sandstone composition (Mulenga, 1991).

The Ore Shale Unit (OSU), also known as the Copperbelt Orebody Member, sits on top of the FWA (Sillitoe *et al.*, 2017). It consists of dark grey, finely laminated siltstone with irregularly occurring calcareous arenite horizons and common dolomite lenticels. Overlying the OSU is the Hangingwall Quartzite (HWQ), while the Hangingwall Aquifer (HWA) and the Shale with Grit (SWG) make up the remaining portion of the Lower Roan Group(Mulonda, 2023). The third major aquifer at Konkola, the HWA, occurs at a stratigraphic depth ranging from approximately 35 m to 180 m (Konkola Copper Mines, 2010).

The Upper Roan Group primarily consists of evaporatic and dolomitic rocks, such as gypsum and anhydrite, alongside a minor presence of siliciclastic rocks. It is succeeded by the Mwanshya Group, which lies atop the Upper Roan Dolomite (URD). Following the Mwanshya Group, a distinct diamictite known as the Grand Conglomerate serves as a key stratigraphic marker. The Kakontwe Limestone Formation is the most recent geological layer above the Grand Conglomerate (Mulonda, 2023).

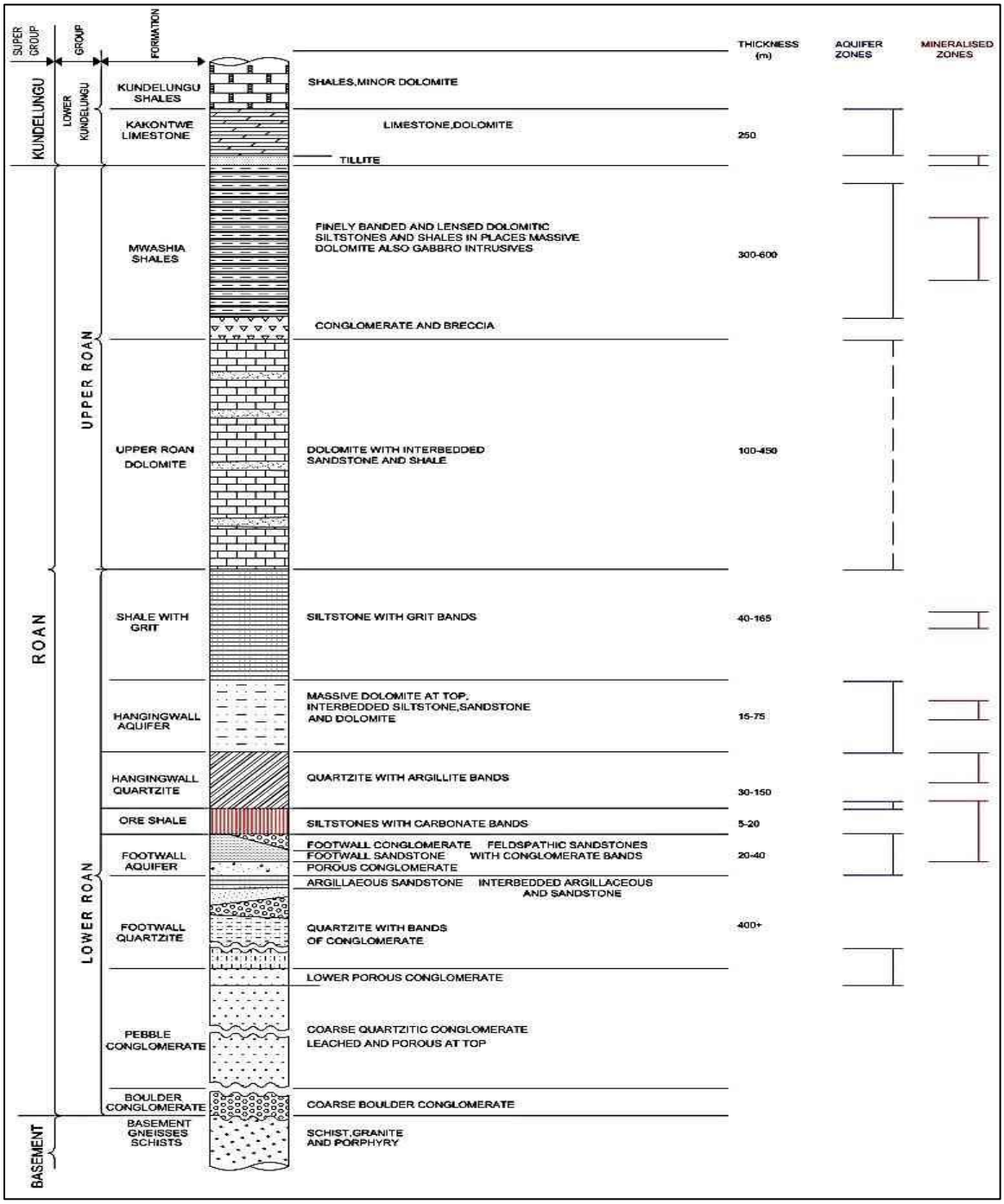


Figure 3-12: General stratigraphic column of the Konkola Mine (Konkola Copper Mines, 2010).



Figure 3-13: Photographs of rock units from the field and diamond drill cores.

3.3.4 Structural setting

The Kirilabombwe Anticline, which encircles the Konkola ore deposit, is the main structural feature of the Konkola Mining site (Torremans *et al.*, 2013). This anticline marks the northwestern end of the Kafue Anticline, the primary regional structure of the Zambian Copperbelt (Mulenga, 1991). According to Torremans *et al.* (2013), the Kirilabombwe Anticline is a tight, upright fold with a subvertical axial plane, an interlimb angle of 35° to 45° and a northwest plunge of 10° to 15°. It has a fold axis striking at N75W, as evidenced by analysed boreholes along the anticline axis and in situ measurements (Figure 3-11). The Kirilabombwe Fault, a distinct fault zone, runs parallel to the axial plane of the anticline. Geological structures such as fault zones, joints and fissures act as fluid pathways between shallow and deep geological environments, while also serving as effective barriers that restrict fluid flow (Bense *et al.*, 2013).

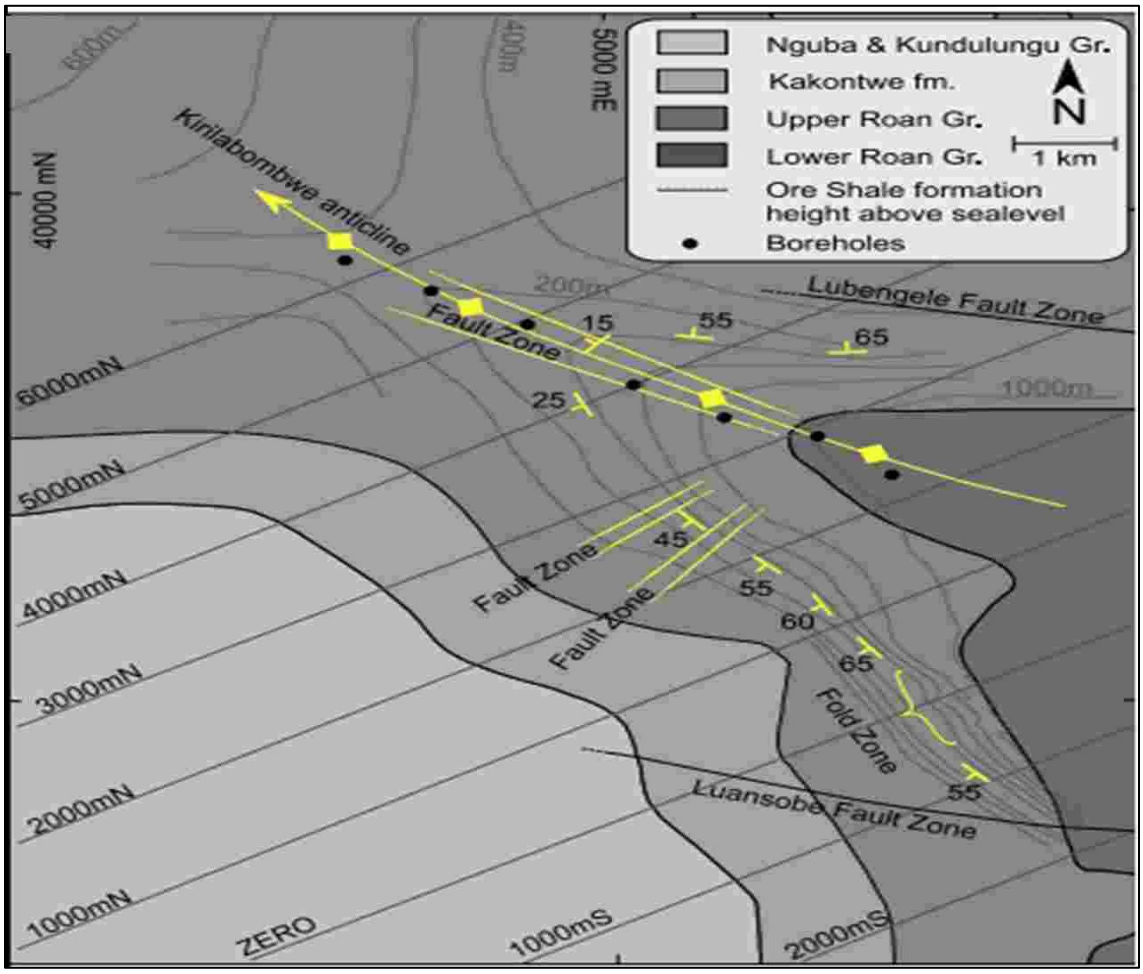


Figure 3-14: Structural map of Konkola Mine depicting the Kirilabombwe anticline surface outline (Torremans *et al.*, 2013).

The Konkola Mine area is sandwiched between two major fault zones, as shown in Figure 3-10. The Lubengele Fault Zone, located to the north, consists of faults dipping 79° to the south, while the Luansobe Fault Zone, in the south, consists of faults dipping 82° to the north (Mulenga, 1991a; Selley *et al.*, 2005). The Cross Axis and the Kirilabombwe Axis Faults are positioned between these two mentioned faults. Together, these structures create a conjugate shear system that is primarily characterised by lateral displacement.

The primary joints trend almost parallel to the Anticline axis at N135° (Mulenga, 1991). Similarly, the minor joints, oriented at N045°, run parallel to the axis of the Cross Axis Fault. These fractures are predominantly open, providing ideal pathways for fluid movement across different geological formations (Mulenga, 1991). When these joints are not open, they are typically filled with materials such as clay, specularite, carbonates, vein quartz and secondary copper minerals, representing typical tension joints.

3.5 Hydrogeology

Konkola Mine is located within the Lubengele Catchment, with a minor southern section drained by the Kakosa Stream. The total catchment area spans 187 km^2, receiving between 1,100 mm and 1,600 mm of rainfall annually, with an average yearly evaporation of 1,762 mm (Straskraba *et al.*, 1991). The streams in the area generally flow towards the south. The Lugengele Stream, along with its tributaries, the Mingomba and Kakosa Streams, are perennial watercourses in the region. The Lubengele and Kakosa Streams are significant tributaries of the Kafue River, which manages the mine's surface drainage and is recognised as Zambia's second largest river (Mulenga, 1991).

The mine area's hydrogeological characteristics are highly complex. The Konkola deposit is located between two aquifers on the hanging wall side and two on the Footwall side (Mulenga, 1991). These aquifers are identified as the FWQ/ LPC aquifer and FWA, both located below the ore body, as well as the HWA and the Kakontwe Limestone Aquifer, both positioned above it (refer to Table 3-1). The FWA primarily consists of siliciclastic rocks, whereas the HWA is predominantly characterised by carbonate-rich rocks (Mulenga and De Freitas, 1991).

Table 3-2: Konkola Mine Hydrostratigraphic column (Advisian WorleyParsons Group, 2017).

Hydrostratigraphic Column of Konkola Mine					
Super Group	Group	Formation	Lithology	Thickness (m)	Aquifer Zones
Kundelungu	Lower Kundelungu	Kundelungu Shales [KUS]	Shales, minor dolomite	Unknown	Aquitard semipervious
		Kakontwe Limestone [KAL]	Limestone, dolomite with tillite at the contact with underlying Mwasha Shales.	250	Major aquifer
Roan	Upper Roan	Mwasha Shales [MW]	Finely banded and lensed dolomitic siltstones and shales, in place massive dolomite, also gabbro intrusive. Conglomerate and breccia at the base at the interface with the URD.	300-600	Aquitard semipervious
		Upper Roan Dolomite [URD]	Dolomite with interbedded sandstone and shale.	100-450	Major aquifer
	Lower Roan	Shale with Grit [SWG]	Siltstone with grit bands.	40-165	Major aquifer at the contact with the underlying HWA
		Hangingwall Aquifer [HWA]	Interbedded siltstone, sandstone and dolomite. Massive dolomite at the top.	15-75	Major aquifer at the interface with the overlying Shale with Grit
		Hangingwall Quartzite [HWQ]	Quartzite with argillite bands. Occasionally wet and fractured at the base.	30-150	Aquitard semipervious
		Ore Shale [OS]	Siltstone with carbonate bands.	~5-20	Aquitard semipervious
		Footwall Aquifer [FWA]	Feldspathic sandstone with conglomerate bands (Footwall Conglomerate, Footwall Sandstone, and Porous Conglomerate)	20-40	Major aquifer
		Footwall Quartzite [FWQ]	Quartzite bands & argillaceous sandstone at the contact with Footwall Aquifer. Highly fractured, jointed and extremely wet at the base.	>400	Aquitard semipervious
		Pebble Conglomerate LPC PBC	Leached and porous at top at the contact with Footwall Quartzite, LPC and coarse quartzitic conglomerate and impermeable at the base, PBC.	>300 (125m in #3 (50m LPC and 75m in PC))	LPC and fractured base section of the overlying FWQ (together approx. 150m thick) are major aquifer zone.
		Boulder Conglomerate	Coarse boulder conglomerate.	Unknown	Aquiclude
Basement		Basement Gneisses, Schists	Schist, granite and porphyry.	Unknown	Aquiclude

3.5.1 Aquifers

The study area's groundwater occurrence can be classified into three distinct aquifers (Straskraba *et al.*, 1991). Although the URD and the Kakontwe Limestone, which are located in the Hangingwall, are also considered main aquifers, they are lithologically separated by an aquiclude (SWG) (Mulenga, 1991). The aquifers at Konkola Mine exhibit a combination of primary (intergranular) and secondary (fracture) permeability. The three distinct aquifers are described below:

Lower Porous Conglomerate aquifer (LPC)

This aquifer is approximately 150 metres thick and comprises the LPC and FWQ (lower part). The LPC is leached and porous, with a micaceous or clay matrix, and water is primarily confined to the vugs. In contrast, the base of the FWQ is extensively fissure-controlled and jointed, leading to the formation of secondary fissures.

According to Mulenga (1991), two significant incidents have been recorded involving open fissures. The first incident occurred in 1976 at the 390 mL at No. 3 Shaft, where water with a flow rate of 60,000 m^3/day and a pressure of 11 bars was encountered during the development of the main haulage. The fissure continued to discharge water at an average rate of 30,000 m^3/day until it finally stopped in 1983, seven years later. The second incident took place in 1982 at the 880 mL at Shaft Number 1. A pilot borehole of 72-mm diameter, drilled from the Drain Crosscut into the LPC, encountered water at a flow rate of 11,300 m^3/day and a pressure of 37 bars (370 kN/m^2). Mining operations were temporarily suspended for several days until the borehole was successfully sealed with grout.

Footwall aquifer (FWA)

The FWA is located immediately below the orebody and is the second major aquifer in the succession. This unit comprises a sequence of conglomerate and sandstone lithologies, which include the PC, FWSST, and FWC. The thickness of the FWA ranges from approximately 20 to 40 metres (Mulenga, 1991).

The FWSST consists of sandstone that is medium to coarse in grain size, containing layers of conglomerate and argillite, sandwiched between two conglomerates. These conglomerates are lithologically similar and are characterised by quartzite, feldspar, and granite pebbles embedded within a matrix of clay or mica. Groundwater inflows in the FWA are both stratigraphically controlled and associated with faults and zones of extensive fissures (Mulenga, 1991).

Hangingwall aquifer (HWA)

The HWA aquifer is located above the orebody, primarily in the upper section of the HWQ, as well as in the overlying SWG and URD formations. Under pristine conditions, this aquifer is well separated from the orebody and the underlying FWA as well as from the overlying URD aquifer. However, the collapse of open stopes induced by mining activities has created a hydraulic connection between this aquifer, the mine workings, the Ore Shale and the underlying FWA. The HWA poses significant water inflow challenges at the mine due to its proximity to and position above the orebody (Straskraba *et al.*, 1991).

3.5.2 Aquicludes

The three significant aquicludes at Konkola Mine include the Argillaceous Sandstone (AGSST), the unfractured sections of FWQ, Mwashia Shale and HWQ. However, the presence of joints, fractures and fissures resulting from both natural faulting and mine-induced blasting creates hydraulic connections across these aquicludes (Mulenga, 1991). Thus, they can be described as aquitards.

Figure 3-15 illustrates the 760m plan for the Konkola flats area, where sampling points for the fractured aquifer were done. Boreholes DVN 1615 (for sample KON 08) and BPN 898 (for water sample KON 09) are shown in Figure 3-15. A section was created to highlight the structures along BPN 898, with Figure 3-16 presenting the cross-section that shows the identified structures.

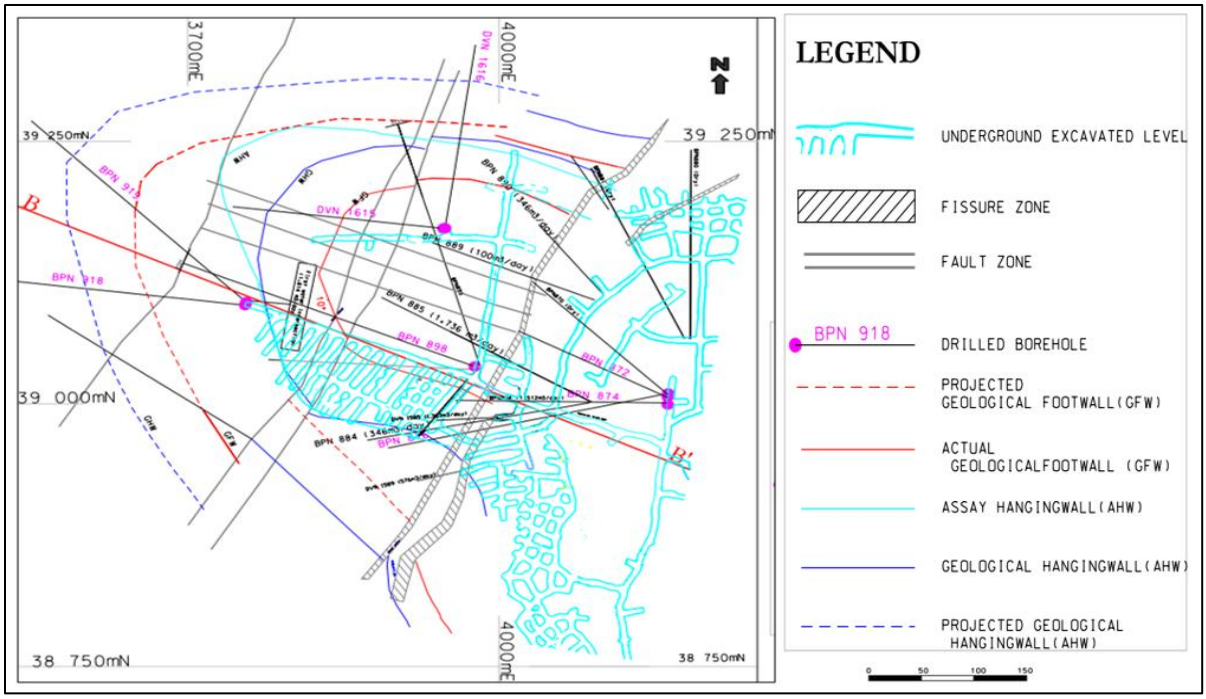


Figure 3-15: 760m level plan of the Konkola Flats area showing plotted diamond drill holes and West to East section line BB'.

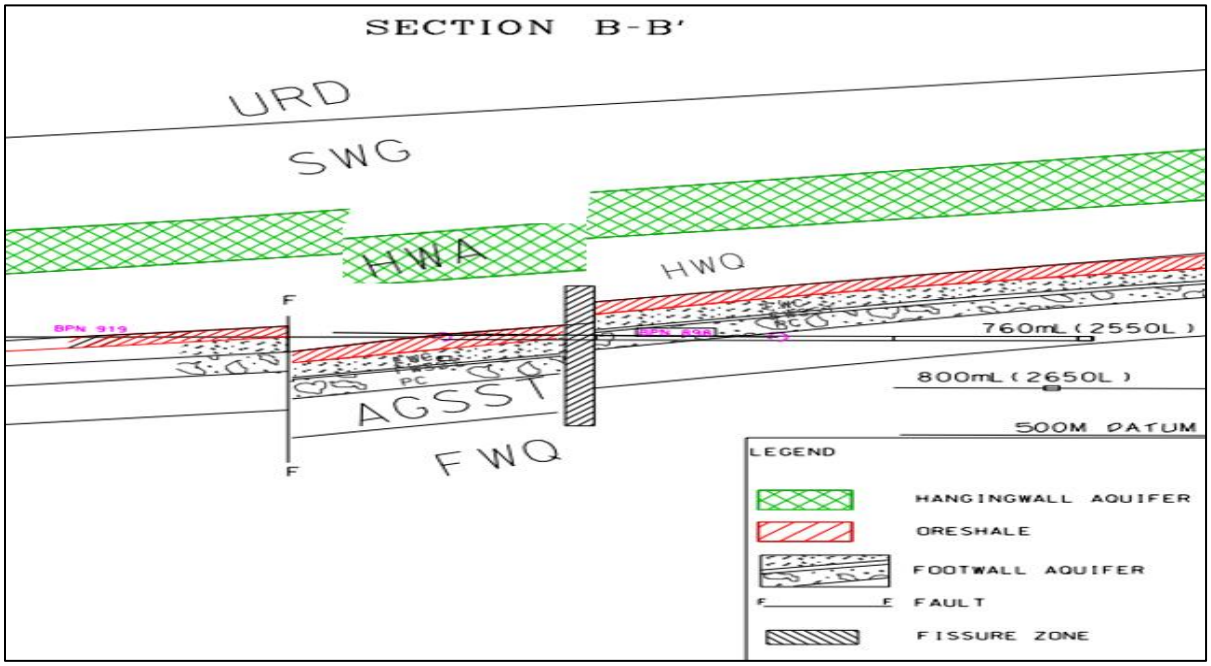


Figure 3-16: A West (B) to East (B') cross-section parallel to KON 09 (BPN 898) sampling point showing mapped geological structures.

4. METHODOLOGY

Several hydrogeological methods were employed in this research to improve the comprehension of the Konkola Mine area's hydrogeological system. These approaches included verbal communication with both surface and underground mineworkers, hydrogeological and geological mapping, sample collection, and desktop studies. During the desktop research, maps were analysed, mine related literature was reviewed, and hydrochemical differences in the collected samples were modelled using computer software.

4.1 Desktop investigations

The initial phase of the investigation focused on reviewing existing literature regarding the hydrogeology and geology of the Konkola Mine and its adjacent areas. Additionally, surface and underground survey data, mine plans, hydrological maps, aerial images, rainfall data and hydrogeological assessments conducted by consultants at KCM were reviewed. Software was utilised to develop a structural model of the ore deposit and underground plans, particularly in areas where sampling was conducted.

The locality map of Chililabombwe (KCM), shown in Figure 3-1, and the digital elevation model (DEM) of the study area, depicted in Figure 3-6, were generated using ArcMap (version 10.6.1). These maps highlight key features, including significant faults and geological structures present in the study area.

MicroStation V8i is a CAD software platform used for 2D and 3D design, generating graphics from various elements and objects. In this project, it was utilised to create both surface and underground 2D plans, highlighting the locations of sampling points. Additionally, it was used to generate the geological map shown in Figure 3-5 and the mining plan depicted in Figure 3-2. This information helps in understanding the positioning of sampling points and the stratigraphy of the study area.

GEOVIA Surpac 6.7.4, a 3D software, was used to generate three dimensional geological structures, providing a comprehensive overview of the mine's structures and potential water conduits.

AquaChem 3.70 software was used to represent hydrochemical data on Piper and Expanded Durov diagrams.

Stiff diagrams plots were generated using a web-based Hydrochemical Analysis Tool (https://https://aquifer.hatarilabs.com/hatari/p3y7qlgzd0/gallery; accessed December 10th, 2024). Excel was employed for plotting stable isotope results and correlation diagrams. This survey helped understand the area's hydrological conditions, identify the main water facies, pinpoint potential groundwater sources in the subsurface and determine the most effective method to trace the water flow.

4.2 Fieldwork

The field methodology involved various data collection efforts aimed at verifying the findings from desktop investigations, particularly concerning the hydrogeology and geology of the region. The stages of these field investigation activities are as follows:

4.2.1 Geological survey

A detailed geological survey was carried out to characterise the rocks and structural features in the study area. A distometer was utilised for measuring distances, while a geological compass was used to take structural readings during fieldwork.. The structural parameters recorded included strike, dip direction, dip angle, and the overall trend of the structures that were examined. Field data, along with information gathered from desktop studies, were utilised to create a geological cross-section that provides a clearer understanding of the stratigraphic sequence of the rocks. The data collected from the mapping was used to update the 3D geological surfaces in Surpac.

4.2.2 Core logging

This activity entailed a thorough examination and assessment of recently drilled boreholes within the Konkola Flats area at KCM. According to Read and Beale (2013), diamond drilling is a dependable technique for collecting geological data, which is essential for determining the main hydrostratigraphic units. The analysis focused on boreholes that intersected fractured aquifers, supplemented by geological mapping to understand underground water flow. During this research, a total of eight boreholes were drilled in the Konkola flats area (see Table 4-1). Out of these, two boreholes (BPN 898 and BPN 891) were logged and plotted on 2D plans using Microstation software. Additionally, water samples collected from borehole BPN 898 underwent hydrochemical analysis, as well as ESI and tritium analyses.

Table 4-1: Drilled diamond drill boreholes in the Konkola Flats area at KCM.

SN		COLLAR			SURVEY		DEPTH
	HOLE ID	Northing (m)	Easting (m)	Collar Elevation (masl)	Azimuth (˚)	Inclination (˚)	(m)
1	DVN1615	39154	4014	610	277	87	195
2	DVN1616	39156	3955	609	192	36	186
3	BPN898	39036	3981	606	293	1	254
4	BPN872	39007	4135	607	297	13	111
5	BPN874	38999	4136	606	272	8	170
6	BPN876	39010	4136	606	257	7	230
7	BPN918	39094	3796	607	277	1	200
8	BPN919	39097	3797	607	315	1	250

4.2.3 Hydrogeological Investigations

The hydrogeological field-based investigation employed a sampling technique to choose suitable personnel based on their competence and expertise for both surface and underground operations. Moriarty (2011) describes quota sampling as a form of purposive sampling in which the researcher specifies the number of participants to be included during the research design stage. The researcher applied knowledge gained from the coursework in Geol7022 (Hydrogeochemistry) and Geol7023 (Environmental Isotopes) regarding sample handling to educate participants on the necessary precautions for collecting and handling water samples.

The non-probability sampling method known as convenience sampling was employed for the underground sampling. According to Etikan et al. (2016), convenience sampling, also referred to as haphazard or accidental sampling, is a type of non-random sampling where individuals from the target population are selected based on practical criteria such as ease of accessibility, geographical proximity, availability at a particular time or willingness to participate. The underground sampling sites in the fractured zone were chosen based on known and mapped fracture zones within the Konkola Flats area and nearby regions, as clearly defined by existing underground plans (see Figure 4-3).

4.2.4 Water Sampling

A total of 10 water samples were collected from both underground and surface areas across the mine. During field sampling, various water quality parameters, including water temperature, pH, EC and TDS, were analysed. This was done to ensure precise measurement of the physical and chemical characteristics that reflect the water sources. Measurements were conducted using the YSI 556 Multi-Probe System, with the instruments calibrated each morning prior to measurement using a buffer solution, following the manufacturer's guidelines. The samples were identified with the labels KON 01 through KON 10. The water samples were sent to Alfred H Knight in Kitwe, Zambia, for chemical testing. Stable isotope testing was conducted at the Hydrogeology Laboratory at the University of the Witwatersrand's School of Geosciences. Additionally, tritium assessments for seven of these samples were carried out at the iThemba Laboratory in Johannesburg.. Table 4-2 outlines the sampling point locations and describes the physical characteristics of the samples.

.

4.3 Laboratory analyses

4.3.1 Analytical Description and Preservation

To maintain the integrity of the samples, the bottles were rinsed with deionised water supplied by the laboratory prior to sampling. Sampling was carried out in a way that accurately represents the in-situ conditions of the aquifers. Each sampling location was mapped and photographed for documentation. Additionally, to ensure quality assurance standards, one of the sampling locations was duplicated (KON 02 and KON 03 were taken from the same location).

4.3.1.1 Hydrochemistry (Major Ion) Analyses

A total of 10 samples were collected from both groundwater and surface water sources for hydrochemical analysis. The water samples were collected in 2L polyethylene bottles provided by the laboratory (Alfred H Knight). The samples were then properly labelled with their physical appearance noted. They were stored in a cool, dark environment and delivered to Alfred H Knight in Kitwe, Copperbelt Province, Zambia.

The water samples were analysed for major ions – Ca^{2+}, Mg^{2+}, Na^{+}, K^{+}, Cl^{-} and SO_4^{2-}. These parameters were measured using an Inductively Coupled Plasma Optical Emission Spectrometer (ICP-OES). Additionally, field measurements of physico-chemical parameters, including pH, EC, temperature (°C) and TDS, were conducted using a YSI 556 Multi-Probe System.

4.3.1.2 ESI analyses

Ten ESI (^{18}O and ^{2}H) water samples were collected in 10 mL glass bottles from both surface and underground sources. To prevent fractionation due to sunlight, the samples were stored in a dark, cool room. Of these, seven samples were collected from underground sources, while three were collected from surface rivers and streams. The samples were analysed using the Liquid Water Isotope Analyzer (LWIA) model 45-EP laser equipment in the Hydrogeology Lab at the University of the Witwatersrand. The LWIA comprises a laser analysis device, an internal computer, a liquid auto-sampler, a compact membrane vacuum pump and a room air intake line that directs air through a diorite column for moisture removal (Abiye *et al.*, 2018). ESIs of hydrogen and oxygen serve as valuable instruments for determining the origin or source of the water, facilitated by using an MWL. In this study, the local meteoric water line (LMWL) for Ndola Station ($\delta^2H = 7.63\delta^{18}O+9.14‰$), which is the only dataset from Zambia available in the International Atomic Energy Agency (IAEA) database and the GMWL ($\delta^2H = 7.91\ \delta^{18}0 + 8.72‰$, Terzer *et al.*, 2013) were used to interpret the findings.

4.3.1.3 Tritium

Seven tritium water samples were collected in 500-mL polyethylene plastic bottles from underground areas, excluding three surface water samples (KON 05, KON 06 and KON 07). The sample bottles were treated with 10 mL of HCl and rinsed with distilled water before sampling. To minimise air contact, the bottles were completely filled with water and kept in a cooler box prior to being delivered to iThemba LABS in Johannesburg, South Africa, for analysis. Tritium plays an essential role in the relative dating of water, as it provides information on how long groundwater has been beneath the surface. This is particularly relevant for groundwater samples, as groundwater is isolated from the atmosphere, where tritium is generated (Mohuba, 2020). The average residence times were calculated using Equation 4 from Clark and Fritz (1997)

$$t = -17.93 \ln (a_t{}^3H / a_0{}^3H) \qquad \text{(Equation 4)}$$

Where:

t = Average residence time in years

$a_t{}^3H$ = Remaining activity after decay over time.

$a_0{}^3H$ = The first Tritium activity

4.3 Data Presentation

4.3.1 Water Chemistry

Piper, Durov and Stiff diagrams were used to plot major ion data in order to identify the predominant ions present in water and their relationships. According to Li et al. (2014), trilinear Piper diagrams are commonly used to classify the hydrochemical characteristics of a dataset. This analysis helps to determine the sources of these ions and the processes contributing to their presence. Additionally, the diagrams provide insight into various processes influencing the hydrochemical properties of water, including the mixing of different water sources (Mohuba, 2020). The Piper diagram graphically displays multiple water samples to facilitate the analysis of their hydrogeochemical properties (Guan *et al.*, 2019). In contrast, the STIFF diagram visually represents the ratios of major ionic components in water, expressed in milliequivalents per litre (meq/L) or equivalents per million (e.p.m) (Freeze and Cherry, 1979). This diagram effectively illustrates the distribution of cations and anions, facilitating the identification of dominant cations and anions in various samples (Singhal and Gupta, 1999). Furthermore, STIFF diagrams aid in

investigating potential sources of these ions, enhancing the understanding of sample chemistry and possible underground inflow sources.

The Durov diagram is a trilinear graphic that displays the concentrations of important cations and anions as percentage milliequivalents across two distinct triangles. The triangles converge at a central square, symbolising the general chemical characteristics of the samples (Freeze and Cherry, 1979). This illustration offers valuable insights into various water types and hydrochemical processes like ion exchange, basic dissolution, and the mixing of waters from various sources.

4.3.2 Stable isotope

In this study, a plot of $\delta^{2}H$ against $\delta^{18}O$, along with a Local Meteoric Water Line (LMWL) and the Global Meteoric Water Line (GMWL), was employed to investigate the origin of water samples collected from fractured aquifers at the KCM area to determine their relationship to the local groundwater. The study employed the Ndola Local Meteoric Water Line (NMWL). The LMWL represents the correlation between the isotopes of hydrogen ($\delta^{2}H$) and oxygen ($\delta^{18}O$) in rainwater. This relationship provides a framework for assessing the relative enrichment or depletion of isotopic composition in the collected water samples (Abiye *et al.*, 2015). Various processes, including water-rock interactions (affecting oxygen only), hydrogen sulphide exchange reactions (affecting hydrogen only) as well as condensation and evaporation, can lead to deviations from the LMWL.

ESI data can be effectively analysed by referencing the meteoric line, which is based on extensive historical records of stable isotope data from precipitation in areas that share comparable climate, geography, and location (Mengistu *et al.*, 2015).

4.3.3 Tritium

Tritium is a radioactive hydrogen isotope used to determine the effective age of water, both before and after 1957, which marks the beginning of hydrogen bomb testing. The average residence times of groundwater are estimated using Equation 4 in this study, assuming a tritium half-life of 12.43 years (Clark and Fritz, 1997; Mazor, 2003).

The current study integrates hydrochemical analysis, ESI techniques and tritium tracer methods to investigate the origin and flow paths of water in aquifers at KCM. The findings aim to inform the development of effective strategies for sustainable groundwater resource management.

5. RESULTS AND DISCUSSION

In this study, a total of 10 water samples were collected from various locations at the Konkola Mine, covering both underground and underground water sources. For the underground samples, four were collected from dewatering boreholes, two from exploration holes and one from the extraction drive. For surface sampling, there was one sample collected from the Kafue River and two from its tributaries, specifically the Lubengele Stream and the Kakosa Stream. Table 5-1 outlines the sampling point locations and describes the physical characteristics of the samples and Table 5-2 shows the surface and groundwater hydrochemical analyses of samples at KCM.

Table 5-1: Surface and underground sampling points and physical appearance of the samples

Sample ID	Water Source	Site	Physical Appearance
KON-01	Groundwater	950mL 3800mN Dewatering Crosscut	Clear Water
KON-02	Groundwater	950mL 3350mN Dewatering Crosscut	Clear Water
KON-03	Groundwater	950mL 3350mN Dewatering Crosscut	Clear Water
KON-04	Groundwater	940mL 10mN Dewatering drive	Clear Water
KON-05	Surface Water	KAFUE RIVER	Clear Water
KON-06	Surface Water	LUBENGELE STREAM	Cloudy
KON-07	Surface Water	KAKOSA STREAM	Cloudy
KON-08	Groundwater	760mL 5000mN Extraction Drive-South	Clear Water
KON-09	Groundwater	760mL 4800mN Extraction Drive	Clear Water
KON-10	Groundwater	760mL 2200mW Access Crosscut	Clear Water

Table 5-2: Surface and groundwater hydrochemical analyses of samples at KCM.

Sample ID		KON-01	KON-02	KON-03	KON-04	KON-05	KON-06	KON-07	KON-08	KON-09	KON-10
	Units										

pH		7.28	7.22	7.39	6.92	7.44	6.81	7.32	6.88	7.21	6.83
Temp	°C	26.06	26.25	26.73	26.82	27.33	21.80	22.70	25.61	25.57	27.97
TDS	mg/L	521	590	540	170	301	540	190	420	440	480
EC	µS/cm	815	859	858.0	285.0	483	761	286	650	678	769
HCO3	mg/L	281.2	275.0	256.2	106.2	187.5	262.5	116.7	252.1	229.2	245.8
Calcium	mg/L	65.8	75.1	69.3	24.1	27.5	71.3	17.0	56.5	56.5	65.0
Magnesium	mg/L	30.40	31.06	31.16	6.56	18.86	27.20	5.37	23.94	26.19	26.23
Sodium	mg/L	4.7	5.7	5.7	7.0	1.5	14.7	6.7	8.3	8.1	5.8
Potassium	mg/L	7.1	6.9	6.9	7.0	1.5	14.7	6.7	8.3	8.1	7.9
Sulphate	mg/L	109	131	132	33	12	142	29	76	76	100
Chloride	mg/L	4.5	3.0	6.9	5.5	15.4	7.4	11.4	3	4	4.0

5.1. Physicochemical and Hydrochemistry

5.1.1 Temperature (°C)

The measured groundwater temperatures range from 25.57°C to 27.97°C, with an average of 26.43°C. The surface water temperature ranges from 21.8°C to 27.33°C, with an average of 23.94°C. The FWA aquifer water (27.97°C) is warmer than the HWA aquifer water (average 26.35°C). The relatively low groundwater temperatures in the fractured aquifers could be associated with the mixing of FWA and HWA aquifer water, as stated by Mulenga (1991). Moreover, fault zones and fractured zones act as significant pathways for water to flow into the mine (Mulenga, 1991).

5.1.2 pH (Hydrogen ion activity)

The slightly acidic surface waters (KON 06) could be attributed to tailings from the nearby Lubengele Tailings Dam. This result is further supported by the high sulphate content observed. The sampling sites from the HWA aquifer (i.e. KON 01, KON 02 and KON 03) match natural waters' pH (Table 5-1). The pH of the FWA and LPC waters is slightly lower compared to that of the HWA water, which could be due to their different origins.

5.1.3 Total dissolved solids (TDS)

The measured TDS values ranged from 170 mg/L to 590 mg/L, with an average of 419.2 mg/L. Therefore, based on the classification scheme by Freeze and Cherry (1979), the water in the study area is primarily classified as freshwater (Table 5-2).

Table 5-3: Simple classification of groundwater based on TDS content, modified after Freeze and Cherry (1979).

Category	Category TDS (mg L-1)
Freshwater	Freshwater 0–1000
Brackish water	Brackish water 1000–10000
Saline water (seawater)	Saline water (seawater) 10000–100000 (35000)
Brine water	Brine water >100000

5.1.4 Electrical conductivity (EC)

Similar to TDS, EC is a measure of the amount of dissolved ions in water, which enhances its ability to conduct an electric current (Hiscock, 2005). The groundwater EC measurements range from 285 µS/cm to 859 µS/cm, with an average of 701 µS/cm (Table 5-1). Talling and Talling (1965), defined freshwater as having an EC measurement of less than 600 µS/cm, moderately saline water as having an EC value between 600 µS/cm and 6000 µS/cm, and saline water as having an EC value greater than 6000 µS/cm. Therefore, most of the water in the study area ranges from fresh to moderately saline.

5.1.5 Hydrochemical facies

The various hydrochemical facies identified within the research area are illustrated in the Piper, Stiff and Expanded Durov diagrams. The Piper diagram classifies the concentrations of major ions (Ca^{2+}, Mg^{2+}, Na^{+},K, SO_4^{2-}, Cl^{-} and HCO_3^{-}) in water (Piper, 1944). The clustered waters on the Piper diagram indicate a common composition and origin. Based on the Piper interpretation in Figure 5-2, most of the groundwater is classified as the calcium-bicarbonate (Ca-HCO_3) facies. The dominant cations are Ca^{2+} and Mg^{2+}, while HCO_3^{-} is the dominant anion. The possible sources of Ca^{2+} and Mg^{2+} are the dissolution of dolomite, limestone and calcareous siltstones, which predominantly compose the HWA (KON 01, KON 02 and KON 03). Similarly, the HCO_3^{-} concentrations in the water likely result from the dissolution of dolomite, limestone and calcareous siltstones as well as the dissolution of CO_2 from the atmosphere, which seeps into the soil – an indication of freshwater (Clark and Fritz, 1997). The similar hydrochemical facies displayed in Figure 5-2 clearly indicate active interaction between surface water and groundwater.

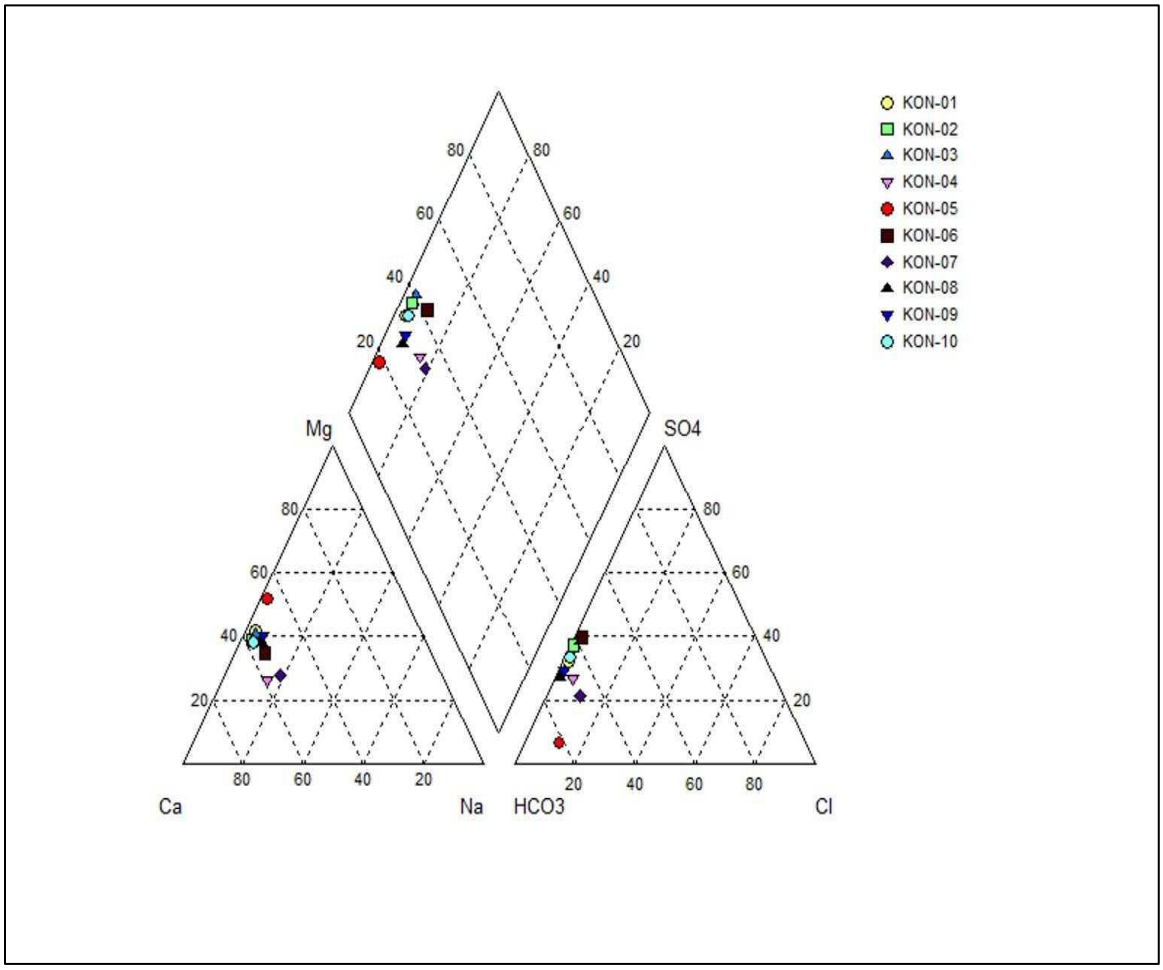


Figure 5-1: Piper diagram showing surface and groundwater of water sampled from KCM.

Stiff diagrams provide a graphical representation of both hydrochemical facies and salinity through the use of a polygon (Clark, 2015). The shape of the polygon highlights the main anion and cation constituents, while the width of the plot reflects their concentrations in milliequivalents (Stiff, 1951). The cations and anions in different samples are well visualised, allowing for easy identification of the dominant ions (Singhal *et al.*, 2010). Additionally, the greater the concentration of ions, the larger the area of the polygon (Fetter, 2014). According to the plots on the Stiff diagram, the water samples were categorised into two types. The first type is Ca-Mg-HCO_3, which includes samples KON 01 to KON 04 and KON 06 to KON 10, as shown in Table 5-3. This class is characterised by a high Ca^{2+} signature. The dominant ions in this water are Ca^{2+} (cation) and HCO_3^- (anion). The water type indicates the presence of calcareous rocks and the dissolution of CO_2 from the atmosphere, which is enriched in the soil. Therefore, dolomite, limestone and calcareous siltstones, which predominantly compose the Hangingwall formations, are the main sources of Ca^{2+}. The mineral content of the rock generally reflects the chemical

composition of the groundwater that has flowed through it (Mazor, 2003). Despite having similar hydrochemical facies, groundwater samples from the distinct aquifers (HWA, FWA, LPC aquifer and the fractured aquifer) vary in their concentrations of the dominant ions (Ca^{2+}, Mg^{2+} and HCO_3^-), as illustrated by the different shapes of the polygons in Figure 5-3. The HWA waters (KON 01, KON 02 and KON 03) have higher concentrations of Ca^{2+} and HCO_3^- compared to the other aquifers. This may be due to most of the water being recharged first into the HWA. The FWA water (KON 10) has slightly lower concentrations of Ca^{2+} and HCO_3^- than HWA water but contains higher concentrations of the dominant ions compared to the fractured aquifer and the LPC aquifer. The water in the fractured aquifer (KON 08 and KON 09) has concentrations of dominant ions that fall between those of HWA and FWA waters, suggesting that it could be a mixture of HWA and FWA waters. This is further supported by pH, temperature and Piper diagram analyses.

The second type of water is categorised as the Mg-HCO_3 water type (KON 05), as shown in Table 5-3. Mg^{2+} is the dominant cation, and similar to the first water type, HCO_3^- is the dominant anion. The hydrochemical facies of KON 05 indicate that the dissolution of dolomite has enriched the water with Mg^{2+}. KON 05 represents water from the Kafue River, which can be characterised as natural freshwater with minimal connectivity to the water in the fractured aquifer in the study area.

The area of the polygon corresponds to the concentration of ions (Fetter, 2014). Therefore, samples KON 04 (LPC) and KON 07 (surface water), which have smaller areas, indicate freshwater.

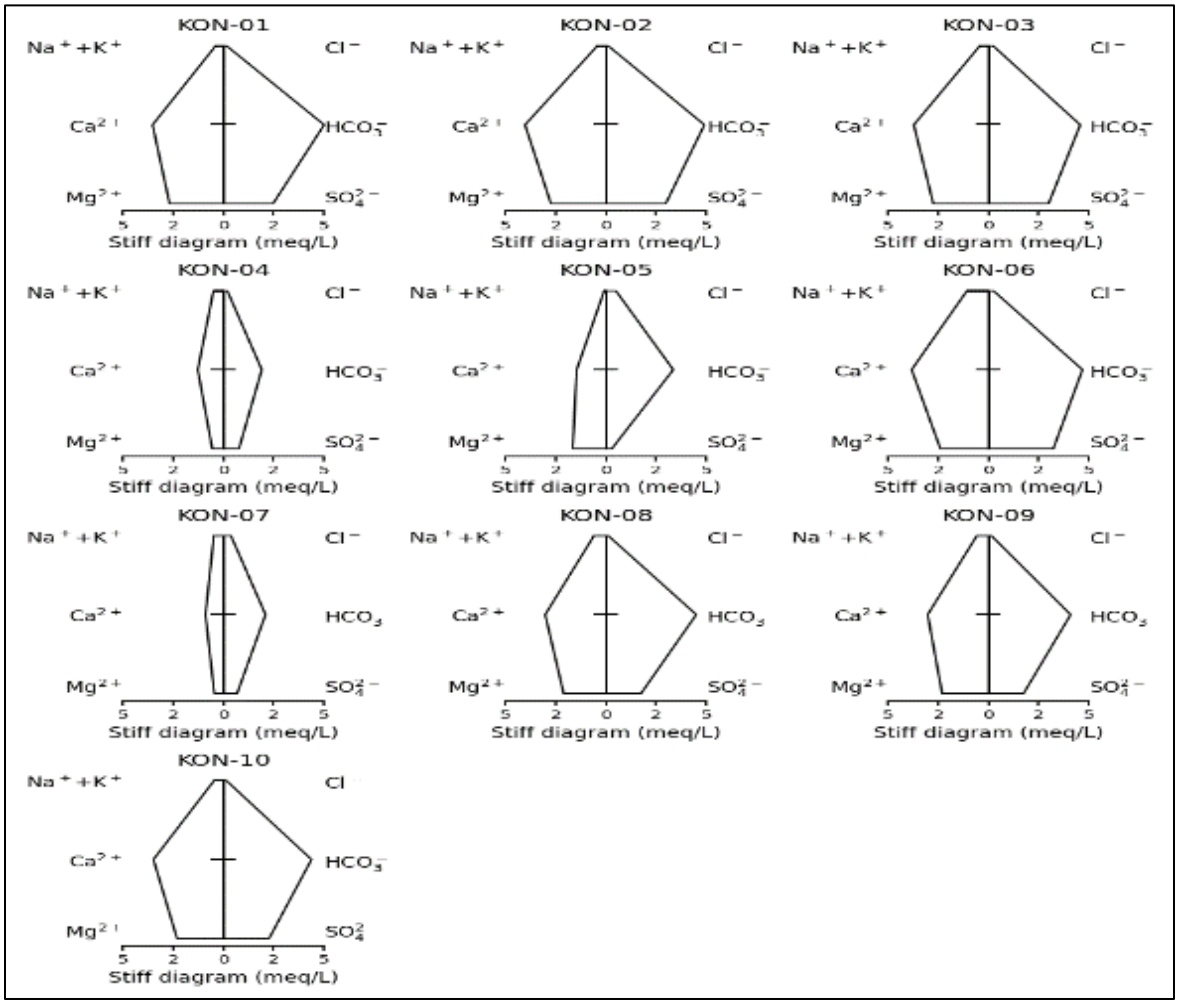


Figure 5-2: Stiff diagram (Stiff, 1951) graphically representing hydrochemical facies of water at KCM.

Table 5-4: Water types based on Stiff diagram interpretation of samples at KCM

SampleID	Dominant Cation	Dominant Anion	Water Type	Aquifer
KON-01	Ca^{2+}	HCO_3^-	$CaHCO_3$	HWA
KON-02	Ca^{2+}	HCO_3^-	Ca-HCO_3	HWA
KON-03	Ca^{2+}	HCO_3^-	Ca-HCO_3	HWA
KON-04	Ca^{2+}	HCO_3^-	Ca-HCO_3	LPC
KON-05	Mg^{2+}	HCO_3^-	Mg-HCO_3	SURFACE
KON-06	Ca^{2+}	HCO_3^-	Ca-HCO_3	SURFACE
KON-07	Ca^{2+}	HCO_3^-	Ca-HCO_3	SURFACE
KON-08	Ca^{2+}	HCO_3^-	Ca-HCO_3	FRACTURED
KON-09	Ca^{2+}	HCO_3^-	Ca-HCO_3	FRACTURED
KON-10	Ca^{2+}	HCO_3^-	Ca-HCO_3	FWA

Figures 5-4 and 5-5 show the Gibbs diagram used to determine the relationship between surface water composition and the lithological composition of the aquifer (Gibbs, 1970). The Gibbs diagram consists of three distinct fields: evaporation dominance, precipitation dominance and rock-water interaction dominance. All surface water samples plot within the rock-water interaction dominance area, as shown in Figure 5-3 (A). According to Gibbs (1970), this suggests that rock-water interaction is the dominant process compared to precipitation and evaporation. However, the application of the diagram to groundwaters should be considered within the broader context of hydrogeochemical processes, which are significantly different from those in surface water due to longer residence times and varying geochemical environments, such as redox conditions(Marandi and Shand, 2018). Therefore, the groundwater samples in Figure 5-3(B) suggest that water-rock interaction and the dissolution of carbonate minerals are the dominant processes. Figure 5-3 (C) further confirms that the dissolution of evaporate minerals is the dominant process in groundwater (Sahib *et al.*, 2016).

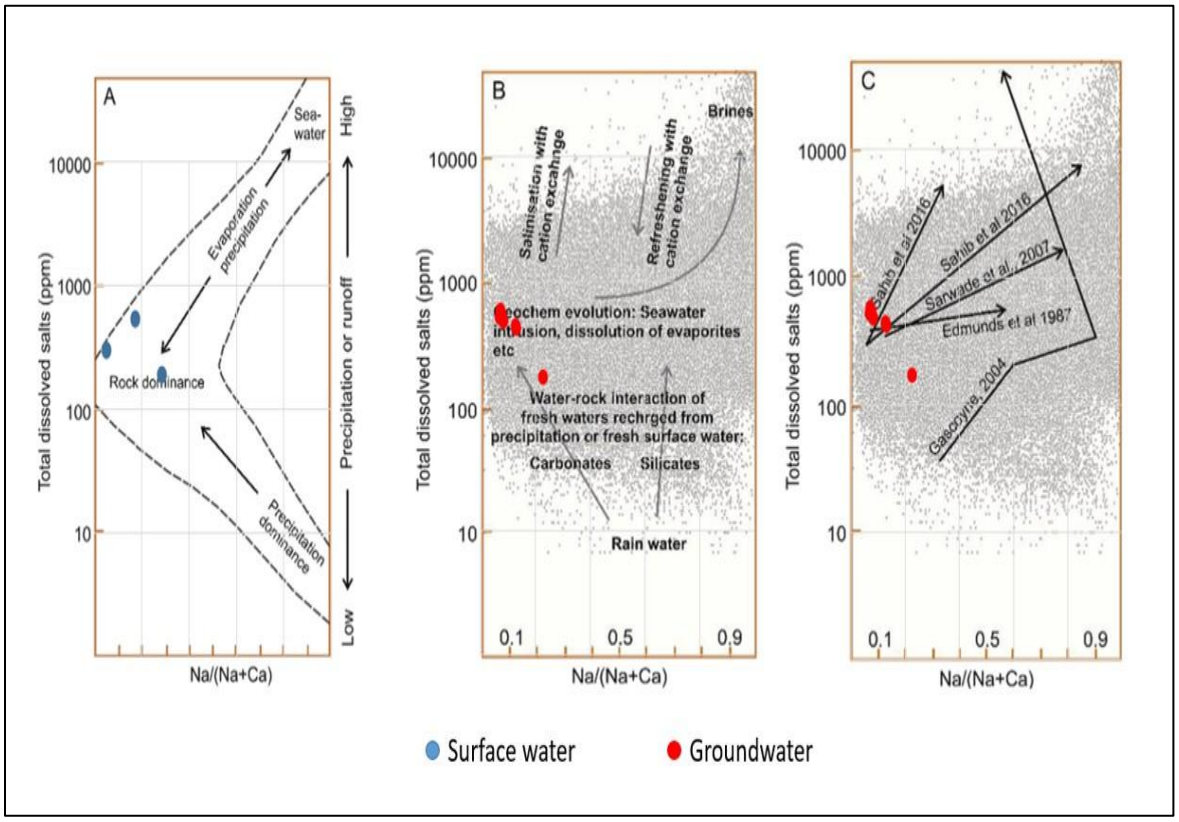


Figure 5-3: TDS vs Na/ (Na/(Na+Ca) diagrams of all water samples from the KCM area. The diagrams depict water chemistry for surface water (Gibbs, 1970), diagram (A) and in groundwater (B). The evolution of groundwater quality caused by (C) the dissolution of evaporite minerals (Sahib et al., 2016). The grey patterned cloud on B and C represents the groundwater samples taken from the USGS Brackish Groundwater Database(Qi and Harris, 2017).

The Durov diagram (Figure 5-6) was employed to enhance the geochemical analysis of processes in groundwater and surface water at KCM by plotting the percentage concentrations of major ions in milliequivalents (Durov, 1948). The plot in Figure 5-5 shows that groundwater samples from the fractured aquifer (KON 08 and KON 09) have undergone a simple dissolution or mixing process, likely due to rock-water interaction, as indicated by the Gibbs diagram.

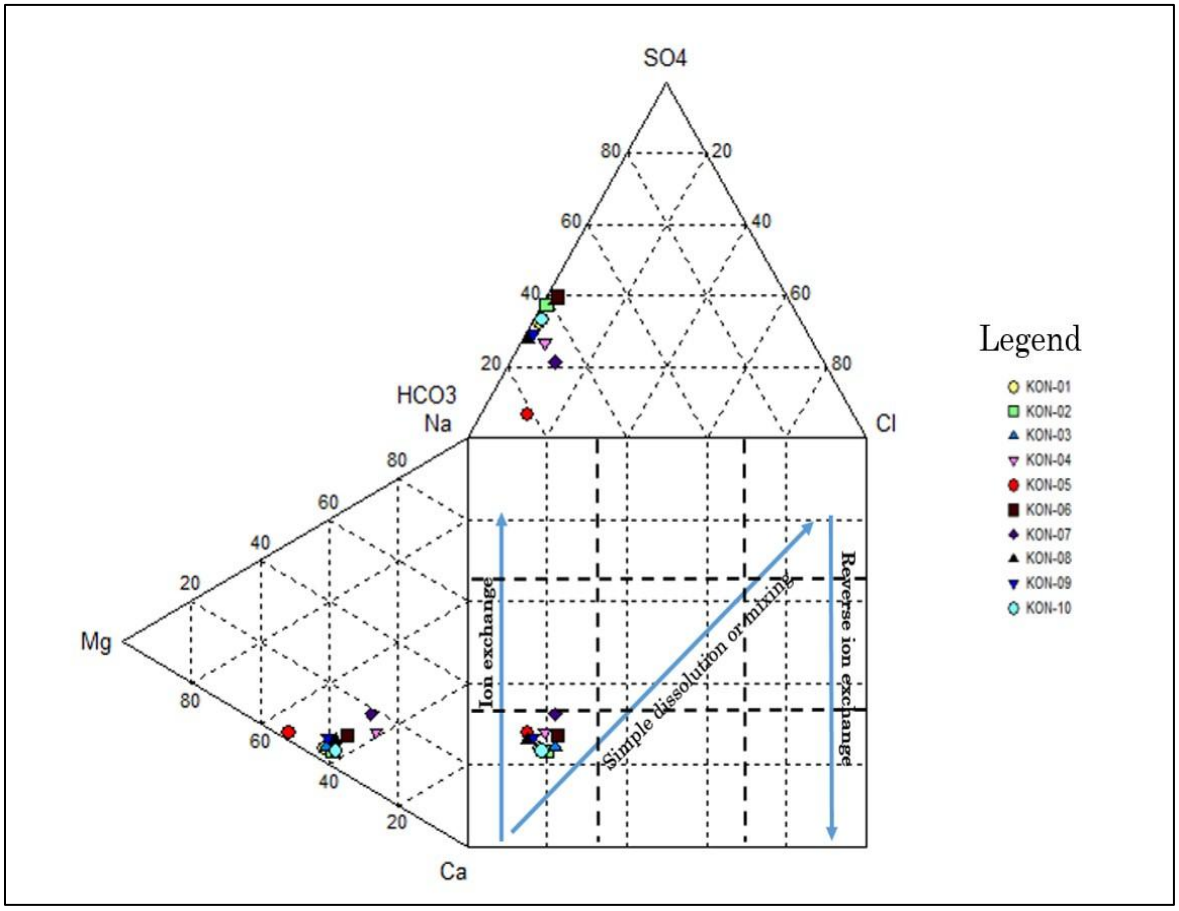


Figure 5-4: Expanded Durov diagram for KCM representing hydrochemical processes

The hydrochemical analysis indicates that the primary ions present in the water samples from KCM are calcium and magnesium. These ions likely originate from the dissolution of dolomites and limestones during interactions between water and rock. As noted by Datta and Tyagi (1996), the scatter plot of (Ca + Mg) against (HCO_3 + SO_4) in Figure 5-5 reveals that ionic concentrations positioned above the equiline are indicative of carbonate weathering, while those along the equiline result from both carbonate and silicate weathering processes. The data presented in Figure 5-5 shows that the majority of water samples are plotted above the equiline, with a smaller number situated on and below it. This pattern suggests that carbonate weathering is the primary contributor to the ions found in the water, while the few samples that fall below the equiline point to the influence of

silicate weathering. The process is summarised in the following reactions, where carbonic acid (derived from atmospheric CO_2 and water) reacts with calcium carbonate in the soil to produce bicarbonate ions, as illustrated in equations 6,7 and 8.

$CO_2 + H_2O \rightarrow H_2CO_3$ (formation of carbonic acid) **Equation 6**

$CaCO_3 + H_2CO_3 \rightarrow Ca^{2+} + 2HCO^-_3$ (calcite dissolution) **Equation 7**

$NaAlSi_3O_8 + H_2CO_3 + 9H_2O \rightarrow Al_2Si_2O_5(OH)_4 + 2Na^+ + 4H_4SiO_4 + 2HCO^-_3$ (silicate weathering) **Equation 8**

The process of carbonate weathering, driven by water saturated with carbon dioxide and carbonic acid, is intensive (Lakshmanan *et al.*, 2003). This acidic water has a strong ability to dissolve carbonate minerals present along its journey. In the study area, magnesium likely originated from the dissolution of dolomite, as indicated in Equation 9.

$CaMg(CO_3)_2 + 2H_2CO_3 \rightarrow Ca^{2+} + Mg^{2+} + 4HCO^-_3$ (dolomite dissolution) **Equation 9**

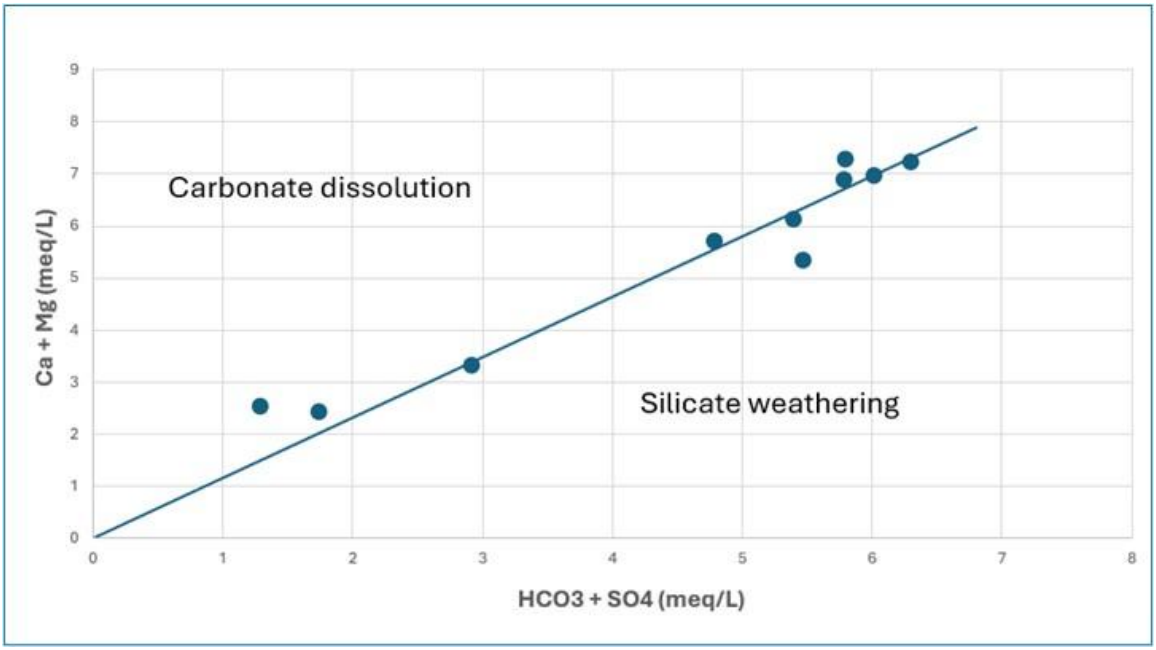


Figure 5-5: Scatter diagram of (Ca + Mg) vs. ($HCO_3 + SO_4$) showing silicate weathering and carbonate dissolution.

5.2 Stable Isotopes

The results from the stable isotope analysis of 10 water samples are shown in Figure 5-5 and Table 5-4. The samples exhibit two distinct isotopic fields, allowing for the characterisation of the water sources in the fractured aquifers, the identification of mixing processes, the analysis of mechanisms influencing recharge, the determination of groundwater flow paths and the understanding of changes in groundwater chemistry. Clark

and Fritz (1997) recommend that for local studies, surface water and groundwater data should be analysed in relation to the LMWL. This approach is justified by the influence of local climate variations on rainfall and evaporation.

The initial field, referred to as the condensation field, is identified by isotopic values that plot above the MWLs. In contrast, the second zone, known as the evaporation field, is characterized by isotopic data that fall below the MWLs. In this study, the GMWL and the LMWL for Ndola are used, based on the assumption that the isotopic composition of rainfall in Chililabombwe is similar to that of Ndola. The equation for the LMWL notably compares to the GMWL through the following equations:

$$\delta^2H = 7.63\delta^{18}O + 9.14‰$$ **Equation 10** (Banda *et al.*, 2023)

$$\delta^2H = 7.91\ \delta^{18}0 + 8.72‰$$ **Equation 11** (Terzer *et al.*, 2013)

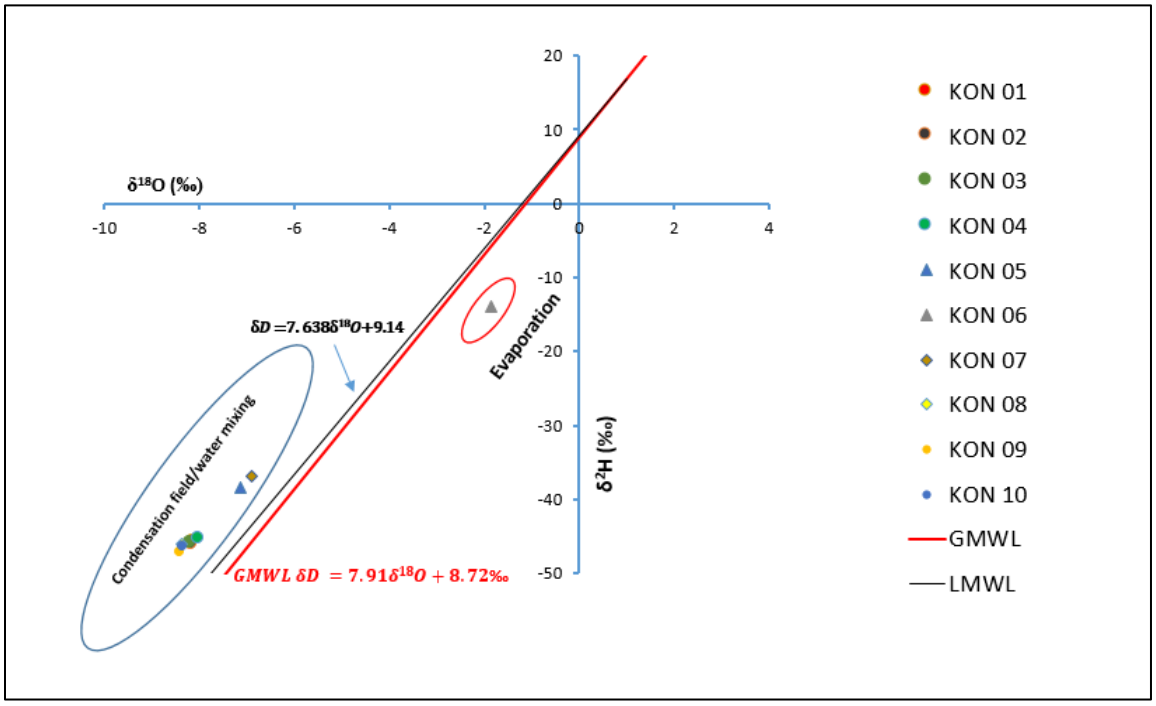


Figure 5-6: Stable isotope correlation diagram of water samples at KCM with associated LMWL

All the analysed surface and groundwater samples exhibit a depleted isotope signature, indicating that both were replenished during colder periods or from moisture originating in high-latitude regions. While both groundwater and surface water samples show depletion, groundwater samples exhibit a greater degree of depletion compared to surface water samples. The stable isotope ($\delta^{18}O$ and $\delta^{2}H$) results for the HWA range from -45.8 ± 0.6‰ and -8.20 ± 0.1‰ for KON 03 to -46.00 ± 0.8‰ and -8.17 ± 0.1‰ for KON 02, plotting above the LMWL/GMWL. The HWA sampled water is highly depleted in $\delta^{18}O$ and $\delta^{2}H$. Similarly, the LPC aquifer shows significant depletion, with values of -45.3 ± 2.4‰ and -8.02 ± 0.2‰ for KON 04. Additionally, the $\delta^{18}O$ and $\delta^{2}H$ results for the fractured aquifer and the FWA show similarities to those of the HWA (KON-01, KON-02 and KON-03) and LPC aquifers (KON-04). These isotopic similarities suggest a connection between different aquifers, potentially due to groundwater infiltration from surface water bodies and upper calcareous and siliceous aquifers into the lower fractured aquifers. The stable isotope plot in Figure 5-7 further illustrates a mixing pattern in the groundwater samples, with the end-members being deep-circulating FWA (KON 10) and fractured water samples (KON 08 and KON 09).

The isotopic signature of the surface water samples (KON 05, KON 06 and KON 07) reveals both depleted and relatively enriched levels of $\delta^{18}O$ and $\delta^{2}H$. The surface water sample KON 06, which is plotted below the LMWL and the GMWL, suggests that evaporation is a primary factor driving isotope fractionation. In contrast, KON 05 and KON

07 are plotted above both the LMWL and GMWL, indicating that the local precipitation might have been affected by condensation or the blending of various air masses prior to recharge, a process influenced by regional air circulation (Abiye *et al.*, 2015). According to (Clark and Fritz, 1997), this could also be attributed to low humidity in the vapour during precipitation and also recharge prior to evaporation.

The plot in Figure 5-7, however, shows clustering of groundwater, indicating that the water in the aquifers originates from the same source.

Table 5-5: Results of ESIs in surface water and groundwater for KCM.

Sample Name	$\delta^{2}H$ (‰)	$^{\pm 2}H$ StDev (‰)	$\delta^{18}O$ (‰)	$^{\pm 18}O$ StDev (‰)	Water Source
KON 01	-45.6	0.9	-8.14	0.1	**Groundwater (HWA)**
KON 02	-46.0	0.8	-8.17	0.1	**Groundwater (HWA)**
KON 03	-45.8	0.6	-8.20	0.1	**Groundwater (HWA)**
KON 04	-45.3	2.4	-8.02	0.2	**Groundwater (LPC)**
KON 05	-38.3	0.7	-7.12	0.1	**Surface Water (Lubengele Stream)**

KON 06	-13.8	0.7	-1.85	0.1	**Surface Water (Kafue River)**
KON 07	-36.9	0.8	-6.90	0.1	**Surface Water (Kakosa Stream)**
KON 08	-46.1	0.5	-8.39	0.1	**Groundwater (Fractured)**
KON 09	-47.0	1.0	-8.42	0.1	**Groundwater (Fractured)**
KON 10	-46.1	1.0	-8.37	0.1	**Groundwater (FWA)**

5.2.1 Deuterium excess or D-excess

D-excess is a measure of the relative proportions of ^{18}O and ^{2}H in water, visually represented as an index of deviation from the global MWL (d=10) in $\delta^{18}O$ versus $\delta^{2}H$ space (Abiye *et al.*, 2015). D-excess is determined based on the LMWL, as it aids in identifying the origin of the moisture that contributed to cloud formation and the resulting rainfall (Abiye *et al.*, 2015). The following equation is used to calculate d-excess according to the LMWL:

$d = \delta^{2}H - 7.63\delta^{18}O$ **Equation 12** (Banda *et al.*, 2023)

The d-excess values for the study area range from 0.2‰ to 17.9‰, as presented in Table 5-4. All groundwater samples exhibit high d-excess values. According to Clark and Fritz (1997), high d-excess values may indicate recharge by rainfall originating from moisture formed under conditions of very low humidity and cool temperatures, resulting in highly depleted moisture. Therefore, the high d-excess values in the groundwater suggest the prevalence of local moisture from extremely low vapour humidity. Figure 5-8 shows two clusters of samples with varying d-excess values. The surface water sample KON 06 does not reflect the original moisture source conditions, as it underwent isotopic changes due to evaporation from a surface water body before recharge. Additionally, variations in the other samples indicate the influence of both regional and local moisture circulations. This interpretation is supported by the highly depleted isotopes exhibited in samples KON 02 (HWA) and KON 09 (Fractured aquifer), which exhibit low tritium content, indicating a regional circulation pattern directing moisture to the recharge area.

Table 5-6: Stable isotope of surface water and groundwater from KCM with associated deuterium excess.

Sample Name	Water Source	δ^2H (‰)	$\delta^{18}O$ (‰)	D-excess (‰)
KON 01	**Groundwater (HWA)**	-45.6	-8.14	16.5
KON 02	**Groundwater (HWA)**	-46.0	-8.17	16.3
KON 03	**Groundwater (HWA)**	-45.8	-8.20	16.8
KON 04	**Groundwater (LPC)**	-45.3	-8.02	15.9
KON 05	**Surface Water (Lubengele Stream)**	-38.3	-7.12	16.0
KON 06	**Surface Water (Kafue River)**	-13.8	-1.85	0.2
KON 07	**Surface Water (Kakosa Stream)**	-36.9	-6.90	15.7
KON 08	**Groundwater (Fractured)**	-46.1	-8.39	17.9
KON 09	**Groundwater (Fractured)**	-47.0	-8.42	17.2
KON 10	**Groundwater (FWA)**	-46.1	-8.37	17.7

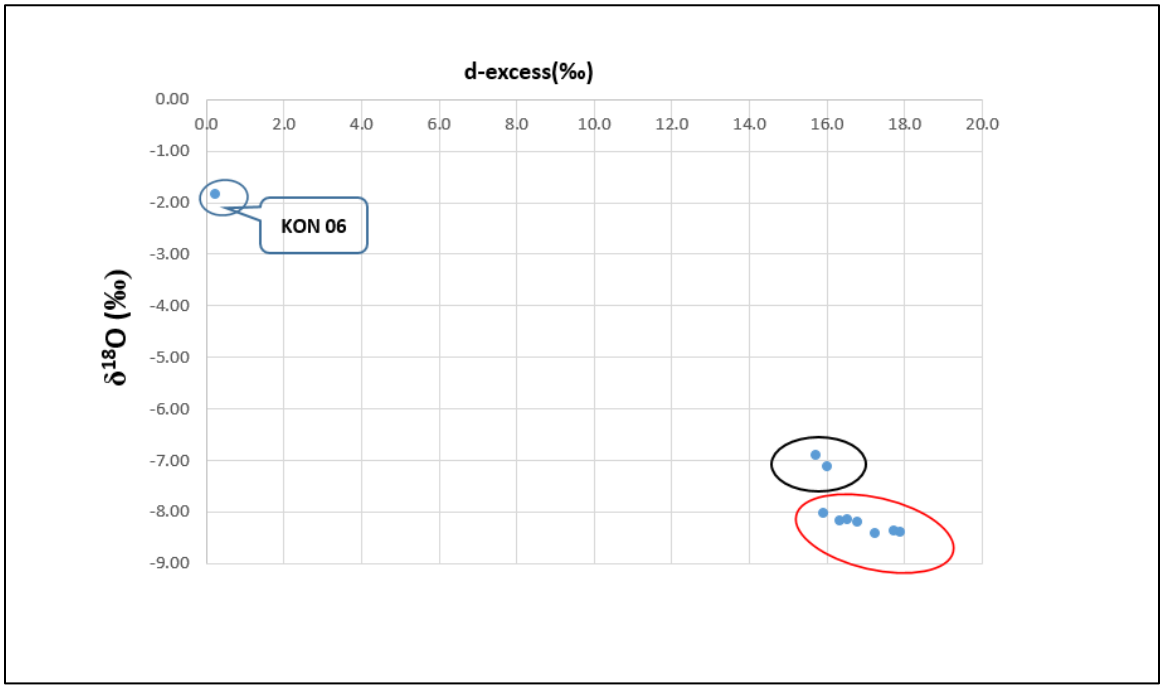


Figure 5-7: Scatter plots of δ18O and deuterium excess for water samples from KCM

5.3 Tritium Dating

Tritium is a radioactive isotope of hydrogen with a greater atomic mass, symbolised as ^{3}H or T (Mazor, 2003). Tritium analysis enables the determination of the mean residence time of groundwater and further confirms the link between surface water and groundwater (Mulenga, 1991). In November 2024, seven groundwater samples (KON 01 to KON 04 and KON 07 to KON 10) were collected for tritium analysis. The results, along with the residence times of the different samples, are presented in Table 5-5. The mean tritium content in the groundwater samples varied between 0.1 ± 0.3 T.U. for KON 02 and 1.0 ± 0.3 T.U. for three samples (KON 01, KON 04 and KON 08), with an average concentration of 0.7 ± 0.3 T.U. Additionally, the estimated rainfall tritium concentration at Lumwana Copper Mine in the North-Western Province of Zambia is 1.9 ± 0.3 T.U. (Mbilima, 2023), which has been used for residence time calculations in this study. Lumwana Copper Mines is located approximately 220 km northwest of KCM in Chililabombwe. Recent groundwater recharge periods can be identified by comparing the tritium levels in groundwater with those found in recent rainfall (Levin and Verhagen, 2013). The HWA sample KON 02 had the lowest tritium content. However, since KON 02 and KON 03 are duplicate samples, the differences in tritium levels may indicate potential contamination, mixing of younger water with older groundwater, or spatial variability within the HWA. KON 01 (HWA) has a short residence time of 12.1 years, indicating that the water is modern and the aquifer has high permeability, allowing for rapid recharge.

According to Abiye (2013), low measurable tritium levels suggest a longer residence time for groundwater, likely due to delays in the zone that is unsaturated or a low ratio of recharge to storage in that zone. Therefore, the shortest residence time of 10.8 years (KON 04/ LPC) indicates that the aquifer allows rapid recharge, which could be attributed to the geological nature of the LPC aquifer, known for its leached and porous characteristics in most areas. The two samples taken from the fractured aquifer, KON 08 and KON 09, exhibit variability. KON 08 shows modern recharge characteristics with a tritium value of 1.0 T.U., whereas KON 09 has a significantly lower value of 0.3 T.U., indicating a mixture of older and younger water. These samples, which further supported evidence of water mixing in the fractured zones at KCM, were taken from boreholes situated in the Cross Axis and the Axis Fault zones. As Mulenga (1991) indicated, a portion of the water in these fractured areas has been recently recharged, while other portions are sub-modern, meaning they were recharged before the 1950s. Furthermore, the long residence time depicted in KON 09 may suggest the presence of groundwater that circulates deeply from the regional aquifer (Mulenga, 1991).

Table 5-7: Tritium concentrations and associated mean residence times for samples from KCM.

Sample Identification	Water Type	Tritium (T.U.)	Residence Time Years	Aquifer Type
KON 01	Groundwater	1.0 ± 0.3	12.1	**HWA**
KON 02	Groundwater	0.1 ± 0.3	46.2	**HWA**
KON 03	Groundwater	0.6 ± 0.3	21.6	**HWA**
KON 04	Groundwater	1.0 ± 0.3	10.8	**LPC**
KON 08	Groundwater	1.0 ± 0.3	12.0	**Fractured**
KON 09	Groundwater	0.3 ± 0.3	30.7	**Fractured**
KON 10	Groundwater	0.8 ± 0.3	15.4	**FWA**

Figure 5-7 presents a scatter plot of tritium and $\delta^{18}O$ within the study area. Reduced tritium concentrations in the primary aquifers (HWA, FWA and LPC) are predominantly observed in the HWA, suggesting a longer residence time of water within these aquifers. In contrast, KON 01 (HWA) exhibits a high tritium concentration, indicating a shorter residence time or recent recharge. Consequently, the primary direction of groundwater flow is from the HWA (KON 01) and LPC (KON 04) towards the FWA aquifer (KON 10). The tritium results support the evidence from hydrochemistry and stable isotopes, confirming that two distinct types of water contribute to mine recharge. Additionally, the fractured zone serves as the primary area where water mixing occurs.

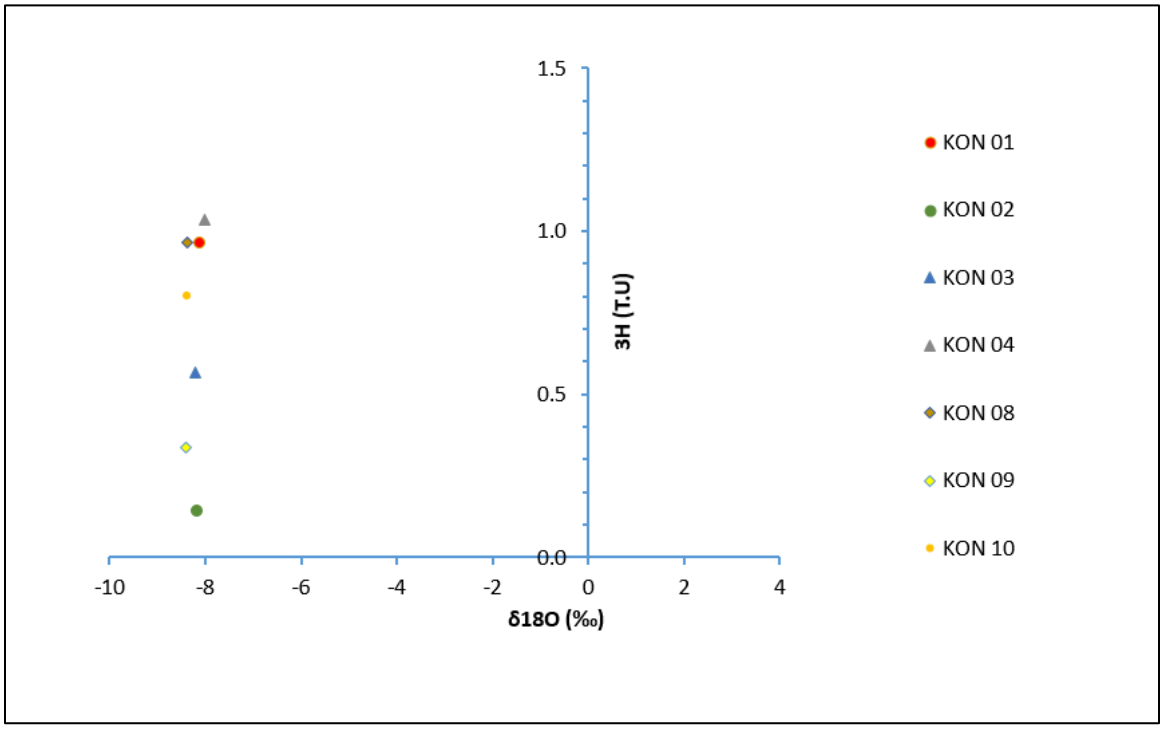


Figure 5-8: Scatter plot of Tritium and $\delta^{18}O$ within the KCM area.

Figure 5-8 illustrates the correlation between tritium levels and mine depths, based on the premise that the residence time (or apparent age) of groundwater samples is determined using a tritium concentration of approximately 1.9 T.U. from recent rainfall. Given that the half-life of tritium is 12.43 years, groundwater samples showing concentrations above 0.95 T.U. indicate water recharge within the last 12.43 years. Notably, sample KON 04 (from the LPC aquifer) exhibits the highest tritium concentration at 1.03 T.U., suggesting its recharge occurred roughly 11 years ago. This finding suggests a potential hydraulic link between the aquifer system and the mine cavity, which extends to depths of up to 950 metres. Additionally, samples from the fractured aquifer display signs of both recent recharge and the influence of older water. It is possible that deep groundwater migrates into the mine cavity through underlying geological structures. Based on the evaluation of tritium levels, the mine is recharged by the following two types of water:

a. Current rainfall and sub-modern recharge: These have a high tritium concentration, ranging from 0.95 T.U. to 1.9 T.U., with a residence time of 10 to 20 years.
b. Old recharge: This has a low tritium concentration (<0.27 T.U.) and a residence time of over 30 years, suggesting groundwater sourced from deep circulation.

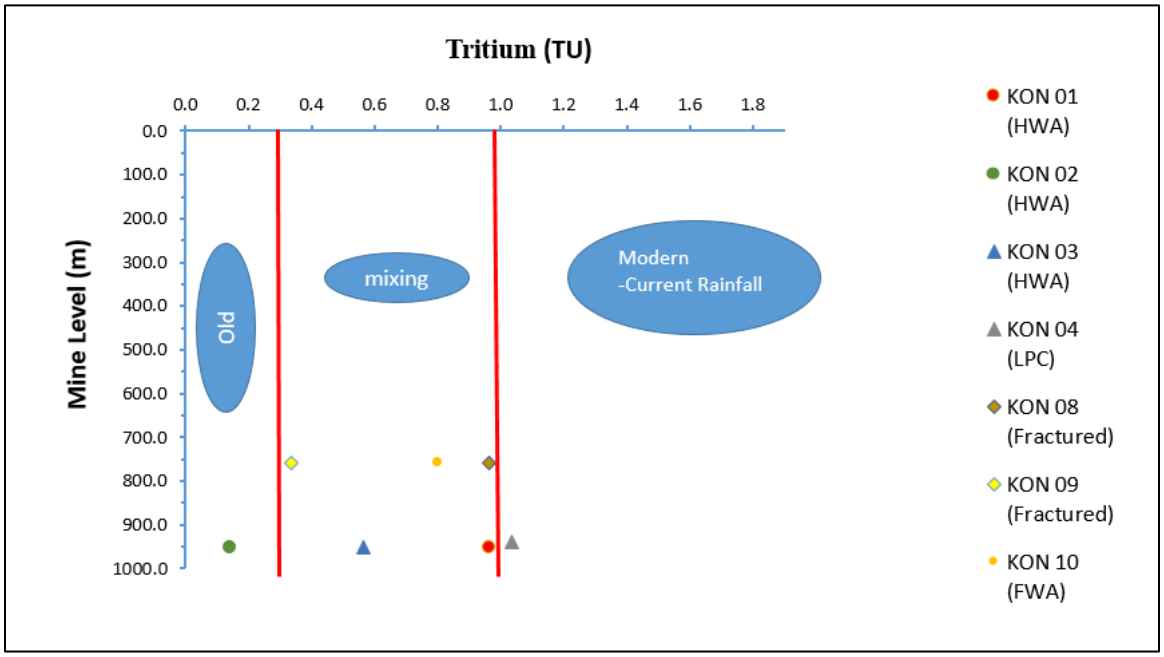


Figure 5-9: Scatter plot depicting the correlation between Tritium levels and mine depths.

5.3 Tracing the Possible Pathways of the Water and Mixing of Groundwater Flow in Aquifers in the Konkola Flats area at KCM.

The fractured zones in the Konkola Flats at KCM were mapped from underground. Two selected boreholes were drilled through the fractures, logged and sampled for water to gain a comprehensive understanding of the hydrogeochemical characteristics of these zones. Additionally, the mapped data was plotted on mine plans. Mapping and a thorough examination of the core revealed multiple fault zones varying in orientation and scale, with thicknesses ranging from a few centimetres to several metres. According to borehole data from BPN 898 and mapping at the 760mL 4800mN Crosscut, the fault zones primarily consist of intensely broken rock pieces embedded within a finer grained material. The fragments within these zones are mostly angular and sharp. The grain distribution is usually poorly sorted and in some areas, the average grain size is smaller than that of the adjacent rock on both sides of the fault zone. The intensity of fracturing within the fault zones varies, with some sections displaying relatively low fracture density while others exhibit higher intensity, as depicted in Figure 5-9. Furthermore, a detailed description of rock units and lithological attributes for BPN 898 is presented in Table 5-7.



Figure 5-10: Observed Fractured Zone of the footwall sandstone in DVN 898 that allows water flow and is associated with sample KON 08. The oxidized, fractured footwall sandstone comprises variable stains of iron oxide.

Table 5-8: Detailed description of rock units and lithological attributes for BPN 898

Borehole I.D	From (m)	To (m)	Description (Rock Unit and Lithology)
BPN 898	0	67.6	AGSST - Grey pink medium grained sandstone, moderately weathered and mineralized with malachite ore minerals
	67.6	80	FWC - Pink grey coarse grained conglomerate, moderately weathered and no visible mineralization observed
	80	11.48	FWC - Pink grey coarse grained conglomerate, moderately weathered and interbedded with feldspathic sandstone
	114.8	128	OSU - Grey fine grained thinly bedded shale, moderately weathered with some micro folding structures and massive mineralization with charcocite ore minerals
	128	143	OSU - Grey fine grained thinly bedded shale, moderately weathered Charcocite ore minerals observed, micro folding structures were observed
	143	149	OSU - Grey fine grained thinly bedded shale moderately weathered with micro folding structures Charcoal ore minerals observed along bedding planes
	149	152	OSU - Grey fine grained thinly bedded shale moderately weathered with micro folding structures Specks of charcoal ore minerals

	152	159.2	OSU - Grey fine grained thinly bedded shale moderately weathered with micro folding structures and Charcocite ore minerals observed
	159.2	163	FWSST - Grey to pink medium grained with shale bands sandstone, moderately weathered (evidence of faulting), Some charcocite ore minerals along shale bands observed and comprise part of HWQ
	163	191	FWSST - Grey pink medium grained sandstone, moderately weathered and fractured with observed malachite and charcocit ore minerals and comprise part of HWQ, evidence of faulting
	191	198	FWSST - Grey medium grained sandstone, highly weathered and fracture (fault zone) and no visible ore minerals observed
	198	254.1	HWQ - Grey pink medium grained quartzite with different metamorphic energies and textures, Some sections more crystallized than others and no visible mineralization observed

The term ‘fractures’ refers to various types of cracks, fissures, joints and faults within a geological formation (Berkowitz, 2002). Among these, joints and faults are the two primary categories of fractures. In the Konkola Flats area at KCM, some fault surfaces contain quartz vein fillings, as illustrated in Figure 5-10. The mixing of sediments due to tectonic activity in fault zones generally reduces permeability (Bense *et al.*, 2013).



Figure 5-11: Underground picture showing massive quartz vein within the footwall sandstone; pen for scale

Figures 5-11 (A to D) and Figure 5-12 show the water collection points from both surface and underground sources, along with a schematic representation of the sampling locations. Samples were collected from various locations across different aquifers, including HWA, LPC, and FWA, as well as from surface water bodies.



Figure 5-12: Water collection points from surface and underground at KCM. (A) KON 08, (B) KON 10, (C) KON 01 and (D) KON 05

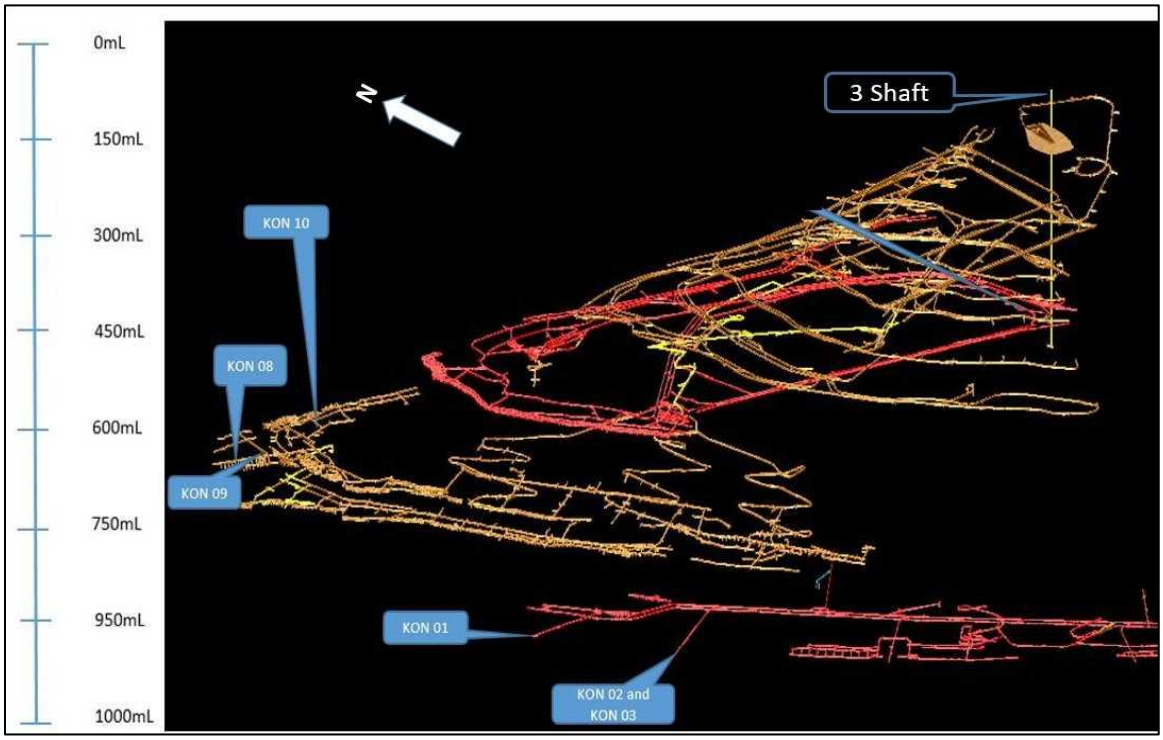


Figure 5-13: Schematic figure of KCM in 3D (Surpac DTM), showing No. 3 Shaft and the sampling points

The hydrochemical analysis indicates that aquifer samples from the study area can be categorised into two distinct hydrochemical facies, as depicted in Figure 5-2 of the Piper trilinear diagrams. These facies are primarily influenced by water-rock interactions, as illustrated in Figures 5-3 of the Gibbs diagrams. The chemical composition of the water typically reflects the mineralogy of the surrounding lithology (Mulenga, 1991). The Piper diagrams provide insight into the relative proportions of major ions in groundwater, enhancing the understanding of its overall hydrochemical characteristics. It was determined that interactions between water and rock are the dominant process influencing the composition of groundwater. Consequently, the hydrochemistry of KCM groundwater was examined in relation to various rock types, highlighting the importance of these interactions (Mulenga, 1991). As water infiltrates the rock, it leaches certain components, enabling the deduction of the groundwater's geological history, the identification of rock types through which it has percolated and a better understanding of its source within the hydrological cycle (Singh, 1986; Mazor, 2003). The aquifers at KCM can be categorised into two types, based on their mineral composition. The HWA are primarily composed of calcareous materials, including dolomite, limestone and calcareous siltstone. In contrast, the Footwall Aquifers (FWA and LPC) consist of siliceous materials such as feldspathic sandstones, conglomerates and quartzites.

Groundwater samples from the HWA boreholes (KON 01, KON 02 and KON 03) exhibited high concentrations of dissolved ions, including bicarbonate (HCO_3^-: 256–281 mg/L), calcium (Ca^{2+}: 65.8–75.1 mg/L) and sulphate (SO_4^{2-}: 109–132 mg/L). These values contribute to the relatively high TDS, ranging from 521 to 590 mg/L and elevated EC values of 815–859 µS/cm. The groundwater is circumneutral, with a pH range of 7.22–7.39. It is classified within the Ca-HCO_3 hydrochemical facies, primarily due to accelerated rock-water interactions (Mazor, 2003). The dominance of calcium (Ca^{2+}), magnesium (Mg^{2+}) and bicarbonate (HCO_3^-) suggests that the water is replenished by meteoric sources, with some dissolution of carbonate minerals (Abiye, 2023). Additionally, stable isotope analysis of the HWA samples indicated that local rainfall may have undergone condensation before recharging, as the water samples plotted above LMWL. According to Clark and Fritz (1997), comparing surface water and groundwater data with the LMWL is crucial for local studies, as climatic variations significantly influence rainfall and evaporation processes. The HWA samples exhibited varying tritium content, suggesting mixed recharge conditions. KON 01 displayed evidence of modern recharge, while KON 02 indicated the presence of older water or mixing with ancient groundwater. The tritium values were 0.96, 0.14 and 0.56 T.U. for KON 01, KON 02 and KON 03, respectively. The long residence time of KON 02 (46.2 years) may explain its slightly depleted isotopic signature, likely due to mixing with older groundwater.

Conversely, groundwater samples from the LPC aquifer borehole KON 04 show relatively low TDS (170 mg/L) and EC (106.2 µS/cm). These low values are attributed to the low presence of dissolved ions, specifically calcium (24.1 mg/L) and magnesium (6.56 mg/L). The lower TDS and EC indicate freshwater recharge, likely from direct rainfall infiltration or diffuse recharge (Leketa and Abiye, 2021). The presence of calcium (Ca^{2+}) and bicarbonate (HCO_3^-) suggests carbonate weathering; however, their lower concentrations compared to those in HWA indicate limited rock-water interaction. Additionally, the depleted isotope results suggest that recharge may originate from depleted rainfall associated with high-latitude moisture sources. Furthermore, the tritium value of 1.0 T.U. aligns with the hydrochemical and stable isotopic data, confirming that the LPC aquifer is being replenished by recent water. The similarity in stable isotope signatures and hydrochemical facies between the HWA and LPC suggests a common recharge source. The FWA groundwater (KON 01) falls within the Ca-Mg-HCO_3 hydrochemical facies due to percolating water from both the HWA and LPC aquifers. The correlation diagram between δ^2H and $\delta^{18}O$ provides further insight into the recharge processes in the FWA, as indicated by its clustering with other groundwater samples (see Figure 5-4).

The hydrochemical analysis of samples from the fractured aquifer (KON 07 and KON 08) indicates a Ca-HCO_3 hydrochemical facies, with a moderate TDS range of 420 to 440 mg/L and an EC range of 650 to 678 µS/cm, suggesting interaction with carbonate minerals or rock. The samples contained variable but detectable amounts of tritium. KON 08 exhibits modern recharge, with a tritium concentration of 1.0 T.U. and a residence time of 12 years,

indicating active and rapid groundwater flow through the fractures. In contrast, KON 09 has a lower tritium value (0.3 T.U.), suggesting older or sub-modern water. The observed variance in tritium concentration and residence times (12 years for KON-08 vs 30.7 years for KON-09) in the fractured aquifer indicates water mixing within the system. Furthermore, the stable isotope signature (δ^2H and $\delta^{18}O$) of the fractured aquifer samples, plotted above the LMWL and GMWL, shows a groundwater isotope composition ranging from -46.1‰ to -47.0‰ for δ^2H and -8.39‰ to -8.42‰ for $\delta^{18}O$. This suggests that the recharge precipitation for this site originated from a series of depleted rainfall events (Van Wyk *et al.*, 2011). The depleted isotopic signatures of the fractured aquifer indicate recharge by rainwater originating from high altitudes or heavy, typically depleted rainfall events (amount effect).

5.3 Mixing of Groundwater in Aquifers at KCM (Konkola Flats Area)

Figure 5-18 shows the mixing graph of $\delta^{18}O$ versus chloride for water samples from various sampling sites at KCM. The graph indicates that multiple recharge sources contribute to variations in $\delta^{18}O$ and Cl^- values. These variations may be attributed to different recharge sources, such as rainfall, river water, deep groundwater circulation and the mixing of different waters. Surface water samples (KON 05 and KON 06) exhibit higher Cl^- concentrations (greater than 10 mg/L) compared to other samples. These samples deviate from the main cluster of lower Cl^- concentrations, suggesting the influence of evaporation, as Cl^- remains in solution while water evaporates, leading to $\delta^{18}O$ enrichment. Groundwater samples from the HWA (KON 01, KON 02 and KON 03), FWA (KON 10) and the fractured aquifer (KON 08 and KON 09) have low Cl^- concentrations (approximately <5 mg/L) and $\delta^{18}O$ values ranging between -8‰ and -7‰. These samples are closely clustered, indicating similar recharge conditions, likely from precipitation or fresh groundwater. They represent younger groundwater that has undergone minimal mixing. In contrast, KON 07 from the fractured aquifer shows slightly enriched $\delta^{18}O$ values, suggesting mixing with an isotopically heavier source or seasonal variations in precipitation, as $\delta^{18}O$ in rainfall fluctuates with the seasons (Clark and Fritz, 1997).

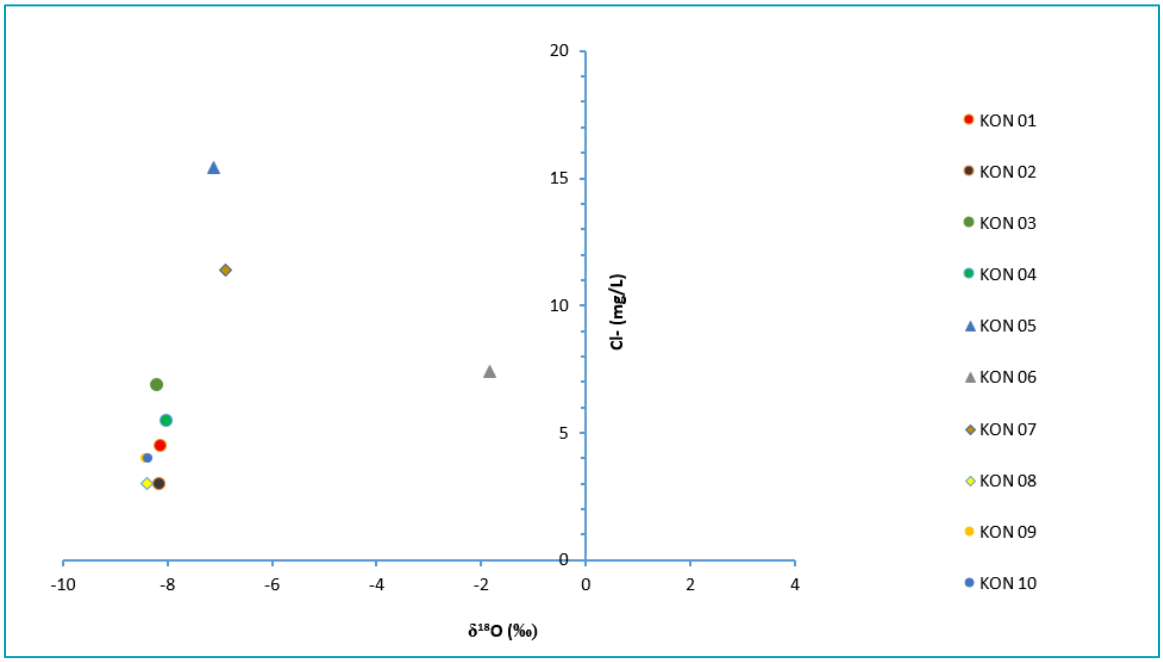


Figure 5-14: Mixing graph of $\delta^{18}O$ versus chloride of the water samples from the sampling sites at KCM

Chen *et al.* (2014) observed the relationship between TDS and stable isotopes ($\delta^{18}O$ and $\delta^{2}H$) in a coal mine in China, providing insights into the groundwater flow direction. Typically, as groundwater flows, TDS gradually increase, with the lowest levels in recharge areas and the highest in discharge areas. This occurs due to chemical and biochemical interactions between the groundwater and the geological materials it passes through (Freeze and Cherry, 1979).

The relationship between TDS and the stable isotopes of oxygen ($\delta^{18}O$) and hydrogen ($\delta^{2}H$) is shown in Figure 5-19 (A and B) from the water samples collected at KCM. Samples from recharge sources, such as the LPC aquifer (KON 04) and surface water (KON 07 and KON 05), exhibit lower TDS levels (<350 mg/L). The surface sample KON 06 is influenced by evaporation, leading to elevated $\delta^{18}O$ and $\delta^{2}H$ values. As the aquifers recharge from the source, they mix with existing groundwater in the flow direction due to diffuse recharge through weathering fractures at high elevations undergoing deep circulation (Leketa *et al.*, 2018). Consequently, $\delta^{18}O$ and $\delta^{2}H$ values become depleted, while TDS increases due to water-rock interactions. The HWA samples (KON 01, KON 02 and KON 03) exhibit high TDS concentrations, likely resulting from these interactions within the aquifer.

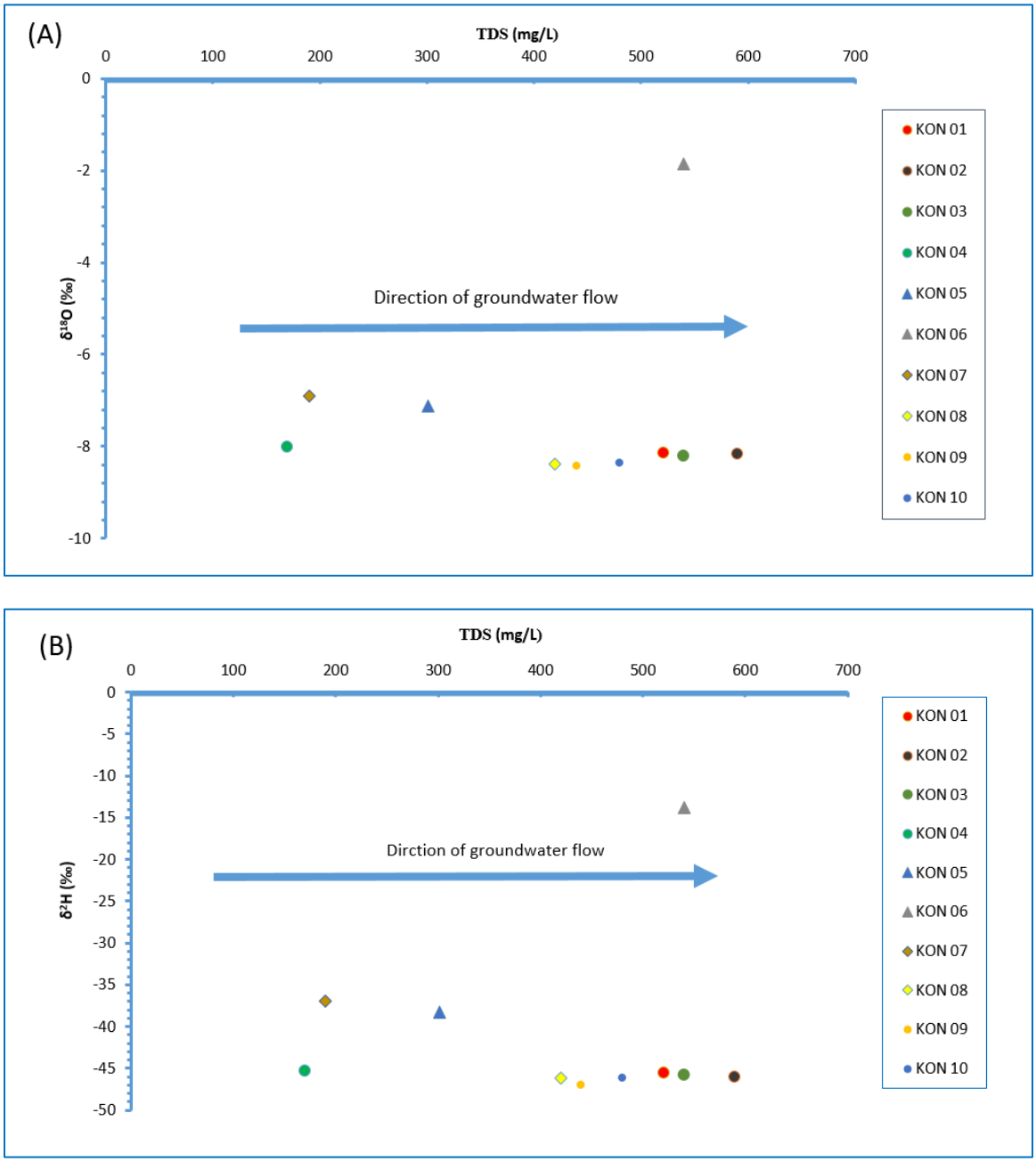


Figure 5-15: Change relationships of environmental stable isotopes with TDS in groundwater flowing direction in the KCM aquifers

5.4 Dewatering Principle for the Fractured Aquifer

Uncontrolled groundwater inflows from fractured zones pose significant challenges in underground mining. Additionally, the cost of pumping excessive water from underground to the surface is often high. Due to the complex hydrogeological conditions at KCM, the current groundwater control system, in place since 1955, requires improvement for greater effectiveness. In any mining operation, the chosen mining method significantly influences the dewatering approach. At KCM, the mining method involves unsupported open stoping, which necessitates dewatering of the strata above the stopes. Based on integrated hydrogeological investigations conducted in this study, an effective dewatering approach has been identified. This approach will enhance the existing dewatering strategy by integrating it with the proposed improvements.

5.4.1 Proposed Dewatering Methods

The three main aquifers mentioned in Chapter 3 (Section 3.5.1) utilise different dewatering techniques at KCM. The following sections explore potential dewatering strategies for each aquifer.

5.4.1.1 Hangingwall Aquifer dewatering

Currently, dewatering of the HWA is achieved through the mining of drainage drifts and the drilling of boreholes from drainage crosscuts. The drainage drives are developed parallel to and slightly below the levels of the haulage drifts (see Figure 5-20). Hydrogeochemical analyses conducted in this study indicate that the HWA is recharged by both local and regional rainfall. The presence of highly depleted stable isotopes and low tritium levels in the sample KON 02 shows that part of this recharge originated from older regional flow systems with long residence time and deep flow paths. This older regional groundwater, although it plays a smaller role in surface recharge, may facilitate long-term inflow, making it challenging to achieve complete hydraulic disconnection from surrounding formations. To enhance dewatering effectiveness, deep vertical boreholes should be installed in addition to the existing underground dewatering boreholes to reduce recharge from local rainfall and regional groundwater circulation. These must be drilled to the shallow regions governed by adjacent rainfall as well as the deeper fractures connected to regional groundwater pathways, in order to minimise long-term water entry and curb reliance on reactive dewatering efforts.

5.4.1.2 Footwall Aquifer Dewatering

The current FWA dewatering is primarily controlled by stratigraphy, except in fractured zones. This is achieved through standard haulage development, while the porous nature of the conglomerates and the jointing in the sandstones provide the aquifer with moderate primary hydraulic conductivity, enabling effective drawdown through gravity drainage. Based on hydrogeochemical findings, the FWA and the fractured aquifer represent the end members of groundwater flow. Therefore, to effectively dewater these aquifers,

groundwater should be intercepted from recharge zones, including the HWA, LPC aquifer and surface water bodies. Additionally, surface water bodies should be diverted away from the mine's caving lines. At KCM, the caving line is determined by a cave angle of approximately 65° at the stoping (production) level (Figure 5-20).

5.4.1.3 Lower Porous Conglomerate Aquifer dewatering

The LPC aquifer is intersected only once during the mining of the main haulage. Groundwater flow in the LPC aquifer is primarily controlled by joints, fractures and vugs. The conventional dewatering technique involves drilling pilot cover holes and sealing the water through cementation (grouting). Hydrogeological findings indicate that the LPC water is locally recharged. While the conventional dewatering technique has proven effective, additional surface dewatering is necessary for optimal results. This can be achieved by installing deep vertical dewatering boreholes in the recharge zones to reduce water infiltration into the LPC aquifer.

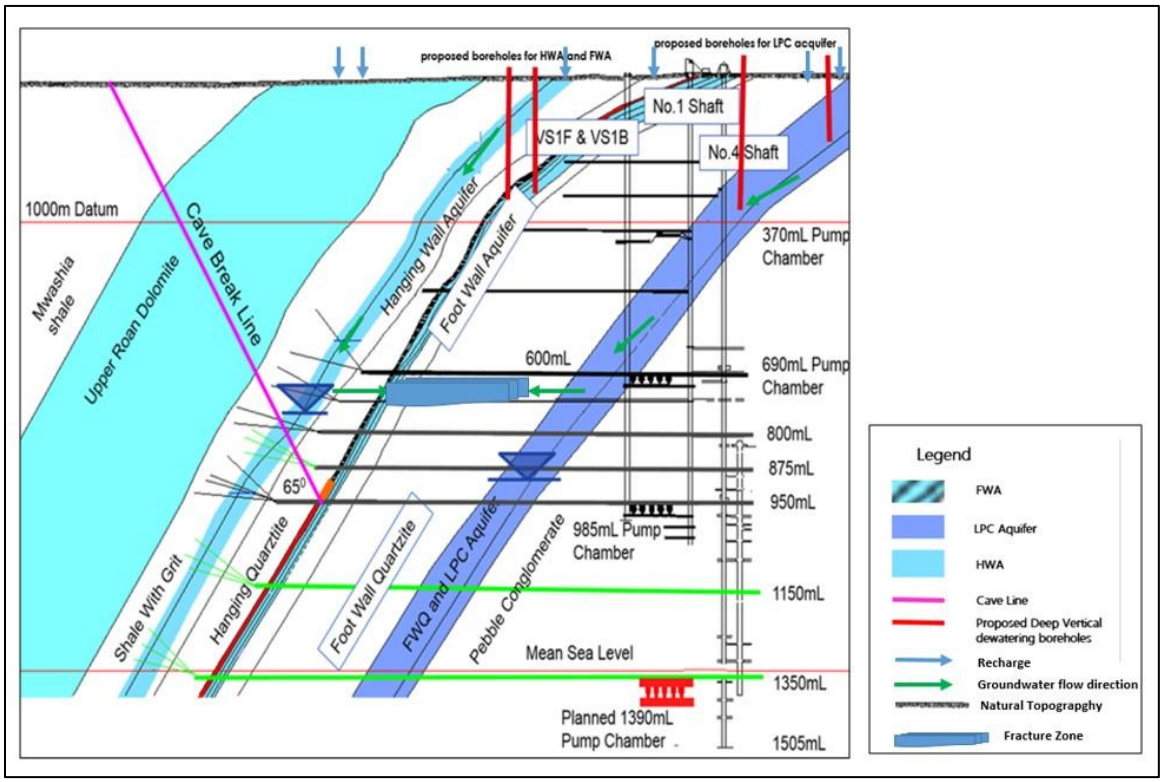


Figure 5-16: Conceptual hydrogeological cross-section of KCM showing the three main aquifers and proposed boreholes. Modified after KCM (2010)

The interpretation of the hydrochemical and isotopic data took into account the inherent limitations of the study. Due to restricted access within the active mine areas, sampling could only be conducted once, which limited the temporal coverage and the ability to assess seasonal variability. Additionally, the high analytical costs associated with laboratory

testing restricted both the number of samples collected and the range of parameters analysed. However, the spatial variability across the study area was adequately represented, as samples from all major aquifers at KCM were included. These limitations were therefore acknowledged without compromising the validity of the hydrochemical and isotopic trend interpreted in this study.

6. CONCLUSION AND RECOMMENDATIONS

6.1 Conclusion

An integrated approach has been employed to evaluate the characteristics of fractured aquifers at KCM in the Konkola Flats area. This assessment involved integrating different data sets, including regional and local geological reviews, site meteorological data, environmental isotopes, hydrochemistry and previous hydrogeological studies conducted at KCM. The hydrochemical data from both surface water and groundwater samples revealed that Ca-Mg-HCO_3 is the dominant facies. The Gibbs diagram analysis indicates that rock-water interaction is the primary process controlling groundwater hydrochemistry in the active mining area. This process occurs through the dissolution of in situ carbonaceous and siliceous rock formations affected by percolating water. Hydrochemical facies analysis established that rainfall is the primary source of recharge for the active mine area. However, the incorporation of environmental isotope data indicated that groundwater contains highly depleted $\delta^{18}O$ and $\delta^{2}H$ signatures, along with low tritium concentrations, especially within the HWA and fractured aquifer. This isotopic profile suggests regional groundwater circulation, likely sourced from higher altitudes or remote recharge zones. Additionally, evidence of water mixing within the fractured aquifer suggests the convergence of different flow systems. This was further illustrated in the expanded Durov diagram, which also indicated that simple dilution or mixing is the dominant process affecting groundwater in the HWA, FWA and surface water.

To further understand the hydrochemical facies, the Stiff diagram provides a graphical representation of hydrochemical facies. Based on this analysis, the water at KCM is classified into two types. The first type is the Ca-Mg-HCO_3 water, which includes HWA (KON-01, KON-02 and KON-03), LPC (KON-04), Lubengele (KON 06), Kakosa Stream (KON 07), the fractured aquifer (KON 08 and KON 09) and FWA (KON 10). This water type indicates the presence of calcareous rocks and the dissolution of CO_2 from the atmosphere, which is enriched in the soil. The dolomite, limestone and calcareous siltstones that predominantly compose the hanging wall formations are the primary sources of Ca^{2+} and HCO_3^- due to CO_2 dissolution. This water type is indicative of freshwater. The second type is the Mg-Ca-HCO_3 water, represented by the Kafue River (KON 05). In this type, Mg^{2+} is the dominant cation and HCO_3^- is the dominant anion. This composition suggests that the dissolution of dolomite rocks has enriched the water with Mg^{2+}.

ESI analyses were employed to better understand the hydraulic linkages between the groundwater and surface water, along with the hydrologic processes. Through stable isotope testing of 10 water samples from the study site, two distinct isotopic groups were identified: the condensation group, where samples were plotted above the LMWL, and the evaporation group, where samples were plotted below the Local and Global MWLs. All

underground samples exhibit a depleted isotope signature, indicating recharge influenced by high-latitude sources and regional air circulation from cooler climate conditions. The stable isotope analysis confirms hydraulic connectivity between the aquifers in the active mine, as all groundwater samples plot within the same cluster. The d-excess values in the study area range from 0.2‰ to 17.9‰, with all samples showing high values, particularly the surface water sample KON 06 from the Lubengele stream. High d-excess values suggest that rainfall recharge may originate from low humidity and cool temperatures, indicating local moisture with very low vapour humidity. The surface water sample KON 06 reflects altered moisture source conditions due to evaporation before recharge.

The interpretation of tritium concentrations confirms the blending of recently recharged and sub-modern water, with tritium values ranging from 0.1 to 1.0 T.U. Samples with high tritium content indicate rapid infiltration and permeable aquifer systems, while sub-modern recharge is associated with deep-circulating or confined groundwater. Variations in tritium concentrations among and within aquifers, particularly in the HWA and fractured aquifer, provide further evidence of the mixing of different water types.

Based on the findings, which were integrated with hydrochemical and environmental isotope analyses, hydraulic connections were observed within the aquifers at KCM. The overall water flow occurs from the HWA and LPC towards the FWA and the fractured aquifer, with the HWA and fractured aquifer serving as the primary zones of groundwater mixing. This study provides valuable insights into groundwater movement and water mixing within the fractured aquifers at KCM. The observed hydraulic and isotopic connectivity between aquifers has direct implications for the dewatering strategy of the mine. The similarity in hydrochemical and isotopic signatures indicates shared recharge pathways, suggesting that dewatering in one aquifer may influence hydraulic heads in neighbouring aquifers. This understanding enables optimisation of pumping borehole placement, prioritisation of high inflow zones and improved prediction of water rebound behaviour during mine closure planning.

6.2 Recommendations

The following recommendations summarise the additional hydrogeological improvements and investigations needed at KCM to improve the results of this research:

1. The monitoring of meteorological data should continue, with a potential increase in the number of weather stations. This will improve the estimation of key hydrological parameters such as rainfall, temperature, evapotranspiration and recharge rates.
2. Ongoing sampling of isotopes and water chemistry from rainfall, surface water bodies and underground sources in the study area is essential. This will provide a more comprehensive understanding of the area’s hydrogeochemistry.

3. Measures to exclude surface water should be improved to minimise seepage, as this study observed a connection between groundwater and surface water.
4. Further geochemical modelling (PHREEQC) to validate geochemical processes and mineral saturation indices

7. REFERENCES

Abiye, T. (ed.) (2013) "The use of isotope hydrology to characterize and assess water resources in South (ern) Africa", *WRS Report No TT570/13 Pretoria*, p. 211.

Abiye, T., Bybee, G. and Leshomo, J. (2018) "Fluoride concentrations in the arid Namaqualand and the Waterberg groundwater, South Africa: Understanding the controls of mobilization through hydrogeochemical and environmental isotopic approaches", *Groundwater for Sustainable Development*, 6, pp. 112–120. doi:10.1016/j.gsd.2017.12.004.

Abiye, T., Molla Demlie, Haile Mengistu, and Khuliso Masindi (2015) "Surface Water and Groundwater Interaction in the Upper Crocodile River Basin, Johannesburg, South Africa: Environmental Isotope Approach", *South African Journal of Geology*. Available at: https://www.academia.edu/54798979/Surface_Water_and_Groundwater_Interaction_in_the_Upper_Crocodile_River_Basin_Johannesburg_South_Africa_Environmental_Isotope_Approach (Accessed: 28 May 2024).

Advisian WorleyParsons Group (2017) *StepWise Options Analysis Report*, p. 141.

Ashton, P., Love, D., Mahachi, H. and Dirks, P. (2001) "AN OVERVIEW OF THE IMPACT OF MINING AND MINERAL PROCESSING OPERATIONS ON WATER RESOURCES AND WATER QUALITY IN THE ZAMBEZI, LIMPOPO AND OLIFANTS CATCHMENTS IN SOUTHERN AFRICA".

Aston, T. R. C. and Singh, R. N. (1983) "A reappraisal of investigations into strata permeability changes associated with longwall mining", *International Journal of Mine Water*, 2(1), pp. 1–14. doi:10.1007/BF02504616.

Banda, K., Mulema, M., Chomba, I., Chomba, M., Levy, J. and Nyambe, I. (2023) "Investigating groundwater and surface water interactions using remote sensing, hydrochemistry, and stable isotopes in the Barotse Floodplain, Zambia", *Geology, Ecology, and Landscapes*. Taylor & Francis. Available at: https://www.tandfonline.com/doi/abs/10.1080/24749508.2023.2202450 (Accessed: 9 December 2024).

Batumike, M. J., Cailteux, J. L. H. and Kampunzu, A. B. (2007) "Lithostratigraphy, basin development, base metal deposits, and regional correlations of the Neoproterozoic Nguba and Kundelungu rock successions, central African Copperbelt", *Gondwana Research*, 11(3), pp. 432–447. doi:10.1016/j.gr.2006.04.012.

Bense, V. F., Gleeson, T., Loveless, S. E., Bour, O. and Scibek, J. (2013) "Fault zone hydrogeology", *Earth-Science Reviews*, 127, pp. 171–192. doi:10.1016/j.earscirev.2013.09.008.

Berkowitz, B. (2002) "Characterizing flow and transport in fractured geological media: A review", *Advances in Water Resources*, 25(8–12), pp. 861–884. doi:10.1016/S0309-1708(02)00042-8.

Bridgwood, E. W., Singh, R. N. and Atkins, A. S. (1983) "Selection and optimization of mine pumping systems", *International journal of mine water*, 2(2), pp. 1–19. doi:10.1007/BF02504559.

Bull, S., Selley, D., Broughton, D., Hitzman, M., Cailteux, J., Large, R. and McGoldrick, P. (2011) "Sequence and carbon isotopic stratigraphy of the Neoproterozoic Roan Group strata of the Zambian copperbelt". University of Tasmania. Available at: https://figshare.utas.edu.au/articles/journal_contribution/Sequence_and_carbon_isotopic_stratigraphy_of_the_Neoproterozoic_Roan_Group_strata_of_the_Zambian_copperbelt/22887680/1 (Accessed: 16 January 2025).

Cailteux, J., Binda, P. L., Katekesha, W. M., Kampunzu, A. B., Intiomale, M. M., Kapenda, D., Kaunda, C., Ngongo, K., Tshiauka, T. and Wendorff, M. (1994) "Lithostratigraphical correlation of the Neoproterozoic Roan Supergroup from Shaba (Zaire) and Zambia, in the central African copper-cobalt metallogenic province", *Journal of African Earth Sciences*, 19(4), pp. 265–278. doi:10.1016/0899-5362(94)90014-0.

Cailteux, J. L. H., Kampunzu, A. B., Lerouge, C., Kaputo, A. K. and Milesi, J. P. (2005) "Genesis of sediment-hosted stratiform copper–cobalt deposits, central African Copperbelt", *Journal of African Earth Sciences*, 42(1–5), pp. 134–158. doi:10.1016/j.jafrearsci.2005.08.001.

Chen, L., Yin, X., Xie, W. and Feng, X. (2014) "Calculating groundwater mixing ratios in groundwater-inrushing aquifers based on environmental stable isotopes (D, 18O) and hydrogeochemistry", *Natural Hazards*, 71(1), pp. 937–953. doi:10.1007/s11069-013-0941-2.

Chilillabombwe Municipal Council (2022) "Chililabombwe District Integrated Development Plan 2022-2031".

Clark, I. (2015) *Groundwater Geochemistry and Isotopes*. CRC Press.

Clark, I. D. and Fritz, P. (1997a) *Environmental isotopes in hydrogeology*. Boca Raton, FL: CRC Press/Lewis Publishers.

Clark, I. D. and Fritz, P. (1997b) *Environmental Isotopes in Hydrogeology*. 0 edn. CRC Press. doi:10.1201/9781482242911.

Cook, P. (2020a) *Introduction to Isotopes and Environmental Tracers as Indicators of Groundwater Flow*. The Groundwater Project. doi:10.21083/978-1-7770541-8-2.

Cook, P. (2020b) *Introduction to Isotopes and Environmental Tracers as Indicators of Groundwater Flow*. The Groundwater Project. doi:10.21083/978-1-7770541-8-2.

Craig, H. (1961) "Isotopic Variations in Meteoric Waters", *Science*, 133(3465), pp. 1702–1703. doi:10.1126/science.133.3465.1702.

De Waele, B. and Mapani, B. (2002) "Geology and correlation of the central Irumide belt", *Journal of African Earth Sciences*, 35(3), pp. 385–397. doi:10.1016/S0899-5362(02)00149-5.

Dildar, J., Manzi, M. S. D., Abiye, T., Gomo, S., Rapetsoa, M. K. and Drennan, G. (2023) "Groundwater Circulation in the Shallow Crystalline Aquifer of Tharisa Mine, South Africa: Evidence from Environmental Isotopes and Near-Surface Geophysics", *Water*, 15(16), p. 2876. doi:10.3390/w15162876.

Etikan, I. (2016) "Comparison of Convenience Sampling and Purposive Sampling", *American Journal of Theoretical and Applied Statistics*, 5(1), p. 1. doi:10.11648/j.ajtas.20160501.11.

Fetter, C. W. (2014) *Applied hydrogeology*. Fourth edition, new international edition. Harlow, Essex: Pearson Education (Pearson custom library).

Freeze, R. A. and Cherry, J. A. (1979) *Groundwater*. Englewood Cliffs, N.J: Prentice-Hall.

Funke, J. W. (1990) "The Water Requirements and Pollution Potential of South African Gold and Uranium Mines", *WRC report KV9/90*, p. 172.

Gibbs, R. J. (1970) "Mechanisms Controlling World Water Chemistry", *Science*, 170(3962), pp. 1088–1090. doi:10.1126/science.170.3962.1088.

Guan, Z., Jia, Z., Zhao, Z. and You, Q. (2019) "Identification of inrush water recharge sources using hydrochemistry and stable isotopes: A case study of Mindong No. 1 coal mine in north-east Inner Mongolia, China", *Journal of Earth System Science*, 128(7), p. 200. doi:10.1007/s12040-019-1232-4.

Hiscock, K. M. (2005) *Hydrogeology: principles and practice*. Malden, MA: Blackwell Pub.

Hiscock, K. M. and Bense, V. F. (2014) *Hydrogeology: principles and practice*. Second edition. Chichester, West Sussex, UK : Hoboken, New Jersey: John Wiley & Sons, Inc.

Hitzman, M. W., Broughton, D., Selley, D., Woodhead, J., Wood, D. and Bull, S. (2012) "The Central African Copperbelt: diverse stratigraphic, structural, and temporal settings in the world's largest sedimentary copper district". University of Tasmania. Available at: https://figshare.utas.edu.au/articles/journal_contribution/The_Central_African_Copperbelt_diverse_stratigraphic_structural_and_temporal_settings_in_the_world_s_largest_sedimentary_copper_district/22925846/1 (Accessed: 15 January 2025).

Huang, X., Wang, G., Liang, X., Cui, L., Ma, L. and Xu, Q. (2018) "Hydrochemical and Stable Isotope (δD and δ18O) Characteristics of Groundwater and Hydrogeochemical

Processes in the Ningtiaota Coalfield, Northwest China", *Mine Water and the Environment*, 37(1), pp. 119–136. doi:10.1007/s10230-017-0477-x.

Kampunzu, A. B. and Cailteux, J. (1999) "Tectonic Evolution of the Lufilian Arc (Central Africa Copper Belt) During Neoproterozoic Pan African Orogenesis", *Gondwana Research*, 2(3), pp. 401–421. doi:10.1016/S1342-937X(05)70279-3.

Konkola Copper Mines (2010) *Geological Maps, Borehole Reports, 1:250 Mine Maps and Cu–Co Assay Results*. Unpublished Reports. Chiliabombwe, Zambia: Konkola Copper Mines.

Leketa, K. and Abiye, T. (2021) "Using Environmental Tracers to Characterize Groundwater Flow Mechanisms in the Fractured Crystalline and Karst Aquifers in Upper Crocodile River Basin, Johannesburg, South Africa", *Hydrology*, 8(1), p. 50. doi:10.3390/hydrology8010050.

Leketa, K., Abiye, T. and Butler, M. (2018) "Characterisation of groundwater recharge conditions and flow mechanisms in bedrock aquifers of the Johannesburg area, South Africa", *Environmental Earth Sciences*, 77(21), p. 727. doi:10.1007/s12665-018-7911-7.

Levin, M. and Verhagen, B. (2013) *THE USE OF ISOTOPE HYDROLOGY TO CHARACTERIZE AND ASSESS WATER RESOURCES IN SOUTH(ERN) AFRICA Tamiru Abiye Report to the Water Research Commission (WRC-South Africa)*.

Li, P., Wu, J. and Qian, H. (2014) "Hydrogeochemistry and Quality Assessment of Shallow Groundwater in the Southern Part of the Yellow River Alluvial Plain (Zhongwei Section), Northwest China", *Earth Sciences Research Journal*, 18. doi:10.15446/esrj.v18n1.34048.

Ma, F., Zhao, H. and Guo, J. (2015a) "Investigating the characteristics of mine water in a subsea mine using groundwater geochemistry and stable isotopes", *Environmental Earth Sciences*, 74(9), pp. 6703–6715. doi:10.1007/s12665-015-4680-4.

Ma, F., Zhao, H. and Guo, J. (2015b) "Investigating the characteristics of mine water in a subsea mine using groundwater geochemistry and stable isotopes", *Environmental Earth Sciences*, 74(9), pp. 6703–6715. doi:10.1007/s12665-015-4680-4.

Marandi, A. and Shand, P. (2018) "Groundwater chemistry and the Gibbs Diagram", *Applied Geochemistry*, 97, pp. 209–212. doi:10.1016/j.apgeochem.2018.07.009.

Master, S., Rainaud, C., Armstrong, R. A., Phillips, D. and Robb, L. J. (2005) "Provenance ages of the Neoproterozoic Katanga Supergroup (Central African Copperbelt), with implications for basin evolution", *Journal of African Earth Sciences*, 42(1–5), pp. 41–60. doi:10.1016/j.jafrearsci.2005.08.005.

Mazor, E. (2003) *Chemical and Isotopic Groundwater Hydrology*. 0 edn. CRC Press. doi:10.1201/9780203912959.

Mbilima, M. (2023) *Hydrogeological assessments and investigation of inflow sources at Lumwana Copper Mine, Zambia*. University of the Witwatersrand.

McGowan, R. R., Roberts, S. and Boyce, A. J. (2006) "Origin of the Nchanga copper–cobalt deposits of the Zambian Copperbelt", *Mineralium Deposita*, 40(6–7), pp. 617–638. doi:10.1007/s00126-005-0032-8.

Mengistu, H., Tessema, A., Abiye, T., Demlie, M. and Lin, H. (2015) "Numerical modeling and environmental isotope methods in integrated mine-water management: a case study from the Witwatersrand basin, South Africa", *Hydrogeology Journal*, 23(3), pp. 533–550. doi:10.1007/s10040-014-1216-z.

Mohuba, S. C. (2020) *HYDROGEOLOGICAL CHARACTERISATION AND GROUNDWATER VULNERABILITY TO POLLUTION MAPPING OF THE THYSPUNT NUCLEAR SITE, EASTERN CAPE*. University of the Witwatersrand.

Moriarty, J. (2011) *Qualitative Methods Overview*. London: National Institute for Health Research School for Social Care (SSCR Methods Reviews).

Muchez, Ph., Brems, D., Clara, E., De Cleyn, A., Lammens, L., Boyce, A., De Muynck, D., Mukumba, W. and Sikazwe, O. (2010) "Evolution of Cu–Co mineralizing fluids at Nkana Mine, Central African Copperbelt, Zambia", *Journal of African Earth Sciences*, 58(3), pp. 457–474. doi:10.1016/j.jafrearsci.2010.05.003.

Mulenga, S. C. (1991) "Groundwater flow through Konkola (Bancroft) copper mine - Zambia". University of London - Imperial College London. Available at: http://spiral.imperial.ac.uk/handle/10044/1/42835 (Accessed: 26 September 2023).

Mulenga, S. C. (1993) "SOLUTION TO KONKOLA MINE WATER INFLOW PROBLEM".

Mulenga, S. C. and De Freitas, M. H. (1991) "Groundwater flow model for Konkola underground copper mine, Zambia", in Institution of Mining and Metallurgy, *African Mining '91*. Dordrecht: Springer Netherlands, pp. 321–328. doi:10.1007/978-94-011-3656-3_32.

Mulenga, S. C., Fernandez-Rubio, R., Leon, A. and Baquero, J. C. (1992) "Estimation of quantitative water inflow from different sources in Konkola Mine, Zambia", *Mine Water and the Environment*, 11(4), pp. 1–22. doi:10.1007/BF02918444.

Mulonda, S. (2023) *Structural Analysis and Geological Modelling of a Stratiform Copper-Cobalt Deposit at Konkola, Central African Copper Belt, Zambia*. University of the Witwatersrand.

Naish, E. J. H. (1993) "Dewatering Concepts at ZCCM's Copperbelt Mines".

Piper, A. M. (1944) "A graphic procedure in the geochemical interpretation of water-analyses", *Eos, Transactions American Geophysical Union*, 25(6), pp. 914–928. doi:10.1029/TR025i006p00914.

Polak, K., Różkowski, K. and Czaja, P. (2016) "Causes and Effects of Uncontrolled Water Inrush into a Decommissioned Mine Shaft", *Mine Water and the Environment*, 35(2), pp. 128–135. doi:10.1007/s10230-015-0360-6.

Porada, H. and Berhorst, V. (2000) "Towards a new understanding of the Neoproterozoic-early palæozoic Lufilian and northern Zambezi belts in Zambia and the Democratic Republic of Congo", *Journal of African Earth Sciences*, 30(3), pp. 727–771. doi:10.1016/S0899-5362(00)00049-X.

Qian, J., Tong, Y., Ma, L., Zhao, W., Zhang, R. and He, X. (2017a) "Hydrochemical Characteristics and Groundwater Source Identification of a Multiple Aquifer System in a Coal Mine", *Mine Water and the Environment*. doi:10.1007/s10230-017-0493-x.

Qian, J., Tong, Y., Ma, L., Zhao, W., Zhang, R. and He, X. (2017b) "Hydrochemical Characteristics and Groundwater Source Identification of a Multiple Aquifer System in a Coal Mine", *Mine Water and the Environment*. doi:10.1007/s10230-017-0493-x.

Ramangoa, M. B. (2021) *Application of hydrochemical and tracer techniques to investigate the source of seepage water in deep gold mines: A case study at South Deep Gold Mine, Gauteng Province, South Africa*. The University of the Witwatersrand.

Read, J. and Beale, G. (2013) *Guidelines for Evaluating Water in Pit Slope Stability*. Csiro Publishing.

Sahib, L. Y., Marandi, A. and Schüth, C. (2016) "Strontium isotopes as an indicator for groundwater salinity sources in the Kirkuk region, Iraq", *Science of The Total Environment*, 562, pp. 935–945. doi:10.1016/j.scitotenv.2016.03.185.

Sammarco, O. and Eng, D. (1986) "Spontaneous inrushes of water in underground mines", *International Journal of Mine Water*, 5(3), pp. 29–41. doi:10.1007/BF02498099.

Selley, D., Broughton, D., Scott, R., Hitzman, M., Bull, S., Large, R., McGoldrick, P., Croaker, M., Pollington, N. and Barra, F. (2005) "A New Look at the Geology of the Zambian Copperbelt", in Hedenquist, J. W., Thompson, J. F. H., Goldfarb, R. J., and Richards, J. P., *One Hundredth Anniversary Volume*. Society of Economic Geologists. doi:10.5382/AV100.29.

Selley, D., Scott, R., Emsbo, P., Koziy, L., Hitzman, M. W., Bull, S. W., Duffett, M., Sebagenzi, S., Halpin, J. and Broughton, D. W. (2018) "Structural Configuration of the Central African Copperbelt: Roles of Evaporites in Structural Evolution, Basin Hydrology, and Ore Location", in Arribas R., A. M. and Mauk, J. L. (eds) *Metals, Minerals, and Society*. Society of Economic Geologists, pp. 115–156. doi:10.5382/SP.21.07.

Sharon L Qi and Alta C Harris (2017) "Geochemical Database for the National Brackish Groundwater Assessment of the United States". U.S. Geological Survey. doi:10.5066/F72F7KK1.

Sillitoe, R. H., Perelló, J., Creaser, R. A., Wilton, J., Wilson, A. J. and Dawborn, T. (2017) "Age of the Zambian Copperbelt", *Mineralium Deposita*, 52(8), pp. 1245–1268. doi:10.1007/s00126-017-0726-8.

Singh (1986) "Mine Inundations", *International Journal of Mine Water*.

Singhal, B. B. S. and Gupta, R. P. (1999) *Applied Hydrogeology of Fractured Rocks*. Dordrecht: Springer Netherlands. doi:10.1007/978-94-015-9208-6.

Singhal, B. B. S., Gupta, Raj P. and Gupta, Ravi P. (2010) *Applied Hydrogeology of Fractured Rocks*. 2. Aufl. Dordrecht: Springer.

Smedley, P. L. and Kinniburgh, D. G. (2002) "A review of the source, behaviour and distribution of arsenic in natural waters", *Applied Geochemistry*, 17(5), pp. 517–568. doi:10.1016/S0883-2927(02)00018-5.

Stiff, H. A. (1951) "The Interpretation of Chemical Water Analysis by Means of Patterns", *Journal of Petroleum Technology*, 3(10), pp. 15–3. doi:10.2118/951376-G.

Straskraba, V., Sharma, D. and Naish, E. (1991) "Konkola Mine Dewatering Study".

Talling, J. F. and Talling, I. B. (1965) "The Chemical Composition of African Lake Waters", *Internationale Revue der gesamten Hydrobiologie und Hydrographie*, 50(3), pp. 421–463. doi:10.1002/iroh.19650500307.

Terzer, S., Wassenaar, L. I., Araguás-Araguás, L. J. and Aggarwal, P. K. (2013) "Global isoscapes for δ^{18} O and δ^{2} H in precipitation: improved prediction using regionalized climatic regression models", *Hydrology and Earth System Sciences*, 17(11), pp. 4713–4728. doi:10.5194/hess-17-4713-2013.

Torremans, K., Gauquie, J., Boyce, A. J., Barrie, C. D., Dewaele, S., Sikazwe, O. and Muchez, Ph. (2013) "Remobilisation features and structural control on ore grade distribution at the Konkola stratiform Cu–Co ore deposit, Zambia", *Journal of African Earth Sciences*, 79, pp. 10–23. doi:10.1016/j.jafrearsci.2012.10.005.

Twite, F., Broughton, D., Nex, P., Kinnaird, J., Gilchrist, G. and Edwards, D. (2019) "Lithostratigraphic and structural controls on sulphide mineralisation at the Kamoa copper deposit, Democratic Republic of Congo", *Journal of African Earth Sciences*, 151, pp. 212–224. doi:10.1016/j.jafrearsci.2018.12.016.

Van Wyk, E., Van Tonder, G. and Vermeulen, D. (2011) "Characteristics of local groundwater recharge cycles in South African semi-arid hard rock terrains – rainwater input", *Water SA*, 37(2). doi:10.4314/wsa.v37i2.65860.

Vutukuri, V. S. and Singh, R. N. (1995) "Mine inundation-case histories", *Mine Water and the Environment*, 14(1), pp. 107–130. doi:10.1007/BF02914857.

World Bank Climate Change Knowledge Portal (2025). Available at: https://climateknowledgeportal.worldbank.org/ (Accessed: 10 March 2025).

WSP (2018) "KONKOLA HYDROGELOGICAL CONCEPTUAL MODEL". Konkola Copper Mines.

Xu, K., Qiao, W., Zhu, G., Feng, L., Wang, Z. and Li, W. (2022) "Hydrogeochemical Characteristics of a Multi-Layer Groundwater System in a Coal Mine Area: A Case Study", *Water*, 14(19), p. 3146. doi:10.3390/w14193146.

Xu, Y. and Beekman, H. E. (2003) *Groundwater Recharge Estimation in Southern Africa*. Paris: Unesco IHPSeries Num 64.

Zhang, H., Xu, G., Chen, X., Wei, J., Yu, S. and Yang, T. (2019) "Hydrogeochemical Characteristics and Groundwater Inrush Source Identification for a Multi-aquifer System in a Coal Mine", *Acta Geologica Sinica - English Edition*, 93(6), pp. 1922–1932. doi:10.1111/1755-6724.14299.